Phylogeography and biodiversity of ophiuroids in the Southern Ocean

by

Matthew P. Galaska

A dissertation submitted to the Graduate Faculty of
Auburn University
in partial fulfillment of the
requirements for the Degree of
Doctor of Philosophy

Auburn, Alabama
August 5, 2017

Ophiuroid, Phylogeography, Southern Ocean
2b-RAD

Approved by

Kenneth M. Halanych, Chair, Professor of Biological Sciences
Jason E. Bond, Professor and Chair of Biological Sciences
Leslie R. Goertzen, Associate Professor of Biological Sciences
Andrew R. Mahon, Assistant Professor of Biological Sciences
Covadonga R. Arias, Associate Professor of Fisheries, Aquaculture and Aquatic Sciences

Abstract

The Southern Ocean surrounding Antarctica is home to a highly endemic benthic fauna, often attributed to the strong oceanic barrier, the Antarctic Polar front. The Antarctic Polar Front and Antarctic Circumpolar Current formed over 24 million years ago when the northern tip of the Antarctic Peninsula separated from the southern tip of South America, thus forming the Drake Passage. Although the Antarctic Circumpolar Current is often attributed as a vector for organismal dispersal in and around the Southern Ocean, the temperature and salinity change of the Antarctic Polar Front has helped to isolate the Southern Ocean from the warmer waters of more northerly latitudes. These two defining forces of the Southern Ocean ecosystem provide important questions, 1) are circumpolar organisms homogenous through their range, 2) does the Antarctic Polar Front act as an absolute barrier to dispersal for non-endemic species?

This research focused on one of the Southern Ocean's benthic ecosystems most conspicuous members, the class Ophiuroidea. Ophiuroidea is the most speciose of all echinoderm classes and represents a rich biodiversity within the Southern Ocean. This biodiversity represents 219 species, 126 are endemic, and many are considered to have circumpolar distributions. Due to the ecological importance of this class, this dissertation has focused on the biodiversity and phylogeography of both endemic and non-endemic species of Southern Ocean ophiuroids.

The work presented here has revealed distinct geographic structure of two circumpolar ophiuroid species, specifically *Ophionotus victoriae* and *Astrotoma agassizii*. *Ophionotus*

victoriae was revealed to have four geographically distinct populations based on two mitochondrial markers and a whole genome single nucleotide polymorphism based approach, specifically 2b-RAD. The first population occurs in the Bellingshausen and Amundsen Sea region, the second population occurs in the Ross Sea and on the western side of the Antarctic Peninsula. The final two populations both occur on the eastern side of the Antarctic Peninsula in the Weddell Sea. This first chapter on *Ophionotus victoriae* follows the formatting of *Ecology and Evolution.*

Additionally, in the non-endemic species *A. agassizii*, genetic connectivity across the Antarctic Polar Front was recovered and is the first benthic invertebrate to have shown this pattern. Although a possible migrant was revealed from the mitochondrial data, the inclusion of whole genome bi-allelic SNP markers, allowed for the recovery of five admixed individuals. Four of the admixed individuals were recovered in South America while one was recovered in the Southern Ocean, providing evidence for bi-directional migration. The work presented in Chapter two on *Astrotoma agassizii* follows the formatting of *Biological Bulletin*. Evolutionary relationships were analyzed within Ophiuroidea using the mitochondrial genome from 10 new ophiuroid species, 9 of which were from the Southern Ocean and 1 from South America. These 10 new mitochondrial genomes more than doubled the number of what was publically available, which allowed our comparison of phylogenetic relationships and comparative gene orders comprising 17 different ophiuroid mitochondrial genomes. The 17 mitochondrial genomes represent a wide taxonomic sampling of the currently accepted evolutionary relationships within Ophiuroidea. These relationships revealed three conserved

gene orders for the 13 coding genes and 2 ribosomal genes within Ophiuroidea. Both the conserved gene orders and Maximum Likelihood phylogenetic analyses support Ophiuroidea being comprised of the two recently suggested superorders, specifically Euryophiurida and Ophintegrida. The third chapter follows the formatting of *Molecular Phylogenetics and Evolution*.

Acknowledgments

I would like to thank my dissertation advisor, Ken Halanych, for overseeing my research over the course of this process. Thank you for taking me on field expeditions, encouraging me to share my work at conferences and allowing me to work independently. I would also like to thank my committee members: Jason Bond and Les Goertzen, who have helped provide guidance, feedback and a valuable perspectives on my research. Andrew Mahon, thank you for not only being a committee member, a collaborator on many of my projects but also someone who has helped to keep me sane through this whole process. Scott Santos, I'd like to thank you for being a pseudo committee member, collaborator and essentially my secondary advisor. This has made the entire process much more pleasant. I would also really like to thank Cova Arias for agreeing to be my outside reader, I know this is extra work and I greatly appreciate it. To the past and present members of the Halanych lab, it would have been a much more difficult journey without the moral support and friendship that you have provided. While my work has substantially varied from others in the lab, I would like to specifically thank Yuanning Li for the insight and advice in my third chapter. I would also like to specifically thank Damien Waits for the occasional bioinformatic advice. Lastly, I would like to thank my family for supporting me through this process.

Table of Contents

List of Tables

List of Illustrations

CHAPTER 2

CHAPTER 3

CHAPTER 4

List of Abbreviations

ACC	Antarctic Circumpolar Current
APF	Antarctic Polar Front
SA	South America
SO	Southern Ocean

Chapter 1. Introduction

The Southern Ocean is home to some of the most interesting ecological communities in the world. Not only comprising a rich charismatic megafauna consisting of seals, whales and penguins but also the rich benthic assemblages of the Southern Ocean which are the focus here. The Southern Ocean houses high species richness in terms of benthic invertebrates, the vast majority of which occur on the relatively narrow Antarctic continental shelf (Díaz et al., 2011). Given the endemic benthic fauna (Kaiser et al., 2013), there are many questions on how oceanographic barriers limit species dispersal. Presumably, the unique nature of the Southern Ocean's benthic assemblages resulted from the opening of the drake passage, cooling temperatures of the Southern Ocean and formation of the Antarctic Circumpolar Current (ACC) 31 Ma ± 2 Ma (Clarke et al., 2007; Lawver and Gahagan, 2003). The ACC can extend to 4000 meters in depth, often to the sea floor, and approximately 200 km in width (Orsi et al., 1995; Smetacek et al., 1997). Although the ACC is often attributed as a vector for dispersal in and around the Southern Ocean (Nikula et al., 2010), the Antarctic Polar Front (APF) is considered a strong barrier to dispersal (Aronson et al., 2007). Molecular studies that have tested genetic connectivity across the APF have found distinct breaks in nemertean worms (Thornhill et al., 2008), octocorals (Dueñas et al., 2016) ophiuroids (Hunter and Halanych, 2008) and notothenioid fish (Bargelloni et al., 2000).

The ecosystem on the Antarctic Shelf is continuously impacted by the ever changing geology due to glacial scour and, over a longer period, glaciation advance and retreat (Clarke and Crame, 1989). Benthic assemblages are shaped by availability of habitable space on the shelf due to glaciation cycles (Kaiser et al., 2013; Thatje et al., 2005). Glaciations have acted as habitat limiting events in the Southern Ocean (Kaiser et al., 2013), allowing for large population

expansions or reductions. These cycles are responsible for population fragmentation and allopatric speciation (Clarke et al., 2007). Polynyas, open areas of water surrounded by sea ice, act as a refugia and are an area of higher-level primary production (Massom and Stammerjohn, 2010). With several studies discovering cryptic species on the Antarctic Shelf (Hunter and Halanych, 2010, 2008; Janosik and Halanych, 2010; Leese et al., 2010, 2008; Thornhill et al., 2008), there is evidence that glaciation cycles may well serve as a biological "diversity pump" (Clarke and Crame, 1992) in the Southern Ocean.

Additionally, the Southern Ocean is currently, and has been, the focus of climate change studies (Aronson et al., 2009; Meredith and King, 2005; Sewell and Hofmann, 2011). One reason for the Southern Ocean to garner so much attention is due to the Antarctic Peninsula heating up at a rate higher than any other area in the world (Meredith and King, 2005; Vaughan et al., 2003). Ecologically, this is very concerning for temperature tolerances of local fauna and the possibility of reinvasion of species from warmer northern latitudes (McClintock et al., 2008). When the Southern Ocean last cooled down during the Eocene, the temperature change made it uninhabitable for higher level durophagous predators (Aronson et al., 2009) but as temperatures steadily rise, the reinvasion of king crabs (*Neolithodes yaldwyni*) has recently been documented off the Antarctic Peninsula (Aronson et al., 2007; Smith et al., 2012). This could be the first of many species that extends its range into the Southern Ocean.

With climate change impacting the Southern Ocean ecosystem, getting a better understanding of how species are currently distributed and genetically connected throughout the Southern Ocean is imperative. Many benthic invertebrates are thought to have a circumpolar distribution around the SO, which raises the question of whether these species are panmictic throughout their range, are geographically structured or in some instances represent cryptic

species complexes? Ophiuroids were used in this study as they are an ideal candidate for phylogeographic analysis in the Southern Ocean. They are an important member of the Southern Ocean's biodiversity with 219 nominal species;126 are considered endemic (Martín-Ledo and López-González, 2014). In addition to being highly speciose, ophiuroids often represent the majority of the biomass and biodiversity in a single sampling location (Sands et al., 2012). Several species that are thought to be circumpolar in distribution (Hunter and Halanych, 2010, 2008; Sands et al., 2012); have served as candidates for analysis in regard to the effects open ocean barriers have on dispersal. Genetic investigations of Southern Ocean ophiuroids have revealed probable cryptic speciation or unrecognized diversity, two of which are the focus of this dissertation *Ophionotus victoriae* and *Astrotoma agassizii* (Galaska et al., 2017; Hunter and Halanych, 2010; Martín-Ledo et al., 2012). The issue of cryptic speciation arises consistently in molecular studies of the Southern Ocean but is far from limited to echinoderms.

To address our questions of genetic connectivity and recognizing the limitations of single gene mitochondrial or even nuclear markers, this dissertation has a large emphasis placed on whole genome reduced representation single nucleotide polymorphism (SNP)-based data sets. The ability to address questions of admixture and fine scale structure in non-model organisms is unmatched in utility and cost (Reitzel et al., 2013). In particular, we focus on the 2b-RAD protocol (Wang et al., 2012) or type 2b endonuclease restriction associated DNA due to its utility in the ability to target specific fractions of restriction sites based on the estimated size of the organisms genome.

The overall goal of this research was to investigate the biodiversity and phylogeography of ophiuroids, particularly relating to the Southern Ocean. Study of open ocean barriers to dispersal, cryptic speciation and phylogeographic relationships in the Southern Ocean were

directly benefited from pairing such high resolution genetic techniques with supposed circumpolar species. The increase in data provided us with higher accuracy and support in our analyses.

References:

Aronson, R.B., Moody, R.M., Ivany, L.C., Blake, D.B., Werner, J.E., Glass, A., 2009. Climate Change and Trophic Response of the Antarctic Bottom Fauna. PLoS One 4, 6.

Aronson, R.B., Thatje, S., Clarke, A., Peck, L.S., Blake, D.B., Wilga, C.D., Seibel, B.A., 2007. Climate Change and Invasibility of the Antarctic Benthos. Annu. Rev. Ecol. Evol. Syst. 38, 129–154.

Bargelloni, L., Marcato, S., Zane, L., Patarnello, T., 2000. Mitochondrial phylogeny of notothenioids: a molecular approach to Antarctic fish evolution and biogeography. Syst. Biol. 49, 114–129. doi:10.1080/10635150050207429

Clarke, A., Crame, J.A., 1992. The Southern Ocean benthic fauna and climate change: A historical perspective. Philos. Trans. R. Soc. B Biol. Sci. 339, 299–309.

Clarke, A., Crame, J.A., 1989. The origin of the Southern Ocean marine fauna. Geol. Soc. Spec. Publ. 47, 253–268. doi:10.1144/GSL.SP.1989.047.01.19

Clarke, A., Johnston, N.M., Murphy, E.J., Rogers, a. D., 2007. Introduction. Antarctic ecology from genes to ecosystems: the impact of climate change and the importance of scale. Philos. Trans. R. Soc. B Biol. Sci. 362, 5–9. doi:10.1098/rstb.2006.1943

Díaz, a., Féral, J.-P., David, B., Saucède, T., Poulin, E., 2011. Evolutionary pathways among shallow and deep-sea echinoids of the genus Sterechinus in the Southern Ocean. Deep Sea Res. Part II Top. Stud. Oceanogr. 58, 205–211. doi:10.1016/j.dsr2.2010.10.012

Dueñas, L.F., Tracey, D.M., Crawford, A.J., Wilke, T., Alderslade, P., Sánchez, J.A., 2016. The Antarctic Circumpolar Current as a diversification trigger for deep-sea octocorals. BMC Evol. Biol. 16, 2. doi:10.1186/s12862-015-0574-z

Galaska, M.P., Sands, C.J., Santos, S.R., Mahon, A.R., Halanych, K.M., 2017. Geographic

structure in the Southern Ocean circumpolar brittle star Ophionotus victoriae (Ophiuridae) revealed from mtDNA and single-nucleotide polymorphism data. Ecol. Evol. 7, 1–11. doi:10.1002/ece3.2617

Hunter, R.L., Halanych, K.M., 2010. Phylogeography of the Antarctic planktotrophic brittle star *Ophionotus victoriae* reveals genetic structure inconsistent with early life history. Mar. Biol. 157, 1693–1704. doi:10.1007/s00227-010-1443-3

Hunter, R.L., Halanych, K.M., 2008. Evaluating connectivity in the brooding brittle star *Astrotoma agassizii* across the drake passage in the Southern Ocean. J. Hered. 99, 137–48. doi:10.1093/jhered/esm119

Janosik, A.M., Halanych, K.M., 2010. Unrecognized Antarctic biodiversity: a case study of the genus *Odontaster* (Odontasteridae; Asteroidea). Integr. Comp. Biol. 50, 981–92. doi:10.1093/icb/icq119

Kaiser, S., Brandão, S.N., Brix, S., Barnes, D.K. a., Bowden, D. a., Ingels, J., Leese, F., Schiaparelli, S., Arango, C.P., Badhe, R., Bax, N., Blazewicz-Paszkowycz, M., Brandt, A., Brenke, N., Catarino, A.I., David, B., Ridder, C., Dubois, P., Ellingsen, K.E., Glover, A.G., Griffiths, H.J., Gutt, J., Halanych, K.M., Havermans, C., Held, C., Janussen, D., Lörz, A.-N., Pearce, D. a., Pierrat, B., Riehl, T., Rose, A., Sands, C.J., Soler-Membrives, A., Schüller, M., Strugnell, J.M., Vanreusel, A., Veit-Köhler, G., Wilson, N.G., Yasuhara, M., 2013. Patterns, processes and vulnerability of Southern Ocean benthos: a decadal leap in knowledge and understanding. Mar. Biol. 160, 2295–2317. doi:10.1007/s00227-013-2232-6

Lawver, L. a., Gahagan, L.M., 2003. Evolution of Cenozoic seaways in the circum-Antarctic region. Palaeogeogr. Palaeoclimatol. Palaeoecol. 198, 11–37. doi:10.1016/S0031-0182(03)00392-4

Leese, F., Agrawal, S., Held, C., 2010. Long-distance island hopping without dispersal stages: transportation across major zoogeographic barriers in a Southern Ocean isopod. Naturwissenschaften 97, 583–94. doi:10.1007/s00114-010-0674-y

Leese, F., Kop, A., Wägele, J.-W., Held, C., 2008. Cryptic speciation in a benthic isopod from Patagonian and Falkland Island waters and the impact of glaciations on its population structure. Front. Zool. 5, 19. doi:10.1186/1742-9994-5-19

Martín-Ledo, R., López-González, P.J., 2014. Brittle stars from Southern Ocean (Echinodermata: Ophiuroidea). Polar Biol. 37, 73–88. doi:10.1007/s00300-013-1411-8

Martín-Ledo, R., Sands, C.J., López-González, P.J., 2012. A new brooding species of brittle star (Echinodermata: Ophiuroidea) from Antarctic waters. Polar Biol. 36, 115–126. doi:10.1007/s00300-012-1242-z

Massom, R. a., Stammerjohn, S.E., 2010. Antarctic sea ice change and variability - Physical and ecological implications. Polar Sci. 4, 149–186. doi:10.1016/j.polar.2010.05.001

McClintock, J., Ducklow, H., Fraser, W., 2008. Ecological Responses to Climate Change on the Antarctic Peninsula. Am. Sci. 96, 302–310. doi:10.1511/2008.73.302

Meredith, M.P., King, J.C., 2005. Rapid climate change in the ocean west of the Antarctic Peninsula during the second half of the 20th century. Geophys. Res. Lett. 32, 1–5. doi:10.1029/2005GL024042

Nikula, R., Fraser, C.I., Spencer, H.G., Waters, J.M., 2010. Circumpolar dispersal by rafting in two subantarctic kelp-dwelling crustaceans. Mar. Ecol. Prog. Ser. 405, 221–230. doi:10.3354/meps08523

Orsi, A.H., Whitworth, T., Nowlin, W.D., 1995. On the meridional extent and fronts of the Antarctic Circumpolar Current. Deep. Res. Part I 42, 641–673. doi:10.1016/0967-

0637(95)00021-W

Reitzel, A.M., Herrera, S., Layden, M.J., Martindale, M.Q., Shank, T.M., 2013. Going where traditional markers have not gone before: utility of and promise for RAD sequencing in marine invertebrate phylogeography and population genomics. Mol. Ecol. 22, 2953–2970. doi:10.1111/mec.12228

Sands, C.J., Griffiths, H.J., Downey, R. V., Barnes, D.K. a., Linse, K., Martín-Ledo, R., 2012. Observations of the ophiuroids from the West Antarctic sector of the Southern Ocean. Antarct. Sci. 25, 3–10. doi:10.1017/S0954102012000612

Sewell, M. a., Hofmann, G.E., 2011. Antarctic echinoids and climate change: A major impact on the brooding forms. Glob. Chang. Biol. 17, 734–744. doi:10.1111/j.1365-2486.2010.02288.x

Smetacek, V., De Baar, H.J.W., Bathmann, U. V., Lochte, K., Rutgers Van Der Loeff, M.M., 1997. Ecology and biogeochemistry of the Antarctic Circumpolar Current during austral spring: A summary of Southern Ocean JGOFS cruise ANT X/6 of R.V. Polarstern. Deep. Res. Part II Top. Stud. Oceanogr. 44, 1–21. doi:10.1016/S0967-0645(96)00100-2

Smith, C.R., Grange, L.J., Honig, D.L., Naudts, L., Huber, B., Guidi, L., Domack, E., 2012. A large population of king crabs in Palmer Deep on the west Antarctic Peninsula shelf and potential invasive impacts. Proc. Biol. Sci. 279, 1017–26. doi:10.1098/rspb.2011.1496

Thatje, S., Hillenbrand, C.-D., Larter, R., 2005. On the origin of Antarctic marine benthic community structure. Trends Ecol. Evol. 20, 534–40. doi:10.1016/j.tree.2005.07.010

Thornhill, D.J., Mahon, A.R., Norenburg, J.L., Halanych, K.M., 2008. Open-ocean barriers to dispersal: a test case with the Antarctic Polar Front and the ribbon worm *Parborlasia corrugatus* (Nemertea: Lineidae). Mol. Ecol. 17, 5104–17. doi:10.1111/j.1365-

294X.2008.03970.x

Vaughan, D.G., Marshall, G.J., Connolley, W.M., Parkinson, C., Mulvaney, R., Hodgson, D.A., King, J.C., Pudsey, C.J., Turner, J., 2003. Recent rapid regional climate warming on the Antarctic Peninsula. Clim. Change 60, 243–274. doi:10.1023/A:1026021217991

Wang, S., Meyer, E., McKay, J.K., Matz, M. V, 2012. 2b-RAD: a simple and flexible method for genome-wide genotyping. Nat. Methods 9, 808–10. doi:10.1038/nmeth.2023

Chapter 2: Geographic structure in the Southern Ocean circumpolar brittle star *Ophionotus victoriae* (Ophiuridae) revealed from mtDNA and single nucleotide polymorphism data.

Abstract:

Marine systems have traditionally been thought of as "open" with few barriers to gene flow. In particular, many marine organisms in the Southern Ocean purportedly possess circumpolar distributions that have rarely been well verified. Here, we use the highly abundant and endemic Southern Ocean brittle star *Ophionotus victoriae* to examine genetic structuring and determine if barriers to gene flow have existed around the Antarctic continent. *Ophionotus victoriae* possesses feeding planktotrophic larvae with presumed high dispersal capability, but, a previous study revealed genetic structure along the Antarctic Peninsula. To test the extent of genetic differentiation within *O. victoriae*, we sampled from the Ross Sea through the eastern Weddell Sea. Whereas two mitochondrial DNA markers (16S rDNA and COI), were employed to allow comparison to earlier work, a 2b-RAD Single Nucleotide Polymorphism (SNP) approach facilitated sampling of loci across the genome. Mitochondrial data from 414 individuals suggested 3 major lineages, whereas, 2b-RAD data generated 1,999 biallelic loci that identified 4 geographically distinct groups from 89 samples. Given the greater resolution by SNP data, *O. victoriae* can be divided into geographically distinct populations likely representing multiple species. Specific historical scenarios that explain current population structure were examined with Approximate Bayesian Computation (ABC) analyses. Although the Bransfield Strait region shows high diversity possibly due to mixing, our results suggest that within the recent past, dispersal processes due to strong currents such as the Antarctic Circumpolar Current, have not

overcome genetic subdivision presumably due to historical isolation, questioning the idea of large open circumpolar populations in the Southern Ocean.

Introduction:

The Southern Ocean (SO) is characterized by rich biodiversity and largely endemic benthic fauna (Kaiser *et al.* 2013), resulting from an active geological history and organismal adaption to an extreme environment. While the Antarctic Polar Front (APF) serves to isolate the SO from warmer waters at lower latitudes, the Antarctic Circumpolar Current (ACC) is the world's strongest major current that has been presumed to aid dispersal of many marine species within the SO (Bathmann *et al.* 1997; Smetacek *et al.* 1997; Thornhill *et al.* 2008). The fact that the ACC can promote long distance dispersal has help reinforce the historically held assumption that many marine organisms of the SO likely have a circumpolar distribution around Antarctica (Dayton *et al.* 1994). Antarctic currents closer to shore such as the Circumpolar Deep Water, Ross Gyre and Weddell Gyre add complexity in predicting geographic dispersal capabilities of species (Tynan 1998).

In addition to dispersal mediated by oceanic currents, glaciation cycles have also played a role in Antarctic biodiversity through controlling habitat availability (Thatje *et al.* 2005). Glacial maximums during the Cenozoic likely forced species into the deep sea with pockets of refugia on the shelf allowing some species to recolonize and ultimately shape the SO's current community structure (Thatje *et al.* 2005). Polynyas, open regions of water surrounded by sea ice, in the SO may also serve as areas of refuge and often contribute higher levels of primary production (Massom & Stammerjohn 2010). In expansion phases, grounded ice sheets can physically cover large geographic areas of the continental shelf, displacing inhabitants, and physically reshaping environments by removal and rearrangement of benthic habitat. During glacial contraction, new

habitat becomes available allowing for population expansion. Thus, glacial cycles can drive population fragmentation and expansion opportunities (Thatje *et al.* 2005), ultimately serving as a biological "diversity pump" (Clarke & Crame 1992).

Brittle stars are important members of SO biodiversity, comprising at least 219 nominal species and 126 that are endemic from the region (Martín-Ledo & López-González 2014). Three of these species belong to *Ophionotus* (*O. hexactis* (Smith 1876), *O. taylori* McKnight, 1967, and *O. victoriae* Bell 1902); all of which also occur in the SO but are morphologically distinct from each other. *Ophionotus victoriae* Bell, 1902 is the most common and is a highly abundant (Figure 1), conspicuous ophiuroid endemic to the SO. This species has been reported to have a circumpolar distribution (Fell 1961) and occupies many different benthic substrates within Antarctic waters (Fratt & Dearborn, 1984), with the South Sandwich Islands as its northern most limit (Sands *et al.* 2012). *Ophionotus victoriae* has a long lived, planktotrophic larvae, remaining in the water column for several months (Pearse *et al.* 1991), thus allowing for the possibility of long distance dispersal via the ACC. Previous phylogeographic work using the mitochondrial DNA (mtDNA) 16S ribosomal subunit (16S) and cytochrome c oxidase subunit I (COI) gene fragments reported unexpected levels of genetic diversity and divergence along the Antarctic Peninsula and oceanic Islands (South Sandwich Islands and Bouvet Island), suggesting *O. victoriae* possesses higher than expected geographic structure and questions the possibility of cryptic species (Hunter & Halanych 2010). Given this, a larger sampling effort around Antarctica would likely result in the uncovering of additional diversity and potential discovery of cryptic species.

To test for phylogeographic structure in this supposed circumpolar species, and to provide insight on processes of dispersal and historical isolation, molecular tools were used to

examine *O. victoriae* over a >7,000 km range from the Western Ross Sea to the Eastern Weddell. This study, to the best of our knowledge, also includes the first sampling of benthic invertebrates from Wrights Bay, located between the Amundsen and Ross Seas. Herein, we utilized the mitochondrial 16S and COI genes to allow direct comparisons to results of Hunter and Halanych (2010) as well as a high resolution whole genome single nucleotide polymorphism (SNP) based approach, specifically 2b-RAD (Wang *et al.* 2012). This latter approach was chosen as restriction associated DNA (RAD)-tags have been shown to identify fine-scale population structure in marine species beyond the resolution of mtDNA genes (Reitzel *et al.* 2013; Benestan *et al.* 2015). Assessing population structure for organisms like *O. victoriae* of the SO is also important towards anticipating changes in the Antarctic benthic ecosystem as species ranges and structure will likely shift with future climate change (Aronson *et al.* 2007).

Methods:

Sample collection:

Specimens of *O. victoriae* were collected during four National Science Foundation (NSF)-sponsored research expeditions (*RVIB Nathaniel B. Palmer* 12-10, *RV Laurence M. Gould* 04-14, 06-05 & 13-12), three British Antarctic Survey (BAS)-sponsored expeditions (*RRS James Clark Ross* JR144, JR179 & JR230) and from an Alfred Wegener Institute (AWI) campaign (*RV Polarstern* PS77). Upon collection, samples were morphologically examined (mainly by MPG, CJS, and KMH) to verify species designations as described (McKnight 1967; Sieg & Waegele 1990). Oceanic island samples used in Hunter and Halanych (2010) were kindly made available from the NSF IceFish cruise and W. Deitrich (OPP-0132032). In total, the mitochondrial dataset included 414 specimens over 88 sampling localities that span the Ross, Amundsen, Bellingshausen, Antarctic Peninsula, Weddell Seas and oceanic islands, or a geographic distance

of > 7,000 km (Figure 2 and Supplementary Table 1). Samples available for 2b-RAD analyses included 96 specimens from 15 sampling localities ranging from the Ross Sea to the western portion of the Weddell Sea, a geographic distance > 5,000 km.

Data collection:

Genomic DNA was extracted using Qiagen's DNeasy® blood and tissue kit following the manufacturer's protocol. Extracted DNA was utilized in amplification of two mtDNA fragments from the COI and 16S genes. Because COI sequences typically provide considerably more resolution then 16S data (Mahon *et al.* 2008; Thornhill *et al.* 2008; Wilson *et al.* 2009), we allocated resources to maximize the number of individuals sampled for COI. A ~560bp fragment of COI was amplified for 414 samples with the universal COI primer set (Folmer *et al.* 1994) LCO1490 (5′-GGTCAACAAATCATAAAGATATTGG-3′) and HCO2198 (5′-TAAACTTCAGGGTGACCAAAAAATCA-3′). Polymerase chain reaction (PCR) cycling conditions for COI were: initial denaturation at 94°C for 3 min; 40 cycles of denaturation at 94°C for 30 s; annealing at 51°C for 1 min; extension at 72°C for 1 min; and final extension at 72°C for 2 min. Additionally, a ~500bp fragment was amplified for 252 samples using the 16S primer set (Palumbi 2007) 16SarL (5′-CGCCTGTTTATCAAAAACAT-3′) and 16SbrH (5′-CCGGTCTGAACTCAGATCACGT-3′). PCR cycling conditions employed for 16S were: initial denaturation at 94°C for 3 min; 35 cycles of denaturation at 94°C for 30 s; annealing at 46°C for 30 s; extension at 72°C for 30 s; and final extension at 72°C for 3 min. Amplicons for the COI and 16S genes were sent to Genewiz, Inc. (South Plainfield, New Jersey) for bidirectional Sanger sequencing. Chromatograms were assembled and edited using Sequencher® 5.4 (Gene Codes, Ann Arbor, MI) and finished sequences were aligned with MEGA 6 (Tamura *et al.* 2013). Analyses of molecular variance (AMOVA) were performed with Arlequin 3.5.1.2 (Excoffier *et*

al. 2005) to test for genetic differentiation between sampling localities by geographic regions (i.e., the Ross Sea, Bellingshausen Sea-Amundsen Sea, Western Peninsula, Weddell Sea and oceanic islands). Sampling information for AMOVA analyses including pooling scheme can be located in Supplementary Figure 1. TCS analyses (Templeton *et al.* 1992) were used to reconstruct statistical parsimony networks as implemented in PopART (Leigh & Bryant 2015) (http://popart.otago.ac.nz) for COI (414 samples), 16S (251 samples), and a concatenation of both mtDNA fragments (251 samples).

To aid with species delineation based on CO1 sequence data, a histogram of uncorrected pairwise distances (p) (Craft *et al.* 2008)was generated comparing all unique haplotypes of *O. victoriae* (Supplemental Table 8), *Ophionotus hexactis* (GenBank Accession Number KU895454.1), and *Ophiacantha spectabilis* (EU869959.1-EU869961.1). The latter taxa were employed to reveal genetic distance to other related ophiuroid taxa.

For RAD-tag analyses, a subset of 96 samples spanning 15 sampling locations from the Ross through the Western Weddell Seas were examined. Due to logistical issues, only samples from the *RVIB Nathaniel B. Palmer* 12-10 and *RV Laurence M. Gould* 13-12 cruises were available for 2b-RAD processing. Samples were prepared following Wang's et al. (2012) 2b-RAD protocol with the restriction enzyme *Alf*I. To avoid potential issues with PCR inhibitors in *O. victoriae*, samples were extracted using Qiagen's DNeasy® Plant Mini Kit. Selection of an appropriate reduction scheme was done by utilizing the genome size of *Ophioplocus esmarki* (C-value=3.00) (Hinegardner 1974) as a proxy since it is the most closely related ophiuroid to *O. victoriae* for which such information was available. Due to the large estimated genome size of *O. victoriae,* samples were prepped and dual barcoded targeting a reduced subset of *Alf*I sites through a 1/32nd reduction scheme to target roughly 2,000 SNPs. Sequencing was performed at

the Genome Services Laboratory at HudsonAlpha Institute for Biotechnology (Huntsville, Alabama) on an Illumina Hi-Seq 2000 using v4 chemistry and generating 50bp single-end reads.

Raw Illumina reads were demultiplexed by sample, quality filtered and aligned against a custom derived *de novo* reference following bioinformatic steps outlined in Wang et al.'s (2012) 2b-RAD protocol and with scripts provided by Dr. Eli Meyer (Oregon State University) (https://github.com/Eli-Meyer). Specifically, data were first filtered by loci with a minimum coverage of 25X. For all SNPs, loci scored as homozygotic were defined to have a max variance of 1% whereas those that were consider heterozygotic had a minimum of 25% variance. Loci deviating from these definitions were excluded from further analyses. Remaining SNP loci were then further filtered to only include loci that were present in ≥ 80% of individuals. To ensure individuals with large amounts of missing data did not skew analyses, those with ≤ 80% of the remaining SNP loci were also removed from the dataset. Raw data were also processed and analyzed using the software *Stacks* (Catchen *et al.* 2011) but both methods yielded similar interpretation of data and evolutionary patterns and processes (see below).

To determine the potential number of populations (*K)*, STRUCTURE 2.3.4 (Pritchard *et al.* 2000) was utilized with the following parameters: 1) 7 replicates at each potential *K* (1-15); 2) an admixture model with correlated allele frequencies; 3) a 50,000 repetition burn-in period, and; 4) 100,000 additional Markov chain Monte Carlo (MCMC) repetitions. Because SNP data sets can vary in λ (parameter around the allele frequency prior) compared to mtDNA (Pritchard *et al.* 2010), an initial run was used to infer λ to be 0.2447 prior to the full run. Resulting files were then processed with STRUCTURE HARVESTER (Earl & VonHoldt 2012) to determine the most likely values of *K* from Delta *K* analyses as well as CLUMPP (Jakobsson & Rosenberg 2007), and DISTRUCT (Rosenberg 2004) to visualize the *K* outputs.

Because results for *K* from STRUCTURE varied by MCMC run and seemed inconsistent with biological knowledge of *O. victoriae*, we used additional approaches to estimate *K*. SMARTPCA (Patterson *et al.* 2006) was used to further validate population structure by performing principal component analyses (PCA) in the EIGENSOFT software package (Price *et al.* 2006). Samples were analyzed and labeled by both STRUCTURE *K* results and geographic region for PCA analyses. Geographic regions for PCA analyses include: Ross Sea, Bellingshausen Sea, western Antarctic Peninsula, Bransfield Strait and Weddell Sea. One sampling locality in the Bransfield Strait (Op877) was likely an intermixing site based on results of STRUCTURE pairwise F_{ST} and PCA. Thus we performed analyses considering Op877 as belonging to both possible source populations. This did not affect interpretation of results (see below), and thus samples from Op877 were pooled with the population for which it is the most similar to (Weddell-A population). Furthermore, BayeScan (Foll & Gaggiotti 2008) was utilized with 4 threads, 100 runs at a 100,000 burn-in length and 100,000 pilot length to identify any loci that might be under selection and molecular diversity analyses were performed using GENEPOP (Rousset 2008).

DIYABC v2.0 (Cornuet *et al.* 2014) was used for an Approximate Bayesian Computation (ABC) analyses (Beaumont *et al.* 2002) to evaluate historic geographical patterns of divergence. This was achieved in DIYABC v2.0 by calculating summary statistics from prior distribution models in each proposed scenario. Specifically, seven different scenarios based off Antarctic currents and geographic history were evaluated to test whether the population structure was due to glacial refugia, current mediated gene flow or localized restriction of gene flow. All seven historic scenarios tested are shown and described in Supplementary Figure 1. Input populations needed for DIYABC v2.0 analyses were selected based off results of STRUCTURE analyses.

DIYABC v2.0 uses Principal Component Analyses (PCAs) to determine the confidence in each scenario and priors.

All sequences collected here in are reported under GenBank Accession numbers KY048203-KY048268. Raw reads for 2b-RAD SNP data are deposited to NCBI Sequence Read Archive (SRA) accessions SAMN05944630-SAMN5944718. Data matrices and alignments are deposited to Dryad under accession numbers doi:10.5061/dryad.0k1r0.

Results:

Mitochondrial:

Both COI and 16S mitochondrial fragments revealed genetic structure within *O. victoriae.* COI data analyzed from 414 individual yielded an increased nucleotide diversity from an extended geographic range in comparison to 16S or concatenated COI and 16S data for 252 individuals (Table 1). Thus, the following discussion focuses mainly on COI results as this marker provided more phylogeographic signal. Analyses of 16S and concatenated dataset are more fully reported in Supplementary Materials. Tests for selection via Tajima's *D* were negative, but not significant ($P > 0.10$), for both mitochondrial markers (Table 1). AMOVA results for COI data with groupings defined by geographic regions (i.e., Ross Sea, Bellingshausen Sea-Amundsen Sea, Western Peninsula, Weddell Sea and oceanic islands), revealed 37.87% of the molecular variation as occurring between geographic regions (Table 2). Additionally, three major lineages were recovered in the parsimony network analysis of COI (Figure 3A), primarily corresponding to the following geographic regions: I) Amundsen & Bellingshausen Seas with some individuals from the Western Weddell Sea; II) the Western Weddell Sea with oceanic islands; III) the Ross Sea with the Eastern Weddell Sea and Western Antarctic Peninsula. To show how the lineages relate to one another, the network was kept

whole but applying a 95% connection limit will separate genetic lineage I into its own unconnected network.

The histogram of uncorrected pairwise distances (Figure 3B) yielded four distinct modes. The most distant mode (~20.3-22.1%, mean = 21.2%) represented comparisons between *Ochiacantha* and *Ophionotus*, and second mode (~ 4.2-5.3%, mean = 4.6%) represents comparisons between *O. victoriae* and *O.hexactis*. Finally, comparisons within *O. victoriae* samples yielded two distinct modes. The mode closest to the origin (~1.8-4.0% mean = 2.8%) represents comparisons between individuals restricted to subnetwork lineages I, II, and III illustrated in Figure 3A, whereas the other mode (~ 0.2-1.6%, mean = 0.5%) are comparisons of individuals between subnetwork lineages. Given that these subnetworks largely correspond to geographic regions and given results of the 2b-RAD data (below), these latter two modes apparently correspond to intraspecific and interspecific variation, respectively.

2b-RAD analyses:

Following quality filtering and SNP calling, 16,588 loci were recovered (Table 3). To further filter these SNPs, any loci not present in at least 80% of samples were excluded, resulting in 1,999 remaining SNP loci. Next, any individuals with < 80% of the total remaining SNP loci were excluded, resulting in removal of 7 samples, thus leaving 89 individuals for analyses (Table 3). Under calculations of Delta *K* from STRUCTURE HARVESTER for this filtered and reduced dataset, *K* of 8 had the highest average support for Delta *K* after 7 runs, although individual runs of *K* at 2 and 4 had the highest maximum likelihood scores (Supplementary Figure 2). Thus, to assess which K was the most appropriate, STRUCTURE analyses were conducted with *K* set to 8, 4 and 2, then subjected to pairwise F_{ST} tests. At *K*=2 and 4, all populations were significantly different (Table 4) from one another while a *K*=8 identified

several populations with low non-significant F_{ST} values, signifying little to no structure between them and possibly an overestimation of *K*. As a result, *K*=4 was deemed the most appropriate for *O. victoriae*. Supplementary Table 2 provides specific F_{ST} values between all 15 sampling localities used in 2b-RAD SNP analyses. Results of the DISTRUCT graph from STRUCTURE are shown for *K*=4 in Figure 4 (Supplementary Figures 3 and 4 depict *K*=2 and *K*=8, respectively).

Population structure was further investigated with SMARTPCA analyses which revealed geographic structuring in concordance with STRUCTURE. Figure 5 and Supplementary Table 3 portray significant PCA results with samples labeled by genetic populations identified by STRUCTURE's *K*=4. All pairwise comparisons of the four STRUCTURE populations were significantly different as judged by a χ^2 test with a $p<0.01$ cut off (Supplementary Table 3). To understand if major geographic regions coincided with inferred STRUCTURE and SMARTPCA populations, we also pooled samples by geographic regions identified in methods (Supplementary Figure 5 and Supplementary Table 4). SMARTPCA results reveal significant differences between the Ross Sea/western Antarctic Peninsula, the Bellingshausen Sea and the Weddell Sea. However, the Bransfield Strait appears to be an intermixing zone.

BayeScan analysis of filtered SNP loci reported only one locus under possible selection. When the sequence containing this SNP was searched using BLAST on the NCBI webserver, a 100% match came back to two different genes, specifically leucoanthocyanidin dioxygenase and fam206a. Due to the nature of the short 36 base pair fragment, we cannot be positive as to the true identity of the SNP containing fragment. Furthermore, Hardy-Weinberg equilibrium was not violated for any loci (summary analyses for every locus in every population; a $X^2 = 91.12$, DF =108 and p= 0.879).

ABC analyses compared the fit of seven historical scenarios for the four genetic populations identified by STRUCTURE. These seven scenarios were chosen based on results of the mtDNA analyses, geographic history of Antarctica and knowledge of oceanic currents. Each of the four populations include two Weddell Sea populations, a Bellingshausen Sea population and a population that includes both the western Antarctic Peninsula and the Ross Sea (consistent with Figure 4). In the highest scoring scenario, Scenario 1, the Bellingshausen, Weddell, and Ross/Western Peninsula populations separate at approximately the same time with a more recent diversification in the Weddell Sea (Figure 6; all scenarios presented in the Supplementary materials Figure 1).

The combination of mtDNA COI sequence and nuclear SNP data provided strong evidence for regional genetic structure of *O. victoriae*. Based on analyses of total SNP data (STRUCTURE analyses, Figure 4 and pairwise F_{ST} Table 4), four genetically distinct populations are clearly identified: Ross Sea/Western Peninsula (R/WP), Bellingshausen Sea (B), Weddell Sea-A/Bransfield Strait (WA/BS) and Weddell Sea-B (WB) populations. Of the two populations within Weddell Sea, one population (WB) consists of individuals from two different mtDNA lineages (I & II) collected at three sampling localities between Seymour Island (a.k.a. Marambio Island) and the Antarctic Peninsula. The other (WA/BS) was recovered from two sampling localities south of Seymour Island and one sampling location in the Bransfield Strait (WA/BS). Population (B), which occurs between the two geographic regions comprising the (R/WP) population was the most genetically differentiated with an average pairwise F_{ST} of (0.1237) among populations.

Discussion:

Both mtDNA and 2b-RAD data reveal considerable genetic structure across the Western Antarctic in the brittle star *Ophionotus victoriae*, questioning its current status as a single species. As mentioned specimens were examined and morphological differences were not discernable with current taxonomy. However, both mtDNA and 2b-RAD data suggest distinct genetic lineages within what is currently recognized as *O. victoriae.* Although the Bransfield Strait appears to be more diverse then other populations indicating a possible mixing zone, the degree of genetic structuring appears ordered by major geographic regions.

Phylogeographic patterns from mtDNA:

Based on analyses of mtDNA COI, the western Weddell Sea has a recent shared history, or is currently connected with, the oceanic islands, and interestingly the eastern Weddell Sea samples share a discrete haplotype subnetwork with the Ross Sea and Western Peninsula (Figure 3A, lineage III, 2b-RAD data not available for eastern Weddell and oceanic islands). Lineage III, which includes the Ross Sea and eastern Weddell Sea samples was also the most geographically widespread clade and yet the least variable, as no haplotypes are more than two steps from the most common haplotype. This particular lineage could represent support for the assumed circumpolar distribution of *O. victoriae* or at least large-scale geographic dispersal capabilities through the Ross Gyre and out into the ACC.

Previous studies of other Antarctic benthic fauna have also revealed unexpected genetic structure in broadly distributed taxa. For example, the Antarctic crinoid *Promachocrinus kerguelensis* has a pelagic larval stage and was assumed to have a circumpolar distribution, but was ultimately found to be comprised of six different lineages and at least five different unrecognized species on the Antarctic Peninsula alone (Wilson *et al.* 2007). Later analyses

revealed all six lineages to be circumpolar, likely sympatric and eurybathic, with only two unrecognized species (Hemery *et al.* 2012). Similarly, population genetic analyses of two abundant and widespread SO pycnogonids, *Colossendeis megalonyx* and *C. robusta,* revealed multiple cryptic species as well (Krabbe *et al.* 2010; Dietz *et al.* 2015). Genetic studies (Held & Wägele 2005; Hunter & Halanych 2008; Mahon *et al.* 2008, 2009; Leese *et al.* 2008; Thornhill *et al.* 2008; Janosik *et al.* 2010; Sands *et al.* 2015) revealed underestimation of species diversity in the SO and have shown multiple genetic lineages within a single morphologically defined species. Given the genetic structure our analyses recovered, unrecognized species may exist within *O. victoriae,* although no distinguishing morphological characteristics could be determined. In contrast, some species do appear to have a circumpolar distribution such as the Antarctic krill, *Euphausia superba,* which has a holopelagic life cycle. Specifically, Hofmann and Murphy's (2004) hypothesis that while individual adult krill may not circumnavigate the SO in their lifetime, slow continuous gene flow occurs, and this hypothesis was supported by recent, RAD tag analyses indicative of panmixia (Deagle *et al.* 2015). With long-lived pelagic larvae, similar dispersal capabilities are possible for *O. victoriae* as well and a 2b-RAD based analysis is particularly appropriate.

Phylogeographic patterns from 2b-RAD:

Given that echinoderm larvae can remain in the water column for several months in the SO (Pearse *et al.* 1991), a circumpolar distribution for *O. victoriae* was a plausible hypothesis. Although we make the case that *O. victoriae* contains three distinct divergent mtDNA lineages, one lineage shows genetic connectivity over several thousands of kilometers. Specifically, 2b-RAD data revealed the Ross Sea and most of the Western Peninsula individuals (excluding one sampling locality in the Bransfield Strait) to be a single genetic population. One likely reason for

this observation is transportation of planktotrophic larvae by the ACC from the Ross Sea to the Western Peninsula. The ACC contacts the northern tip of the Western Peninsula. Depending on the depth planktotrophic larvae reside, the Circumpolar Deep Water and Upper Circumpolar Deep Water could have a significant impact on their distribution as well (Tynan 1998).

The level of genetic differentiation recovered from 2b-RAD between *O. victoriae* populations in both STRUCTURE and SMARTPCA analyses reveals distinct geographic structure. COI data further corroborates 2b-RAD data in that *O. victoriae* in the Bellingshausen Sea and Amundsen Sea appear to represent a singular, largely disconnected clade (Figure 3A, lineage I). DIYABC analyses most strongly supported scenario 1 where the three geographic regions separated from each other early in their history with a secondary, more recent, diversification in the Weddell Sea. The isolation of the Amundsen and Bellingshausen Seas likely resulted from shifts in the position of the ACC provide a plausible explanation for the genetic differentiation recovered. Antarctic coastal currents likely are a factor in this isolation as they move the opposite direction of the ACC and have been used to explain genetic structure in benthic invertebrates thought to be circumpolar (Riesgo *et al.* 2015).

Overall structure:

The high-resolution 2b-RAD approach was consistent with findings from COI while providing greater genetic resolution. Although 2b-RAD data were more geographically and numerically limited relative to COI, both recovered strong connections between the Ross Sea and Western Peninsula, a distance of over 5,000 km, bypassing the Bellingshausen and Amundsen Seas. This connection is likely the result of transport from the Ross gyre into the ACC, which does not contact the Antarctic shelf again until the western portion of the Antarctic Peninsula (Tynan 1998). As seen in other taxa (e.g., *P. kerguelensis*, Wilson *et al.* 2007; *D. Kerguelensis*

Wilson *et al.* 2013*, O. validus*, Janosik *et al.* 2010; *N. austral*, Mahon *et al.* 2008), the northern tip of the Antarctic Peninsula, especially the Bransfield Strait, is an area of high genetic diversity. SMARTPCA analyses of SNP data provide additional support that the Bransfield Strait is a genetically diverse and likely an intermixing site for *O. victoriae* populations.

Probable causes for this diversity may be mixing of distinct water masses, including water from the ACC, and thus populations in the region (Gill 1973; Smith *et al.* 1999), repeated formation and disintegration of refugia during glaciation events (Clarke & Crame 1992) or other processes that promote mixing of populations. Although the ACC serves as a vector for eastward distribution, westward counter currents closer to the shelf and several large Antarctic gyres (including in the Weddell and Ross Seas) may further distribute, or isolate, populations (Thatje 2012). For example, the Weddell gyre moves clockwise and spills into the Bransfield Straits mixing with warmer waters (García *et al.* 2002; Kaiser *et al.* 2011). Such a situation supports our findings for isolation of the WA/BS population. Bransfield Strait consists of several water masses differing in oxygen and salinity (Gordon *et al.* 2001) compared to those on the western Antarctic Peninsula, along with being hypothesized as an area of refugium during glaciation events (Jażdżewska 2011). The separation of water masses and support for historic refugium both provide an explanation for genetic distinctiveness of the WA/BS population and R/WP population. Mitochondrial data suggest that the eastern Weddell Sea might share more similarities with the Ross Sea and western Peninsula lineage than with the western Weddell Sea. Both types of data recovered a geographically structured distribution for *O. victoriae*. Whereas some lineages have very broad distributions and may be circumpolar, others are more restricted.

Comparing mtDNA to 2b-RAD:

Our study afforded the opportunity to compare traditional mtDNA markers to a whole genome SNP-based approach such as 2b-RAD. Other studies have recognized the ability of RAD data to recover structure that traditional markers have overlooked (Wagner *et al.* 2013; Reitzel *et al.* 2013). Although general phylogeographic structure of large scale SO regions was able to be ascertained through mtDNA, identification of 4 distinct populations and existence of population WB would have gone unrecognized if higher resolution 2b-RAD analyses had not been employed. Population WB comprised 16 specimens whose haplotypes were within COI lineage I, with an additional 4 individuals from lineage II, which could have resulted from incomplete lineage sorting as mtDNA is uniparentally inherited. The 2b-RAD data were able to reveal this higher resolution structure through fewer samples from a smaller geographic range. Further 2b-RAD data in the sub-Antarctic islands and the eastern Weddell Sea would provide greater insight into connectivity of organisms in the SO ecosystem with the Ross and Weddell Seas being of particular interest. As marine systems are often considered to have few barriers, these high-resolution approaches provide us with better tools to answer ecological questions. With climate change prone to reshape current community structure in the SO ecosystem, large high-resolution phylogeographic studies can help to serve as a benchmark or snapshot prior to any further restructuring.

Acknowledgements:

Laurie Stevison provided valuable insight with SMARTPCA analyses, and Peter Beerli was most helpful with trying to troubleshoot Migrate-n. Support from the National Science Foundation (NSF ANT-1043670 to ARM, NSF ANT-1043745 & OPP-0132032 to KMH) and the British Antarctic Survey (BAS) for the funding to collect the specimens and perform the research is

gratefully acknowledged. This research was made possible with assistance from the Captains and crews of NBP12-10, LMG13-12, LMG04-14, LMG06-05, PS77, JR144, JR179 & JR230. We thank Eli Meyer for data pipelines and guidance for processing the 2b-RAD data. We also thank Pamela Brannock for data assistance. This is Molette Biology Laboratory contribution 57 and Auburn University Marine Biology Program contribution 150.

Data Accessibility: All sequences collected here in are reported under GenBank Accession numbers KY048203-KY048268. Raw reads for 2b-RAD SNP data are deposited to SRA SAMN05944630-SAMN5944718. Data matrices and alignments are deposited in Dryad under accession doi:10.5061/dryad.0k1r0.

References:

Aronson RB, Thatje S, Clarke A *et al.* (2007) Climate Change and Invasibility of the Antarctic Benthos. *Annual Review of Ecology Evolution and Systematics*, **38**, 129–154.

Bathmann UV, Scharek R, Klaas C, Dubischarr CD, Smetacek V (1997) Spring development of phytoplankton biomass and composition in mejor water masses of the Atlantic sector of the Southern Ocean. *Deep Sea Research II*, **44**, 51–67.

Beaumont M a., Zhang W, Balding DJ (2002) Approximate Bayesian computation in population genetics. *Genetics*, **162**, 2025–2035.

Benestan L, Gosselin T, Perrier C *et al.* (2015) RAD genotyping reveals fine-scale genetic structuring and provides powerful population assignment in a widely distributed marine species, the American lobster (*Homarus americanus*). *Molecular Ecology*, **24**, 3299–3315.

Catchen JM, Amores A, Hohenlohe P, Cresko W, Postlethwait JH (2011) Stacks: building and genotyping Loci de novo from short-read sequences. *G3: Genes, Genomes, Genetics*, **1**, 171–82.

Clarke A, Crame JA (1992) The Southern Ocean benthic fauna and climate change: A historical perspective. *Philosophical Transactions of the Royal Society B: Biological Sciences*, **339**, 299–309.

Clement M, Posada D, Crandall K a (2000) TCS: a computer program to estimate gene genealogies. *Molecular Ecology*, **9**, 1657–9.

Cornuet JM, Pudlo P, Veyssier J *et al.* (2014) DIYABC v2.0: a software to make approximate Bayesian computation inferences about population history using single nucleotide polymorphism, DNA sequence and microsatellite data. *Bioinformatics*, **30**, 1187–1189.

Craft JD, Russ AD, Yamamoto MN *et al.* (2008) Islands under islands: The phylogeography and evolution of Halocaridina rubra Holthuis, 1963 (Crustacean: Decapoda: Atyidae) in the Hawaiian archipelago. *Limnology and Oceanography*, **53**, 675–689.

Dayton PK, Mordida BJ, Bacon F (1994) Polar marine communities. *Integrative and Comparative Biology*, **34**, 90–99.

Deagle BE, Faux C, Kawaguchi S, Meyer B, Jarman SN (2015) Antarctic krill population genomics: apparent panmixia, but genome complexity and large population size muddy the water. *Molecular Ecology*, **24**, 4943–4959.

Dietz L, Pieper S, Seefeldt M a., Leese F (2015) Morphological and genetic data clarify the taxonomic status of *Colossendeis robusta* and *C. glacialis* (Pycnogonida) and reveal overlooked diversity. *Arthropod Systematics & Phylogeny*, **73**, 107–128.

Earl DA, VonHoldt BM (2012) STRUCTURE HARVESTER: A website and program for visualizing STRUCTURE output and implementing the Evanno method. *Conservation Genetics Resources*, **4**, 359–361.

Excoffier L, Laval G, Schneider S (2005) Arlequin (version 3.0): an integrated software package for population genetics data analysis. *Evolutionary Bioinformatics Online*, **1**, 47–50.

Fell HB (1961) The fauna of the Ross Sea: Ophiuroidea. *New Zealand Department of Scientific and Industrial Research*, **18**, 1–79.

Foll M, Gaggiotti O (2008) A genome-scan method to identify selected loci appropriate for both dominant and codominant markers: A Bayesian perspective. *Genetics*, **180**, 977–993.

Folmer O, Black M, Hoeh W, Lutz R, Vrijenhoek R (1994) DNA primers for amplification of mitochondrial cytochrome c oxidase subunit I from diverse metazoan invertebrates.

Molecular Marine Biology and Biotechnology, **3**, 294–299.

Fratt D, Dearborn J (1984) Feeding biology of the Antarctic brittle star *Ophionotus victoriae* (Echinodermata: Ophiuroidea). *Polar Biology*, **3**, 127–139.

García MA, Castro CG, Ríos AF *et al.* (2002) Water masses and distribution of physico-chemical properties in the Western Bransfield Strait and Gerlache Strait during Austral summer 1995/96. *Deep-Sea Research Part II: Topical Studies in Oceanography*, **49**, 585–602.

Gill AE (1973) Circulation and bottom water production in the Weddell Sea. *Deep Sea Research and Oceanographic Abstracts*, **20**, 111–140.

Gordon AL, Visbeck M, Huber B (2001) Export of Weddell Sea deep and bottom water. *Journal of Geophysical Research*, **106**, 9005.

Held C, Wägele J-W (2005) Cryptic speciation in the giant Antarctic isopod *Glyptonotus antarcticus* (Isopoda: Valvifera: Chaetiliidae). *Scientia Marina*, **69**, 175–181.

Hemery LG, Eléaume M, Roussel V *et al.* (2012) Comprehensive sampling reveals circumpolarity and sympatry in seven mitochondrial lineages of the Southern Ocean crinoid species *Promachocrinus kerguelensis* (Echinodermata). *Molecular Ecology*, **21**, 2502–2518.

Hinegardner R (1974) Cellular DNA content of the Echinodermata. *Comparative Biochemistry and Physiology.*, **49B**, 219–226.

Hofmann EE, Murphy EJ (2004) Advection, krill, and Antarctic marine ecosystems. *Antarctic Science*, **16**, 487–499.

Hunter RL, Halanych KM (2008) Evaluating connectivity in the brooding brittle star *Astrotoma agassizii* across the drake passage in the Southern Ocean. *The Journal of Heredity*, **99**, 137–

48.

Hunter RL, Halanych KM (2010) Phylogeography of the Antarctic planktotrophic brittle star *Ophionotus victoriae* reveals genetic structure inconsistent with early life history. *Marine Biology*, **157**, 1693–1704.

Jakobsson M, Rosenberg N a. (2007) CLUMPP: A cluster matching and permutation program for dealing with label switching and multimodality in analysis of population structure. *Bioinformatics*, **23**, 1801–1806.

Janosik AM, Mahon AR, Halanych KM (2010) Evolutionary history of Southern Ocean *Odontaster* sea star species (Odontasteridae; Asteroidea). *Polar Biology*, **34**, 575–586.

Jażdżewska A (2011) Soft bottom sublittoral amphipod fauna of Admiralty Bay, King George Island, Antarctic. *Oceanological and Hydrobiological Studies*, **40**, 1–10.

Kaiser S, Brandão SN, Brix S *et al.* (2013) Patterns, processes and vulnerability of Southern Ocean benthos: a decadal leap in knowledge and understanding. *Marine Biology*, **160**, 2295–2317.

Kaiser S, Griffiths HJ, Barnes DK a. *et al.* (2011) Is there a distinct continental slope fauna in the Antarctic? *Deep Sea Research Part II: Topical Studies in Oceanography*, **58**, 91–104.

Krabbe K, Leese F, Mayer C, Tollrian R, Held C (2010) Cryptic mitochondrial lineages in the widespread pycnogonid *Colossendeis megalonyx* Hoek, 1881 from Antarctic and Subantarctic waters. *Polar Biology*, **33**, 281–292.

Leese F, Kop A, Wägele J-W, Held C (2008) Cryptic speciation in a benthic isopod from Patagonian and Falkland Island waters and the impact of glaciations on its population structure. *Frontiers in Zoology*, **5**, 19.

Leigh JW, Bryant D (2015) POPART: Full-Feature Software for Haplotype Network Construction. *Methods in Ecology and Evolution*, **6**, 1110–1116.

Mahon AR, Arango CP, Halanych KM (2008) Genetic diversity of Nymphon (Arthropoda: Pycnogonida: Nymphonidae) along the Antarctic Peninsula with a focus on Nymphon australe Hodgson 1902. *Marine Biology*, **155**, 315–323.

Mahon AR, Thornhill DJ, Norenburg JL, Halanych KM (2009) DNA uncovers Antarctic nemertean biodiversity and exposes a decades-old cold case of asymmetric inventory. *Polar Biology*, **33**, 193–202.

Martín-Ledo R, López-González PJ (2014) Brittle stars from Southern Ocean (Echinodermata: Ophiuroidea). *Polar Biology*, **37**, 73–88.

Massom R a., Stammerjohn SE (2010) Antarctic sea ice change and variability - Physical and ecological implications. *Polar Science*, **4**, 149–186.

McKnight D (1967) Echinoderms from Cape Hallett, Ross Sea. *New Zealand Journal of Marine and Freshwater Research*, **1**, 314–323.

Palumbi SR (2007) Nucleic Acids II: The Polymerase Chain Reaction. In: *Molecular Systematics, Second Edition* (eds Hillis DM, Moritz C, Mable BK), pp. 205–245. Sinauer Associates, Inc, Sunderland, Massachusetts U.S.A.

Patterson N, Price AL, Reich D (2006) Population structure and eigenanalysis. *PLoS Genetics*, **2**, 2074–2093.

Pearse JS, McClintock JB, Bosch I (1991) Reproduction of Antarctic Benthic Marine Invertebrates: Tempos, Modes, and Timing. *American Zoologist*, **31**, 65–80.

Price a. L, Patterson NJ, Plenge RM *et al.* (2006) Principal components analysis corrects for

stratification in genome-wide association studies. *Nature Genetics*, **38**, 904–909.

Pritchard JK, Stephens M, Donnelly P (2000) Inference of population structure using multilocus genotype data. *Genetics*, **155**, 945–59.

Pritchard JK, Wen X, Falush D (2010) Documentation for structure software : Version 2 . 3.

Reitzel AM, Herrera S, Layden MJ, Martindale MQ, Shank TM (2013) Going where traditional markers have not gone before: utility of and promise for RAD sequencing in marine invertebrate phylogeography and population genomics. *Molecular Ecology*, **22**, 2953–2970.

Riesgo A, Taboada S, Avila C (2015) Evolutionary patterns in Antarctic marine invertebrates: An update on molecular studies. *Marine Genomics*, **23**, 1–13.

Rosenberg N a. (2004) DISTRUCT: A program for the graphical display of population structure. *Molecular Ecology Notes*, **4**, 137–138.

Rousset F (2008) GENEPOP'007: A complete re-implementation of the GENEPOP software for Windows and Linux. *Molecular Ecology Resources*, **8**, 103–106.

Sands CJ, Griffiths HJ, Downey R V. *et al.* (2012) Observations of the ophiuroids from the West Antarctic sector of the Southern Ocean. *Antarctic Science*, **25**, 3–10.

Sands CJ, O'Hara T, Barnes DK, Martín-Ledo R (2015) Against the flow: evidence of multiple recent invasions of warmer continental shelf waters by a Southern Ocean brittle star. *Frontiers in Ecology and Evolution*, **3**.

Sieg J, Waegele J (1990) *Fauna of Antarctica*. Blackwell verlag GmbH, Berlin, West Germany.

Slatkin M (1995) A measure of population subdivision based on microsatellite allele frequencies. *Genetics*, **462**, 457–462.

Smetacek V, De Baar HJW, Bathmann U V., Lochte K, Rutgers Van Der Loeff MM (1997) Ecology and biogeochemistry of the Antarctic Circumpolar Current during austral spring: A summary of Southern Ocean JGOFS cruise ANT X/6 of R.V. Polarstern. *Deep-Sea Research Part II: Topical Studies in Oceanography*, **44**, 1–21.

Smith DA, Hofmann EE, Klinck JM, Lascara CM (1999) Hydrography and circulation of the West Antarctic Peninsula Continental Shelf. *Deep-Sea Research Part I: Oceanographic Research Papers*, **46**, 925–949.

Tamura K, Stecher G, Peterson D, Filipski A, Kumar S (2013) MEGA6: Molecular evolutionary genetics analysis version 6.0. *Molecular Biology and Evolution*, **30**, 2725–2729.

Templeton a R, Crandall K a, Sing CF (1992) A cladistic analysis of phenotypic associations with haplotypes inferred from restriction endonuclease mapping and DNA sequence data. III. Cladogram estimation. *Genetics*, **132**, 619–33.

Thatje S (2012) Effects of Capability for Dispersal on the Evolution of Diversity in Antarctic Benthos. *Integrative and Comparative Biology*, **52**, 470–482.

Thatje S, Hillenbrand C-D, Larter R (2005) On the origin of Antarctic marine benthic community structure. *Trends in Ecology and Evolution*, **20**, 534–40.

Thornhill DJ, Mahon AR, Norenburg JL, Halanych KM (2008) Open-ocean barriers to dispersal: a test case with the Antarctic Polar Front and the ribbon worm Parborlasia corrugatus (Nemertea: Lineidae). *Molecular Ecology*, **17**, 5104–17.

Tynan CT (1998) Ecological importance of the Southern Boundary of the Antarctic Circumpolar Current. *Nature*, **392**, 708–710.

Wagner CE, Keller I, Wittwer S *et al.* (2013) Genome-wide RAD sequence data provide

unprecedented resolution of species boundaries and relationships in the Lake Victoria cichlid adaptive radiation. *Molecular Ecology*, **22**, 787–98.

Wang S, Meyer E, McKay JK, Matz M V (2012) 2b-RAD: a simple and flexible method for genome-wide genotyping. *Nature Methods*, **9**, 808–10.

Wilson NG, Hunter RL, Lockhart SJ, Halanych KM (2007) Multiple lineages and absence of panmixia in the "circumpolar" crinoid Promachocrinus kerguelensis from the Atlantic sector of Antarctica. *Marine Biology*, **152**, 895–904.

Wilson NG, Maschek JA, Baker BJ (2013) A species flock driven by predation? Secondary metabolites support diversification of slugs in Antarctica. *PLoS ONE*, **8**, 1–8.

Wilson NG, Schrödl M, Halanych KM (2009) Ocean barriers and glaciation: evidence for explosive radiation of mitochondrial lineages in the Antarctic sea slug *Doris kerguelenensis* (Mollusca, Nudibranchia). *Molecular Ecology*, **18**, 965–984.

Table 1. Standard nucleotide indices from mtDNA. Tajima's *D* was found to be not significant in all analyses.

	COI	16S	COI &16S
Number of Samples	414	251	251
Nucleotide diversity	0.0179446	0.00394178	0.00989389
Segregating sites	67	22	73
Parsimony-informative sites	45	14	51
Tajima's *D*	-0.38834, P > 0.10	-1.23336, P > 0.10	-0.411972, P > 0.10

Table 2. Analysis of molecular variance statistics for *O. victoriae* based on COI data.

Source of variation	d.f.	Sum of squares	σ^2	Percentage of variation
Among groups	4	13832.777	30.561	37.87802
Among populations within groups	6	2666.908	17.744	21.99185
Within populations	403	13048.374	32.378	40.13013
Total	413	29548.06	80.638	

Table 3. Filtering steps for 2b_RAD SNP data.

Filter	Samples	SNP Loci
All samples and SNP loci	96	16,588
Remove loci with <80% coverage	96	1,999
Remove samples with < 80% SNP loci	89	1,999

Table 4. 2b-RAD Pairwise F_{ST} values. Significance value ($P < 0.05$).

Region	(R/WP)	(B)	(WA/BS)	(WB)
Ross/ Western Peninsula (R/WP)	-			
Bellingshausen (B)	0.12921	-		
Weddell/Bransfield Strait (WA/BS)	0.09789	0.10985	-	
Weddell (WB)	0.12676	0.13214	0.08039	-

Figure 1. A) Aboral view of *O. victoriae.* B) Oral view of *O. victoriae.* C) Yo-Yo camera image of SO benthic ecosystem consisting of many ophiuroid species including the dominant *Ophionotus victoriae.* This image was taken at a depth of 313 m, near Andersson Island at the south end of Antarctic Sound (-63°40'42.0"S 56°14'18.0"W). Photos A & B kindly provided by Dr. Christoph Held.

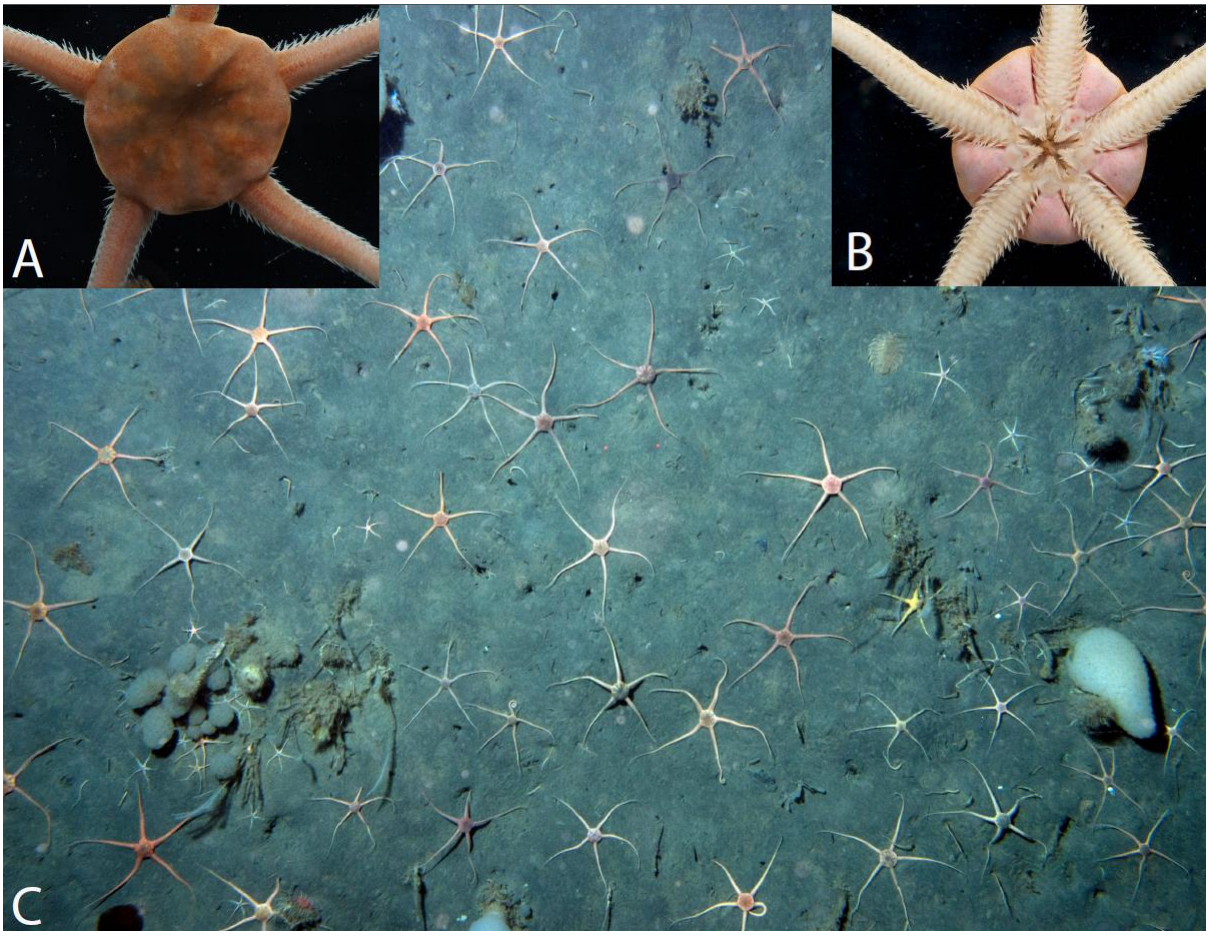

Figure 2. Distribution of *Ophionotus victoriae*. Green dots represent sampling localities with 2b-RAD and mtDNA data while orange dots represent localities where solely mtDNA was utilized. Due to the proximity of some localities, overlap on the map could not be avoided. Sampling localities in the Antarctic Peninsula inset that appear to be on land represent locations now open to the sea since the Larsen Ice Shelf broke away.

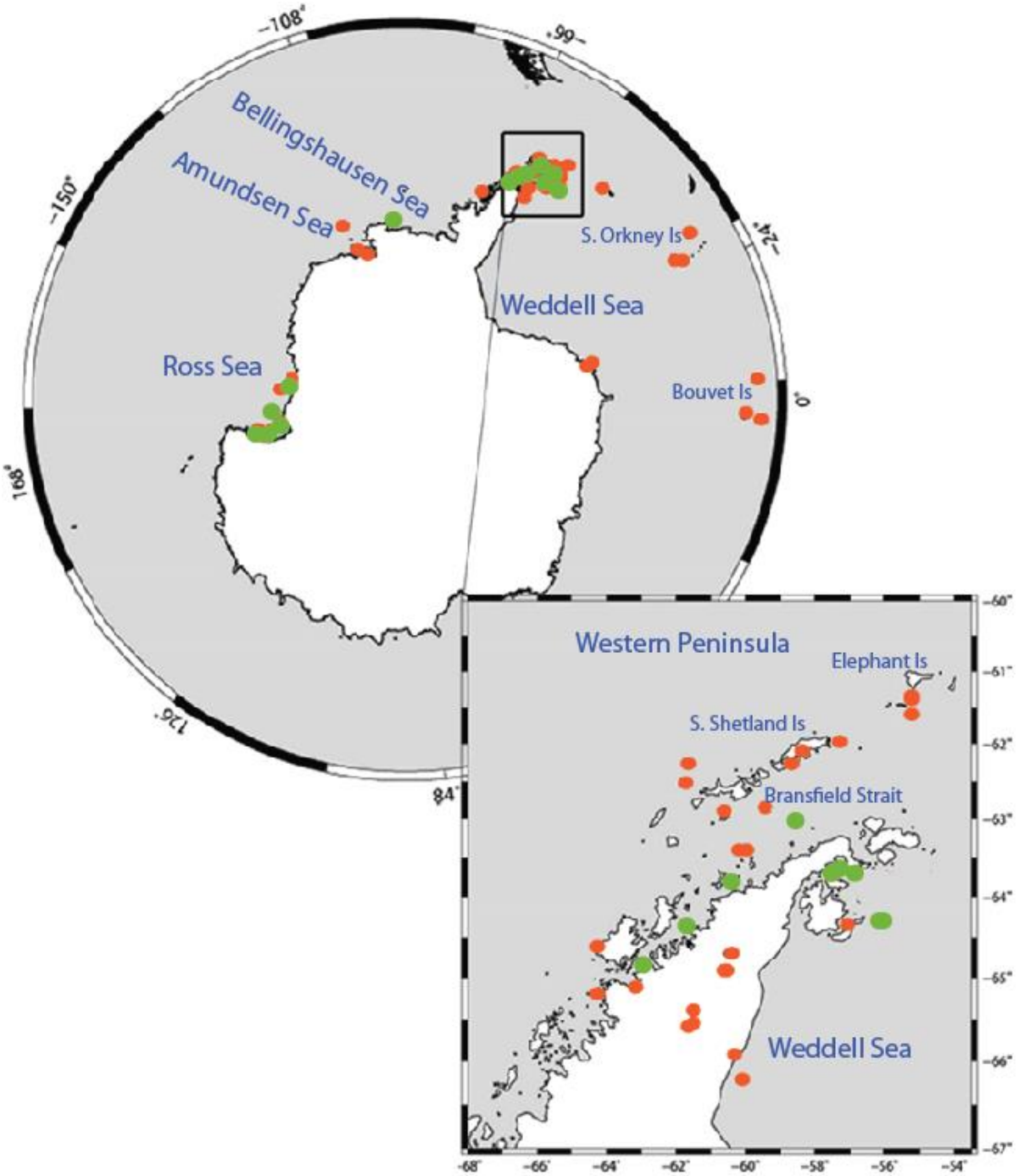

Figure 3. A) Haplotype network of *Ophionotus victoriae* produced by PopART (Leigh & Bryant 2015). The haplotype network is based off COI data from a TCS1.21 (Clement *et al.* 2000) analyses of 414 samples. Filled black dots represent missing haplotypes. In addition, maximum likelihood analyses also revealed three clades. B) Histogram of COI uncorrected pairwise distances (*p*).

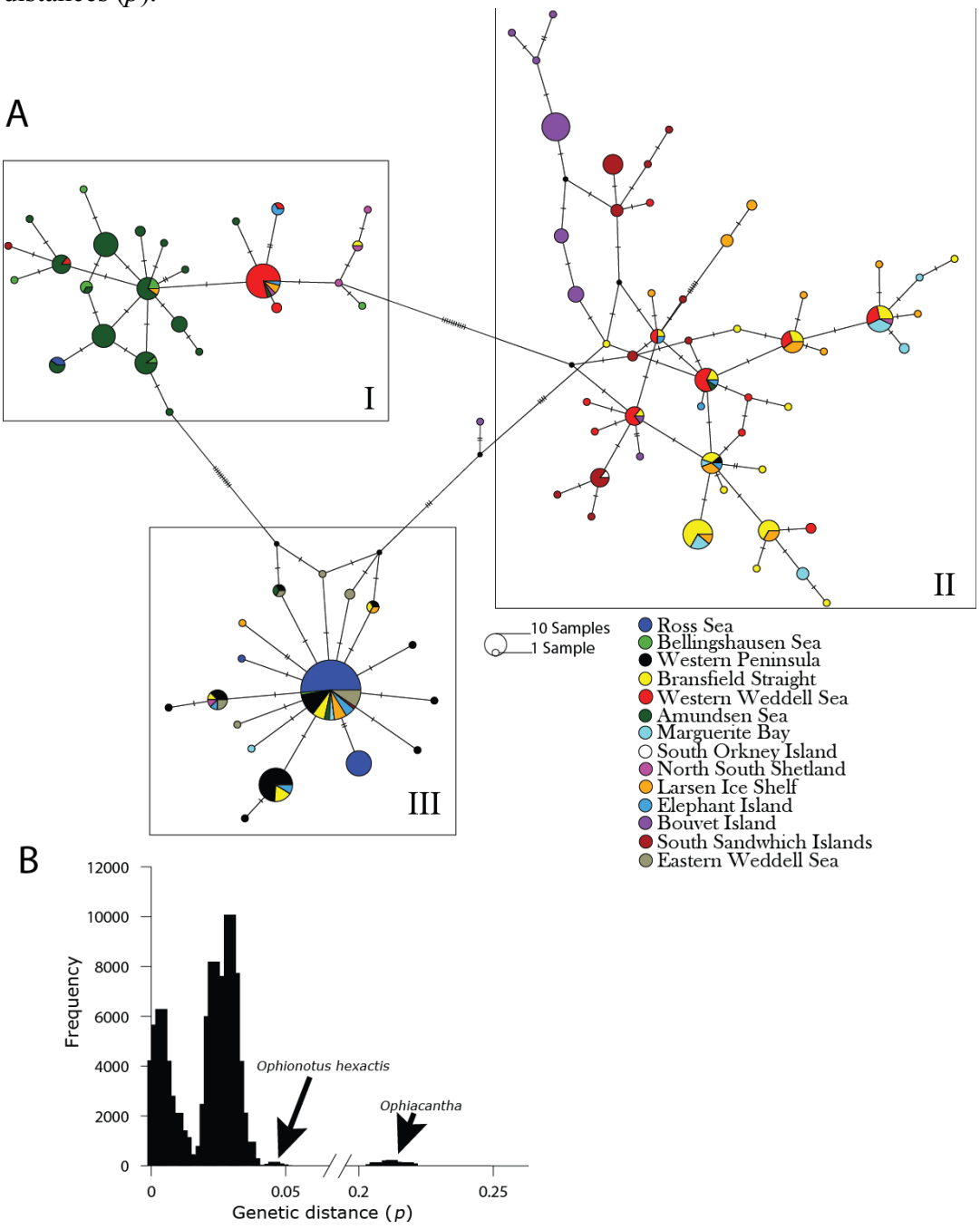

Figure 4. Patterns of population structure for *Ophionotus victoriae* based on SNP data analyzed in STRUCTURE 2.3.4. (Pritchard et al. 2000) and visualized in DISTRUCT (Rosenberg 2004) testing for the true number of populations (*K*). *K*=4 is presented in the graph above as our most likely accurate *K*.

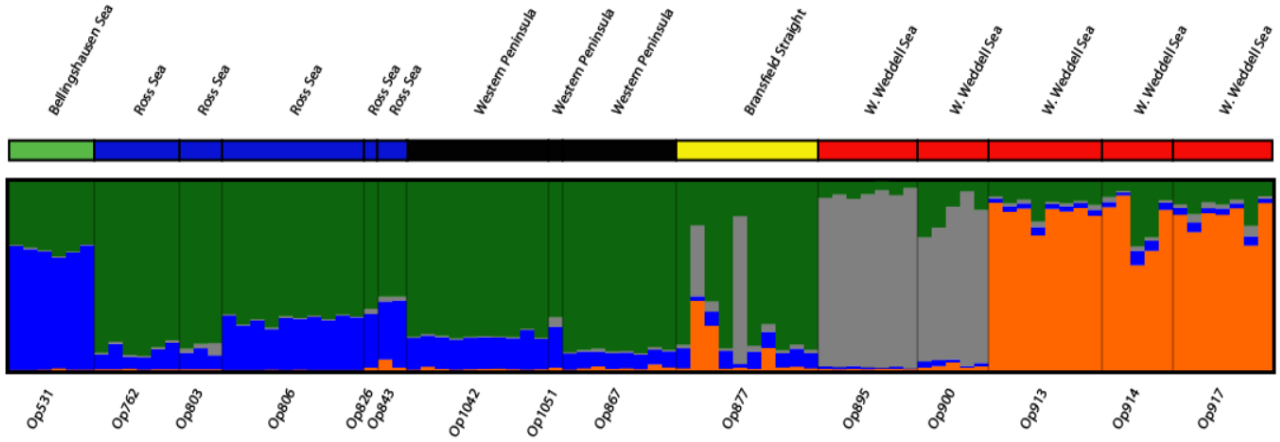

Figure 5. PCA results based on SNP data for samples labeled by the STRUCTURE's *K*=4 genetic populations. Weddell A Bransfield population samples that intermix with the Ross Sea/western Peninsula population were all from the sampling locality in the Bransfield Strait.

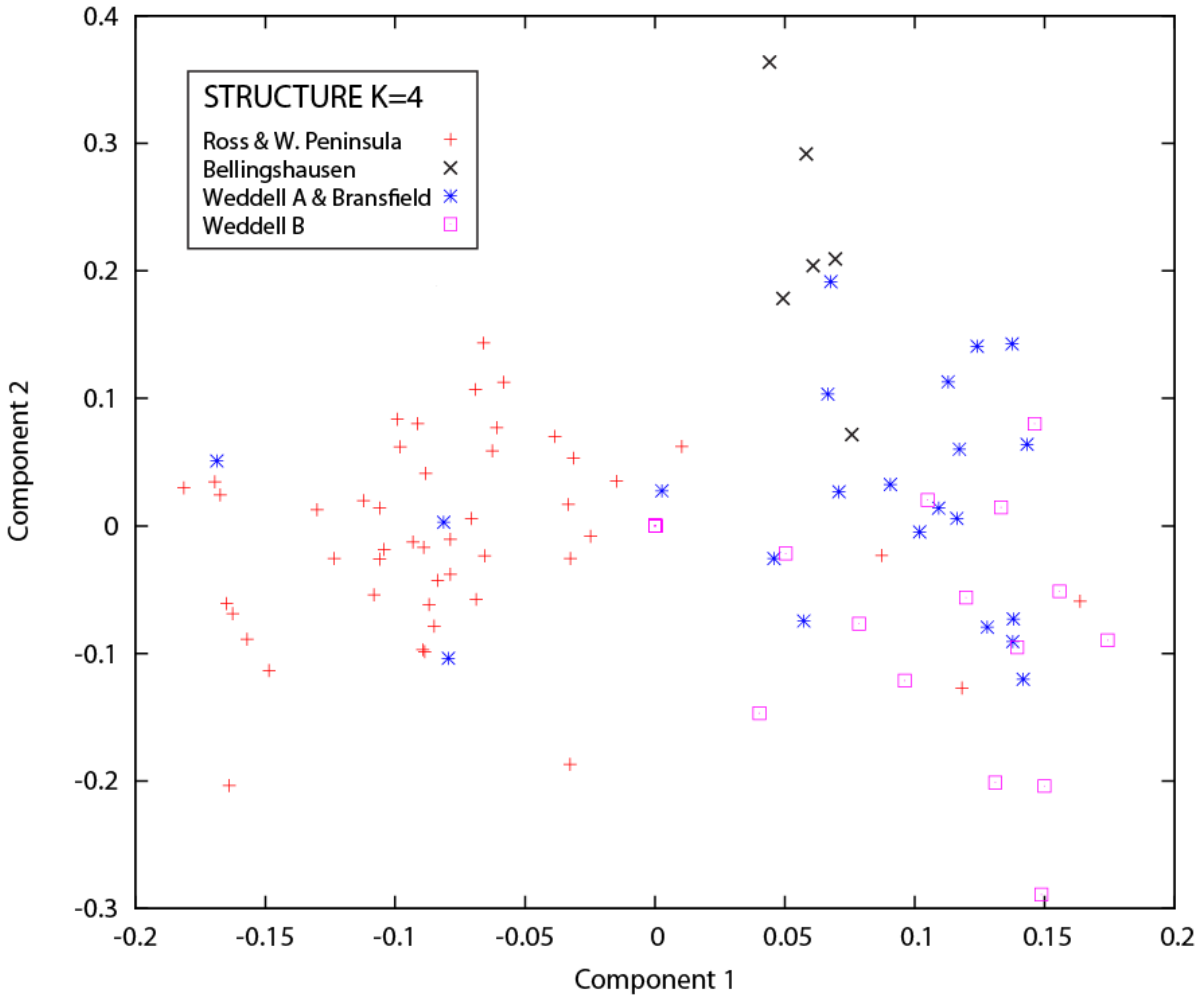

Figure 6. Highest supported scenarios using Bayesian computation (ABC). In these scenarios t# represents time in generations and is based off the four genetic populations identified by STRUCTURE. All three geographic regions split at approximately the same time with a more recent diversification in the Weddell Sea.

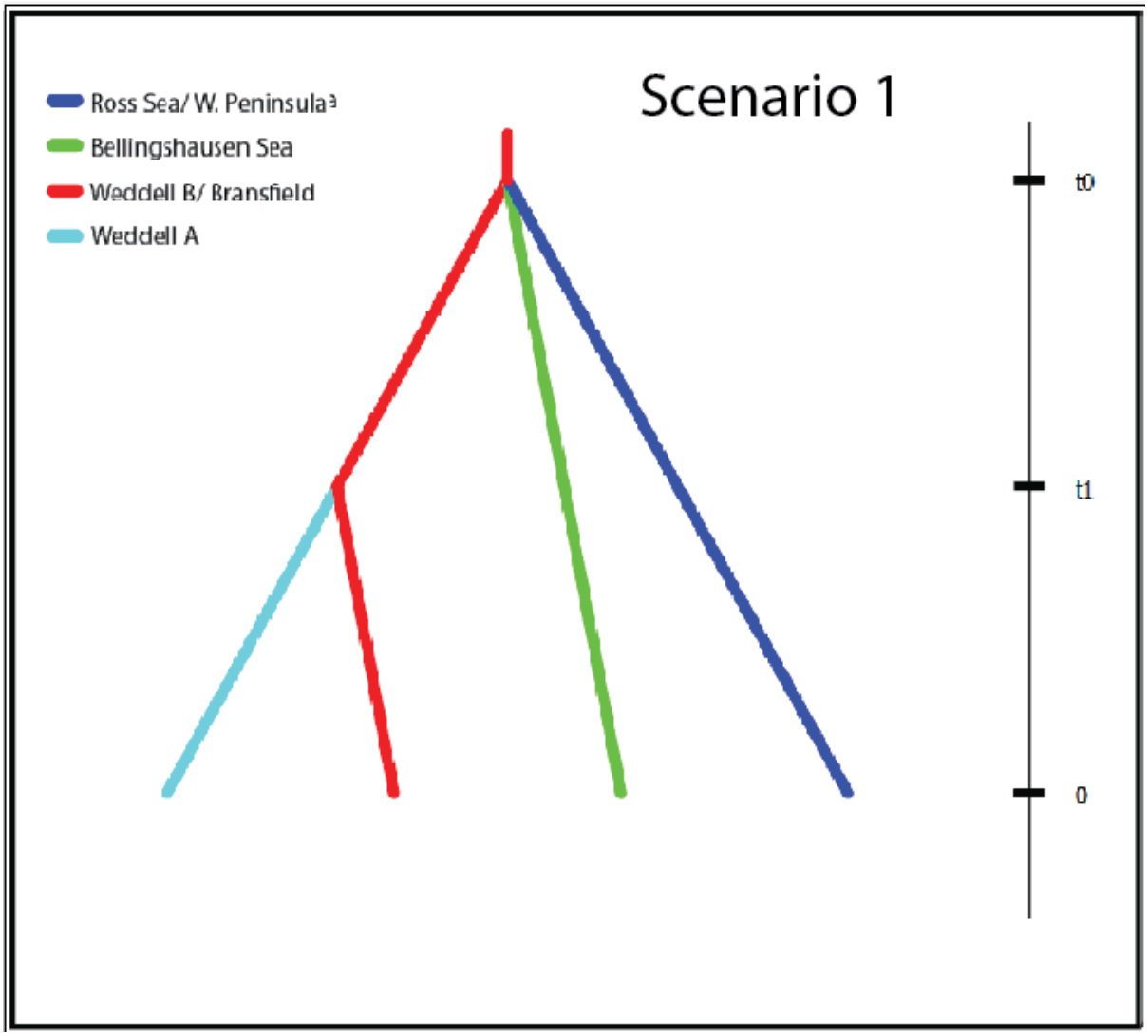

Chapter 3. Crossing the divide: Admixture across the Antarctic Polar Front revealed by the brittle star *Astrotoma agassizii*.

Abstract:

The Antarctic Polar Front (APF) is one of the most well-defined and persistent oceanographic features on the planet and serves as a barrier to dispersal between the Southern Ocean and lower latitudes. High levels of endemism in the Southern Ocean have been attributed to this barrier, whereas the accompanying Antarctic Circumpolar Current (ACC) likely promotes west-to-east dispersal. Previous phylogeographic work on the brittle star *Astrotoma agassizii* based on mitochondrial genes suggested isolation across the APF, even though populations in both South American waters and the Southern Ocean are morphologically indistinguishable. Here, we revisit this finding using a high-resolution 2b-RAD Single Nucleotide Polymorphism (SNP) based approach, in addition to enlarged mitochondrial DNA data sets (16S rDNA, COI, and COII) for comparison to previous work. In total, 955 bi-allelic SNP loci confirmed the existence of strongly divergent populations on either side of Drake Passage. Interestingly, genetic admixture was detected between South America and the Southern Ocean in five individuals on both sides of the APF, revealing evidence of recent or ongoing genetic contact. We also identified two differentiated populations on the Patagonian shelf with six admixed individuals from these two populations. These findings suggest the APF is a strong but imperfect barrier. Fluctuations in location and strength of the APF and ACC due to climate shifts may have profound consequences for levels of admixture or endemism in this region of the world.

Introduction:

Although marine systems are often thought of as "open" to dispersal, strong oceanic barriers can exist, isolating populations over time that may lead to speciation (Clarke *et al.*, 2005; Thornhill *et al.*, 2008; Figuerola *et al.*, 2017). One of the strongest open ocean barriers in the world is the Antarctic Polar Front (APF), which isolates the Southern Ocean from warmer waters at lower latitudes and thus contributes to the high endemism found in the Southern Ocean (Thornhill *et al.*, 2008; Kaiser *et al.*, 2013). However, the APF co-occurs with the Antarctic Circumpolar Current (ACC), which functions as a oceanographic dispersal mechanism for many species in and around the Southern Ocean (Bathmann *et al.*, 1997; Smetacek *et al.*, 1997). Megafauna such as whales, fur seals and marine birds freely move across the APF (Rasmussen *et al.*, 2007), but, in contrast, endemism is particularly high among several marine invertebrate groups inhabiting continental shelves on either side of the APF despite having long-lived life stages capable of dispersal (Ekman, 1953; Hempel, 1985; Arntz WE, Brey T, 1997; Thatje, 2012). For example, molecular studies analyzing genetic connectivity across the APF revealed distinct genetic breaks on either side of the APF in nemertean worms (Thornhill *et al.*, 2008), octocorals (Dueñas *et al.*, 2016), and notothenioid fish (Bargelloni *et al.*, 2000). Although one study suggested migration occurs across the APF in molluscs based on taxonomy (Jörger *et al.*, 2014), supporting molecular data are absent and these animals occurred at abyssal, not shelf, depths. Another group where species are reported to occur on both side of the ACC and APF are the Ophiuroidea, a dominant component of Southern Ocean benthic fauna (Stöhr *et al.*, 2012). For example, molecular work within the brittle star species, *Ophiura lymani*, identified successful radiations out of the Southern Ocean into South America, albeit only during the

Pleistocene (Sands *et al.*, 2015). Presently, genetic connectivity has not been recognized across the APF among extant ophiuroids.

In contrast to the APF, the ACC is often attributed to be a large scale dispersal vector (Nikula *et al.*, 2010), moving clockwise around Antarctica and coming into contact with the southernmost region of South America. Pelagic larvae, such as lecithotrophic larvae produced by the brittle star *Astrotoma agassizii*, have been recovered from the Ross Sea with mitochondrial haplotypes matching those from the Antarctic Peninsula, presumably via dispersal by the ACC (Heimeier *et al.*, 2010). Additionally, the isopod species *Septemserolis septemcarinata,* which has no pelagic stages, can apparently disperse over 2,000 km likely through rafting on kelp mediated by the ACC (Leese *et al.*, 2010). Thus, if a species life history incorporates a planktonic dispersal phase, migration to the Patagonian Self of South America, some ~700 km from the Antarctic Shelf, is possible given the Coriolis effect and Eckmann transport. However, such dispersals events across the APF would require that a species withstand substantial temperature and salinity changes. Previous trans-Drake Passage work on *A. agassizii* using mitochondrial DNA (mtDNA) identified a single clade on the shelf regions of the Southern Ocean and two clades on the South American shelf, with no evidence for genetic connectivity across the APF (Hunter and Halanych, 2008). However, geographic sampling in the Southern Ocean has previously been limited primarily to the Antarctic Peninsula and genetic analyses relied solely on mtDNA, which are uniparentally inherited and not suitable for exploring potential admixture. Morphologically designated as a single species on either side of the Drake Passage, *A. agassizii* is considered a brooder in its geographic ranges of South America but has recently been revealed to possess planktonic lecithotrophic larvae in the Southern Ocean

(Heimeier *et al.*, 2010). Whether these reproductive strategies are unique to either region is unknown, but this difference could imply that *A. agassizii* is comprised of different species.

Here, we address the question of genetic connectivity in the brittle star *A. agassizii*, which has a broad geographic distribution (Fig. 2), by examining populations from both the Western Antarctic and South American continental shelves. Specifically, we sampled a broader geographic range as well as s greater number of individuals than Hunter and Halanych (2008) using both mtDNA and higher-resolution genomic single nucleotide polymorphism (SNP) markers with the 2b-RAD (Wang *et al.*, 2012) approach. A larger geographic range was included in this study for the Southern Ocean to facilitate investigation of spatial genetic structure within *A. agassizii's* Southern Ocean circumpolar distribution. Similar 2b-RAD work on the circumpolar ophiuroid, *Ophionotus victoriae*, revealed four distinct populations that were geographically structured and may represent multiple species (Galaska *et al.*, 2017). This was contrary to the prediction of an intermixed range due to dispersal capabilities of *O. victoriae*'s feeding planktotrophic larvae. In this study, two hypotheses were tested: 1) Southern Ocean and South American lineages of *A. agassizii* are genetically isolated, representing distinct ecological and evolutionary units and, 2) significant genetic structure by geography would be recovered in the Southern Ocean, analogous to what was recently identified in *O. victoriae*.

Methods:

Taxon Sampling:

Individuals of *A. agassizii* were collected during four National Science Foundation (NSF)-sponsored research expeditions (i.e., *RVIB Nathaniel B. Palmer 12-10*, *RV Laurence M. Gould 04-14, 06-05, 13-12*), the *Polarstern* expedition PS77, and four British Antarctic Survey (BAS)-sponsored expeditions (i.e., JR144, JR179, JR230 and JR275). In total, the data set

included 231 individuals collected from the Ross Sea to the Weddell Sea in the Southern Ocean and the Patagonian Shelf off the southeastern coast of SA (Fig. 2, Appendix Table 1 view online).

Sample Preparation and Sequencing:

Genomic DNA was extracted using Qiagen's DNeasy® Blood and Tissue kit following the manufacturer's protocol, and fragments from three mtDNA genes (i.e., cytochrome *c* oxidase subunits I (*COI*) and II (*COII*) and the large ribosomal subunit - *16S-rDNA*) were amplified *via* the polymerase chain reaction (PCR). Samples provided by, and analyzed at the BAS, comprised of 45 individuals amplified for an ~660 bp fragment of *COI* with the primers LCO1490 (5′-GGTCAACAAATCATAAAGATATTG G- 3′) and HCO2198 (5′-TAAACTTCAGGGTGACCAAAAAATCA- 3′) (Folmer *et al.*, 1994) under the following cycling conditions: initial denaturation at 94°C for 3 min; 40 cycles of denaturation at 94°C for 30 s; annealing at 51°C for 1 min; extension at 72°C for 1 min; and final extension at 72°C for 2 min. An additional 186 individuals were amplified and sequenced for fragments of the *COII* and *16S-rDNA* mtDNA genes from samples obtained by the Halanych Lab at Auburn University to allow comparison to the work done by Hunter & Halanych (2008). The *COII* primer set CO2_23AF (5'-MCARCTWGGWTTWCAAGA-3') and CO2_577R (5'-TCSGARCATTGSCCATARAA-3') (Hunter and Halanych, 2008) were utilized to amplify an ~550bp fragment from the same 186 individuals amplified for *16S-rDNA* (see below; Appendix Table 1 view online). Cycling conditions utilized for *COII* were: initial denaturation at 94°C for 3 min; 35 cycles of denaturation at 94°C for 30 s; annealing at 50°C for 30 s; extension at 72°C for 30 s; and final extension at 72°C for 3 minutes. An ~500bp fragment of *16S-rDNA* was amplified using the primers 16SarL (5′-CGCCTGTTTATCAAAAACAT-3′) and 16SbrH (5′-

CCGGTCTGAACTCAGATCACGT-3′) (Palumbi, 2007) under cycling conditions of: initial denaturation at 94°C for 3 min; 35 cycles of denaturation at 94°C for 30 s; annealing at 46°C for 30 s; extension at 72°C for 30 s; and final extension at 72°C for 3 minutes. Amplicons from *COII* and *16S-rDNA* were sent to Genewiz, Inc. (South Plainfield, New Jersey) for bidirectional Sanger sequencing.

Population genetic analyses:

Assembly and editing of bidirectional Sanger sequences were done with Sequencher® 5.4 (Gene Codes, Ann Arbor, MI) and MEGA 6 (Tamura *et al.*, 2013) used to perform alignments *via* MUSCLE (Edgar, 2004) for each mtDNA gene. Network analyses using TCS were done with POPART v1.7 (Clement *et al.*, 2000; Leigh and Bryant, 2015) to visualize relationships between mtDNA haplotypes of *A. agassizii* recovered from *COI*, *COII* and *16S-rDNA* separately, along with a concatenation of *16S-rDNA* and *COII* for all individuals from the Halanych lab that were sequenced for both (Fig. 3). DnaSP v5.10.01 (Librado and Rozas, 2009) was used to perform tests of neutrality, including Tajima's *D* (Tajima, 1989) and Fu and Li's F_s (Fu and Li, 1993), along with standard nucleotide indices from each of the three mtDNA fragments. Uncorrected pairwise (*p*-) distances amongst the *COI*, *COII* and *16S-rDNA* fragments were generated separately in PAUP* v4.0b10 (Swofford, 2003).

RAD-based SNP data collection:

From the 231 individuals included in this study, a subset of 94 individuals were randomly selected for whole genome SNP-based analyses following Wang's *et al.* (2012) 2b-RAD protocol. These 94 individuals represented localities from the entire geographic range where both *COII* and *16S-rDNA* were also sampled. The 2b-RAD protocol utilized RNAse-treated genomic DNA that was cut with the restriction enzyme *Alf*I, which leaves a 2-bp sticky end on both sides

of the cleaved DNA. A 1/16th reduction scheme was employed through the addition of site-specific ligation adaptors, specifically NG/NG that paired with their complementary 2-bp sticky ends. Samples were then dual barcoded and sent for sequencing at the HudsonAlpha Institute for Biotechnology Genome Services Laboratory (Huntsville, Alabama) on an Illumina Hi-Seq 2500 using v4 chemistry, generating 50bp single-end reads.

Raw Illumina reads were demultiplexed by sample, quality-filtered and aligned against a custom derived reference built *de novo* from our sequences as outlined in Wang et al.'s (2012), using scripts from Meyer (2017), and Stacks v1.35 *denovo_map.pl* (Catchen *et al.*, 2011). The 2b-RAD data were first filtered by loci to exclude samples with coverage of less than 25X. Homozygous SNP loci were then defined to have a maximum variance of 1%, whereas those considered heterozygous had a minimum variance of 25%. Any loci that did not meet these criteria were excluded from further analyses. Lastly, only loci occurring in ≥75% of individuals within a sampling locality were retained.

Multiple analyses were conducted on SNP data set to determine genetic diversity and structure within and between geographic populations and genetic lineages of *A. agassizii*. Initially, SNP data were analyzed using Discriminant Analysis of Principal Components (DAPC) from the adegenet v1.4-2 package (Jombart, 2008; Jombart *et al.*, 2010; Jombart and Ahmed, 2011) in the R v3.3.2 statistical environment (R Core Team, 2016). Specifically, adegenet initially conducts a series of Principal Component Analysis (PCA) on SNP data that is then retained to perform a Discriminant Analysis on all PCAs (DAPC). Performing multiple PCAs allows for identification of genetic clusters while avoiding assumptions of population genetic models (Jombart *et al.*, 2010). The retention of multiple PCA analyses can then be analyzed by DAPC for group variability while avoiding within group variation (Jombart *et al.*, 2010).

Optimal clusters (*K*), likely representing discrete populations, were identified through Bayesian information criterion (BIC) likelihood values from retained principle components (Appendix Fig. 1). Visualization of the DAPC analyses was performed with adegenet in R.

In addition, the Landscape and Ecological Associations (LEA) v1.0 package in R was used to perform population structure inference and admixture coefficient analyses (Frichot and François, 2015). Estimation of *K* in LEA is performed using the cross-entropy criterion (Appendix Fig. 2) and least-squares estimates were used to calculate ancestry proportions (Frichot *et al.*, 2014). Admixture was then visualized in two ways: 1) as bar charts, similar to that from STRUCTURE (see below), and 2) as pie charts, with the inclusion of geographic coordinates, to visualize admixture at each locality, which were overlain onto an orthographic projection map of Antarctica and the Patagonian Shelf with the R package ggplot2 v2.2.1 (Wickham, 2009).

Further analyses of SNP data were performed using STRUCTURE v2.3.4 (Pritchard *et al.*, 2000) under the following parameters: 1) 5 replicates at each potential *K* (1-18); 2) an admixture model with correlated allele frequencies; 3) a 100,000 generation burn-in period, and; 4) 100,000 additional Markov chain Monte Carlo (MCMC) generations. These analyses were run on Southern Ocean and South American populations together as well as for each region separately. Files containing each simulation were then processed with STRUCTURE HARVESTER v0.6.94 to objectively select a value for *K* based on a Delta *K* analyses (Earl and VonHoldt, 2012). The selected *K* for each analysis was visualized using CLUMPP v1.1.2 (Jakobsson and Rosenberg, 2007) as well as DISTRUCT v1.1 (Rosenberg, 2004).

Lastly, summary statistics for SNP data along with analyses of genetic differentiation were performed in the R package HIERFSTAT v0.04-22 (Goudet, 2005). Initially, SNP data was

analyzed assuming a single population to recover summary statistics. However, once discrete populations were identified from the DAPC, LEA and STRUCTURE analyses, additional summary statistics were performed on each. Pairwise F_{ST} differences were calculated in GenoDive v2.0b27 (Meirmans and Van Tienderen, 2004) to test for significance between the Southern Ocean and South American lineages.

Results:

mtDNA:

Sequence data for mtDNA *COII* and *16S-rDNA* were analyzed both separately and concatenated for 186 individuals (Data Set A), with an additional 45 individuals analyzed solely for *COI* (Data Set B), and all three mtDNA fragments revealed genetic structure between the Southern Ocean and South America. The TCS-based haplotype network of *A. agassizii* inferred from *COII* and *16S-rDNA* identified one clade in the Southern Ocean (Clade I) and two distinct clades in South America (i.e., Clades II and III) (Fig. 3a). Although the two South American clades are presented as a single network to show the relationship between them, they separate into distinct networks if a 95% connection limit is applied (data not shown). Notably, an individual with both *COII* and *16S-rDNA* haplotypes thought to be unique to South America was recovered on the Antarctic Peninsula in the Southern Ocean. Histograms of uncorrected *p*-distance values (Fig. 3) revealed two distinct modes in the *COII* and *16S-rDNA* concatenated data set, representing within (0.2%-1.0%) and between (3.8%-6.2%) clade genetic distances. Similar network results were recovered from 45 individuals analyzed for only *COI*, although inferences made from the *COI* data set are limited due to fewer samples. Two similar modes for *COI* uncorrected *p*-distances were recovered for within (0.2%-0.8%) and between (5.8%-7.0%) clades.

Tests of neutrality were found to be not significant for either Tajima's *D* or Fu and Li's F_s for any of the three mtDNA fragments when data sets included all samples, which could be the result of differentiation between populations. Thus, additional tests of neutrality were performed individually on clades identified from network analyses (Fig. 3) for the *COII* fragment since it consisted of the same number of individuals as *16S-rDNA* but possessed higher nucleotide diversity. In this case, Tajima's *D* and Fu and Li's F_s were found to be statistically significant ($P < 0.05$) and negative for Clade I, with values of -2.217 and -3.89, respectively. Tests of neutrality in Clade II were all found to be non-significant while Clade III was found to have a statistically significant and negative value for Fu and Li's F_s (-2.751, $P < 0.05$). Thus, these negatively significant tests of neutrality within Clades I and III suggest either recent population expansions or purifying selection operating on *COII*, which are fairly typical results from mitochondrial data (Wares, 2010). Amplified fragments of *COI*, *COII* and *16S-rDNA* recovered 76, 74 and 30 segregating sites, respectively, and summary nucleotide indices by fragment are presented in Table 1.

2b-RAD:

Quality-filtering of SNP loci yielded a data set of 955 polymorphic SNP loci among 94 individuals from the *COII* and *16S-rDNA* data set, with 33 and 61 from South America and the Southern Ocean sampling localities, respectively (including the individual from the Southern Ocean that was recovered with a SA mtDNA haplotype). For the entire data set, the highest supported *K* for both DAPC and LEA was *K*=5 (Appendix Fig. 1 & 2), with two *K*s each in South America and the Southern Ocean and a fifth *K* comprised of 5 individuals from the two geographic regions (*i.e.,* 4 South American and 1 from the Southern Ocean, Figures 2 & 4).

Similar patterns were obtained when each region was analyzed individually (data not shown). As STRUCTURE has hierarchal model assumptions that are not always met (Jombart *et al.*, 2010; Kalinowski, 2011), the results, though similar, are presented in Appendix Figures 3, 4 & 5 for comparison. Although estimates for the number of discrete populations, as represented by *K*, were consistent between analyses, the true value likely resides somewhere within the range of 2-5. Hereafter, the discussion of results assumes $K = 5$ given the above. Genetic distances between populations as defined by mitochondrial clade are presented in Table 2 and revealed significant ($P < 0.001$) differentiation between the three (i.e., SOI, SAII and SAIII). Summary estimates of genetic diversity recovered from the entire SNP data matrix are presented in Table 3. Fixed differences between clusters identified by DAPC are presented in Table 4. Analyses of the Southern Ocean and South American data as a whole also yielded significant results ($F_{ST} = 0.721$, $P < 0.001$), supporting our first hypothesis that the two regions are genetically isolated. However, the second hypothesis of geographic structure in the Southern Ocean were found to be not significant ($F_{ST} = 0.002$, $P = 0.72$) from DAPC and LEA analyses.

Admixture:

Notably, five individuals were identified apparently resulting from admixture, or genetic mixing, between populations in South America and the Southern Ocean, including one individual from the Southern Ocean possessing a South American mtDNA haplotype. These admixed individuals were recovered in the above analyses (in Figures 2, maroon bars, & in Figure 4, cluster number 3) and identified as such under all values of $K \geq 2$ (Appendix Fig. 3, 5, & 6). Admixture was also recovered from 6 individuals between the two South American populations (Figure 2B, bars with pink and yellow). These individuals were also distinguishable when SNP calls were manually scanned as loci that were fixed in either South America or Southern Ocean

populations were heterozygous in admixed individuals (note admixed individuals may be F_2, F_3 or later generations and thus not all admixed loci are heterozygous). Additionally, no unique alleles were detected in these, apparently admixed, individuals.

Discussion:

Admixture across the APF:

Using a suite of 955 polymorphic SNP loci for *Astrotoma agassizii*, we found evidence of admixture across the Drake Passage that separates the South American and Southern Ocean regions (Figure 2B). Nonetheless, the South American and Southern Ocean lineages previously identified by Hunter and Halanych (2008) are confirmed to be strongly divergent populations ($F_{ST} = 0.721$, $P < 0.001$). Whereas analyses presented here and by others (Hunter and Halanych, 2008; Leese *et al.*, 2008; Thornhill *et al.*, 2008) do reveal significant genetic differentiation between populations in South America and the Southern Ocean, SNP data allowed identification of admixed individuals implying recent, or even current, gene flow occurring bi-directionally across the strong barrier imposed by the APF. Moreover, we support earlier findings (e.g., Hunter and Halanych 2008) of two clades in South America with SNP-based analyses ($F_{ST} = 0.363$, $P < 0.001$), with admixture between them revealed in 6 individuals (Figure 2B). For the Southern Ocean, SNP data also imply some geographic structure, particularly in the Ross Sea. Notably, the variable genetic structure of *A. agassizii* across the Southern Ocean contrasts with that of *O. victoriae*, which possesses population structure reflecting specific geographic regions (Galaska *et al.*, 2017). In comparison, although both *A. agassizii* and *O. victoriae* in the Southern Ocean have been previously reported to have circumpolar distributions and employ broadcast spawning with planktonic larval life history stages, *A. agassizii* appears to have higher dispersal capabilities relative to *O. victoriae*.

Asymmetric migration:

With the unexpected findings of admixture across the APF, important questions arise, including just how permeable the APF is to dispersal of benthic invertebrates. Of course, the rate at which gene flow occurs is likely taxa-dependent and our limited sampling serves as just a coarse estimate at best. Even under these limitations, notable patterns are apparent. For instance, 12.1% of South American individuals sampled for 2b-RAD were apparently admixed between the two regions compared to 1.6% from the Southern Ocean. The fact that admixed individuals had a higher frequency in South America suggests that, in *A. agassizii*, migration is more probable from the Southern Ocean to South America. In recent evolutionary history, dispersal from the Southern Ocean to South America has also been identified in the ophiuroid species *Ophiura lymani* (Sands *et al.*, 2015). Alternatively, survivorship of admixed individuals could be more favorable in South America. With many benthic invertebrates in the Southern Ocean possessing reproductive strategies involving a pelagic larval stage (Stanwell-Smith *et al.*, 1999), coupled with the dispersal potential of the ACC, the use of fine-scale population genetic techniques are likely to uncover a higher number of taxa having trans-APF connectivity.

Data presented here imply *A. agassizii* individuals (most likely larvae) have an ability to migrate long distances (i.e., >900 km) as well as overcome the 3-4ºC temperature cline at the APF between the Southern Ocean and South America. Genetic connectivity by teleplanic larvae is plausible through transport by mesoscale eddies generated by the ACC (Joyce *et al.*, 1981; Johnson and Bryden, 1989; Clarke *et al.*, 2005). Although such connectivity may occur in both northerly and southerly directions, given that the Antarctic Peninsula experiencing unprecedentedly rapid warming due to climate change, higher temperature waters have been suggested to mitigate migration of cold temperature-limited species (Aronson *et al.*, 2007, 2009;

Clarke *et al.*, 2007). Additionally, warming temperatures along the Antarctic Peninsula could increase survivability of individuals from northern latitudes onto the Antarctic Continental Shelf (Meredith and King, 2005). Given this, one possible driver for the higher rate of admixture found in South America is that the temperature and salinity in more northerly latitudes may be increasingly favorable to *A. agassizii's* reproduction, which are implicated as important cues in other echinoderms (Lamare and Stewart, 1998). Migration of species or populations from South America could have played a crucial role in the Antarctic Shelf undergoing recolonization following the post-glacial maximum (Aronson *et al.*, 2007; Thatje, 2012).

Given that the Southern Ocean population of *A. agassizii* appears to be primarily reproducing via lecithotrophic larvae, and the South American population is described as brooding, recovering five individuals resulting from apparent admixture between them is surprising. Although we have conservatively considered the two regions to be distinctly diverged populations due to large genetic differentiation between the Southern Ocean and South America ($F_{ST} = 0.721$, $P < 0.001$), we recognize that *A. agassizii* may represent multiple species. This conclusion is supported by apparent reproductive differences and large genetic differences, with almost a third of the SNP loci fixed between regions (Table 4.). However, morphological support for separate species is lacking.

Due to the Southern Ocean *A. agassizii* possessing a pelagic larval stage, detection of more admixture on the Patagonian shelf, although by limited sampling, would support the idea that migration from Southern Ocean to South America is more common than the converse. However, explaining the introgression of the individual with the South American haplotype sampled from Antarctica is more difficult. For other animals, passive transport by rafting on substrate such as soft coral or macroalgae has been suggested (Leese *et al.*, 2010; Thatje, 2012)

and documented (Helmuth *et al.*, 1994) in benthic invertebrates around the Southern Ocean. If South American *A. agassizii* do have a planktonic lecithotrophic larval stage, transport into the Southern Ocean *via* currents or mesoscale eddies may be possible. With the apparent higher rate of admixture found on the Patagonian Shelf of South America, this area and the western Chilean side of southern South America are an area of high interest for future research. If a first-generation migrant is going to be recovered from the Southern Ocean in South America, we hypothesize that the Chilean side of South America would be an ideal location to sample as it is where the Humboldt Current breaks north from the ACC and comes into contact with the South American continent (White and Peterson, 1996). With the warming climate in the Southern Ocean, specifically around the Antarctic Peninsula (Meredith and King, 2005), the APF's ability to serve as an absolute barrier for many species could account for genetic isolation, but additional assessment of trans-APF species with high resolution molecular techniques will likely yield more cases of connectivity.

Acknowledgements:

We would like to thank the support received from the National Science Foundation (NSF ANT-1043670 to ARM, NSF ANT- 1043745 & OPP- 0132032 to KMH) and the British Antarctic Survey (BAS) for the funding to collect the specimens and perform the research. This research was made possible with assistance from the Captains and crews of NBP12- 10, LMG13- 12, LMG04- 14, LMG06- 05, PS77, JR144, JR179, and JR230. We would also like to thank Dr. Stephen Sefick for useful suggestions with ggplot2 in R. This is Molette Biology Laboratory contribution XX and Auburn University Marine Biology Program contribution XXX.

Data Accessibility:

All sequences collected herein are reported under GenBank accession numbers KY986584-KY986640 (Appendix Table 2 view online). Raw reads for 2b-RAD SNP data are deposited to SRA XXXX-XXXX. Data matrices and alignments are deposited in Dryad under accession doi: XXXX.

References:

Arntz WE, Brey T, G. V. 1997. *Antarctic marine biodiversity: an overview. In: Antarctic Communities: Species, Structure and Survival* (W. D. Battagkua B, Valencia J, ed). Cambridge University Press, Cambridge, UK.

Aronson, R. B., R. M. Moody, L. C. Ivany, D. B. Blake, J. E. Werner and A. Glass. **2009**. Climate Change and Trophic Response of the Antarctic Bottom Fauna. *PLoS One* **4**: 6. Public Library of Science.

Aronson, R. B., S. Thatje, A. Clarke, L. S. Peck, D. B. Blake, C. D. Wilga and B. A. Seibel. **2007**. Climate Change and Invasibility of the Antarctic Benthos. *Annu. Rev. Ecol. Evol. Syst.* **38**: 129–154. Annual Reviews.

Bargelloni, L., S. Marcato, L. Zane and T. Patarnello. **2000**. Mitochondrial phylogeny of notothenioids: a molecular approach to Antarctic fish evolution and biogeography. *Syst. Biol.* **49**: 114–129.

Bathmann, U. V., R. Scharek, C. Klaas, C. D. Dubischarr and V. Smetacek. **1997**. Spring development of phytoplankton biomass and composition in mejor water masses of the Atlantic sector of the Southern Ocean. *Deep Sea Res. II* **44**: 51–67.

Catchen, J. M., A. Amores, P. Hohenlohe, W. Cresko and J. H. Postlethwait. **2011**. Stacks: building and genotyping Loci de novo from short-read sequences. *G3 Genes, Genomes, Genet.* **1**: 171–82.

Clarke, A., D. K. A. Barnes and D. A. Hodgson. **2005**. How isolated is Antarctica? *Trends Ecol. Evol.* **20**: 1–3.

Clarke, A., N. M. Johnston, E. J. Murphy and a. D. Rogers. **2007**. Introduction. Antarctic ecology from genes to ecosystems: the impact of climate change and the importance of scale. *Philos. Trans. R. Soc. B Biol. Sci.* **362**: 5–9.

Clement, M., D. Posada and K. a Crandall. **2000**. TCS: a computer program to estimate gene genealogies. *Mol. Ecol.* **9**: 1657–9.

Dueñas, L. F., D. M. Tracey, A. J. Crawford, T. Wilke, P. Alderslade and J. A. Sánchez. **2016**. The Antarctic Circumpolar Current as a diversification trigger for deep-sea octocorals. *BMC Evol. Biol.* **16**: 2. BMC Evolutionary Biology.

Earl, D. A. and B. M. VonHoldt. **2012**. STRUCTURE HARVESTER: A website and program for visualizing STRUCTURE output and implementing the Evanno method. *Conserv. Genet. Resour.* **4**: 359–361.

Edgar, R. C. 2004. MUSCLE: Multiple sequence alignment with high accuracy and high throughput. *Nucleic Acids Res.* **32**: 1792–1797.

Ekman, S. 1953. *Zoogeography of the Sea*. Sidgwick and Jackson, London.

Figuerola, B., D. K. A. Barnes, P. Brickle and P. E. Brewin. **2017**. Bryozoan diversity around the Falkland and South Georgia Islands: Overcoming Antarctic barriers. *Mar. Environ. Res.* **126**: 81–94. Elsevier Ltd.

Folmer, O., M. Black, W. Hoeh, R. Lutz and R. Vrijenhoek. **1994**. DNA primers for amplification of mitochondrial cytochrome c oxidase subunit I from diverse metazoan

invertebrates. *Mol. Mar. Biol. Biotechnol.* **3**: 294–299.

Frichot, E. and O. François. **2015**. LEA: An R package for landscape and ecological association studies. *Methods Ecol. Evol.* **6**: 925–929.

Frichot, E., F. Mathieu, T. Trouillon, G. Bouchard and O. François. **2014**. Fast and efficient estimation of individual ancestry coefficients. *Genetics* **196**: 973–983.

Fu, Y. X. and W. H. Li. **1993**. Statistical tests of neutrality of mutations. *Genetics* **133**: 693–709.

Galaska, M. P., C. J. Sands, S. R. Santos, A. R. Mahon and K. M. Halanych. **2017**. Geographic structure in the Southern Ocean circumpolar brittle star Ophionotus victoriae (Ophiuridae) revealed from mtDNA and single-nucleotide polymorphism data. *Ecol. Evol.* **7**: 1–11.

Goudet, J. 2005. HIERFSTAT, a package for R to compute and test hierarchical F-statistics. *Mol. Ecol. Notes* **5**: 184–186.

Heimeier, D., S. Lavery and M. Sewell. **2010**. Molecular species identification of *Astrotoma agassizii* from planktonic embryos: further evidence for a cryptic species complex. *J. Hered.* **101**: 775–779.

Helmuth, B., R. R. Veit and R. Holberton. **1994**. Long-distance dispersal of a Sub-Antarctic brooding bivalve (*Gaimardia trapesina*) by kelp-rafting. *Mar. Biol.* **120**: 421–426.

Hempel, G. 1985. *On the biology of polar seas, particulary the Southern Ocean*, Marine bio (J. Gray and M. Christiansen, eds). Wiley, Chichester.

Hunter, R. L. and K. M. Halanych. **2008**. Evaluating connectivity in the brooding brittle star *Astrotoma agassizii* across the drake passage in the Southern Ocean. *J. Hered.* **99**: 137–48.

Jakobsson, M. and N. a. Rosenberg. **2007**. CLUMPP: A cluster matching and permutation program for dealing with label switching and multimodality in analysis of population structure. *Bioinformatics* **23**: 1801–1806.

Johnson, G. C. and H. L. Bryden. **1989**. On the size of the Antarctic Circumpolar Current. *Deep Sea Res.* **36**: 39–53.

Jombart, T. 2008. adegenet: a R package for the multivariate analysis of genetic markers. *Bioinformatics* **24**: 1403–1405.

Jombart, T. and I. Ahmed. **2011**. adegenet 1.3-1: New tools for the analysis of genome-wide SNP data. *Bioinformatics* **27**: 3070–3071.

Jombart, T., S. Devillard and F. Balloux. **2010**. Discriminant analysis of principal components: a new method for the analysis of genetically structured populations. *BMC Genet.* **11**: 1–15.

Jörger, K. M., M. Schrödl, E. Schwabe and L. Würzberg. **2014**. A glimpse into the deep of the Antarctic Polar Front - Diversity and abundance of abyssal molluscs. *Deep. Res. Part II Top. Stud. Oceanogr.* **108**: 93–100. Elsevier.

Joyce, T. M., S. L. Patterson and R. C. Millard. **1981**. Anatomy of a cyclonic ring in the drake passage. *Deep Sea Res. Part A, Oceanogr. Res. Pap.* **28**: 1265–1287.

Kaiser, S., S. N. Brandão, S. Brix, D. K. a. Barnes, D. a. Bowden, J. Ingels, F. Leese, S.

Schiaparelli, C. P. Arango, R. Badhe, *et al.* 2013. Patterns, processes and vulnerability of Southern Ocean benthos: a decadal leap in knowledge and understanding. *Mar. Biol.* **160**: 2295–2317.

Kalinowski, S. T. 2011. The computer program STRUCTURE does not reliably identify the main genetic clusters within species: simulations and implications for human population structure. *Heredity (Edinb).* **106**: 625–32. Nature Publishing Group.

Lamare, M. D. and B. G. Stewart. **1998**. Mass spawning by the sea urchin Evechinus chloroticus (Echinodermata: Echinoidea) in a New Zealand fiord. *Mar. Biol.* **132**: 135–140.

Leese, F., S. Agrawal and C. Held. **2010**. Long-distance island hopping without dispersal stages: transportation across major zoogeographic barriers in a Southern Ocean isopod. *Naturwissenschaften* **97**: 583–94.

Leese, F., A. Kop, J.-W. Wägele and C. Held. **2008**. Cryptic speciation in a benthic isopod from Patagonian and Falkland Island waters and the impact of glaciations on its population structure. *Front. Zool.* **5**: 19.

Leigh, J. W. and D. Bryant. **2015**. POPART: Full-Feature Software for Haplotype Network Construction. *Methods Ecol. Evol.* **6**: 1110–1116.

Librado, P. and J. Rozas. **2009**. DnaSP v5: a software for comprehensive analysis of DNA polymorphism data. *Bioinformatics* **25**: 1451–2.

Meirmans, P. G. and P. H. Van Tienderen. **2004**. GENOTYPE and GENODIVE: Two programs for the analysis of genetic diversity of asexual organisms. *Mol. Ecol. Notes* **4**: 792–794.

Meredith, M. P. and J. C. King. **2005**. Rapid climate change in the ocean west of the Antarctic Peninsula during the second half of the 20th century. *Geophys. Res. Lett.* **32**: 1–5.

Meyer, E. 2017. The Meyer Lab: Bioinformatic scripts. Oregon State University, Corvallis, OR. [Online]. Available: https://github.com/Eli-Meyer [2016, Dec. 20].

Nikula, R., C. I. Fraser, H. G. Spencer and J. M. Waters. **2010**. Circumpolar dispersal by rafting in two subantarctic kelp-dwelling crustaceans. *Mar. Ecol. Prog. Ser.* **405**: 221–230.

Palumbi, S. R. 2007. Nucleic Acids II: The Polymerase Chain Reaction. In: *Molecular Systematics, Second Edition* (D. M. Hillis et al., eds), pp. 205–245. Sinauer Associates, Inc, Sunderland, Massachusetts U.S.A.

Pritchard, J. K., M. Stephens and P. Donnelly. **2000**. Inference of population structure using multilocus genotype data. *Genetics* **155**: 945–59.

R Core Team. **2016**. R: A Language and Environment for Statistical Computing. R Foundation for Statistical Computing, Vienna, Austria.

Rasmussen, K., D. M. Palacios, J. Calambokidis, M. T. Saborío, L. Dalla Rosa, E. R. Secchi, G. H. Steiger, J. M. Allen and G. S. Stone. **2007**. Southern Hemisphere humpback whales wintering off Central America: insights from water temperature into the longest mammalian migration. *Biol. Lett.* **3**: 302 LP-305.

Rosenberg, N. a. 2004. DISTRUCT: A program for the graphical display of population structure. *Mol. Ecol. Notes* **4**: 137–138.

Sands, C. J., T. D. O'Hara, D. K. a. Barnes and R. Martín-Ledo. **2015**. Against the flow:

evidence of multiple recent invasions of warmer continental shelf waters by a Southern Ocean brittle star. *Front. Ecol. Evol.* **3**: 1–13.

Smetacek, V., H. J. W. De Baar, U. V. Bathmann, K. Lochte and M. M. Rutgers Van Der Loeff. **1997**. Ecology and biogeochemistry of the Antarctic Circumpolar Current during austral spring: A summary of Southern Ocean JGOFS cruise ANT X/6 of R.V. Polarstern. *Deep. Res. Part II Top. Stud. Oceanogr.* **44**: 1–21.

Stanwell-Smith, D., L. S. Peck, A. Clarke, A. W. A. Murray and C. D. Todd. **1999**. The distribution, abundance and seasonality of pelagic marine invertebrate larvae in the maritime Antarctic. *Philos. Trans. R. Soc. B Biol. Sci.* **354**: 471–484.

Stöhr, S., T. D. O'Hara and B. Thuy. **2012**. Global diversity of brittle stars (Echinodermata: Ophiuroidea). *PLoS One* **7**: 1–14.

Swofford, D. L. 2003. PAUP*. Phylogenetic Analysis Using Parsimony (*and Other Methods). Version 4.

Tajima, F. 1989. Statistical method for testing the neutral mutation hypothesis by DNA polymorphism. *Genetics* **123**: 585–95.

Tamura, K., G. Stecher, D. Peterson, A. Filipski and S. Kumar. **2013**. MEGA6: Molecular evolutionary genetics analysis version 6.0. *Mol. Biol. Evol.* **30**: 2725–2729.

Thatje, S. 2012. Effects of capability for dispersal on the evolution of diversity in antarctic benthos. *Integr. Comp. Biol.* **52**: 470–482.

Thornhill, D. J., A. R. Mahon, J. L. Norenburg and K. M. Halanych. **2008**. Open-ocean barriers to dispersal: a test case with the Antarctic Polar Front and the ribbon worm *Parborlasia corrugatus* (Nemertea: Lineidae). *Mol. Ecol.* **17**: 5104–17.

Wang, S., E. Meyer, J. K. McKay and M. V Matz. **2012**. 2b-RAD: a simple and flexible method for genome-wide genotyping. *Nat. Methods* **9**: 808–10.

Wares, J. P. 2010. Natural distributions of mitochondrial sequence diversity support new null hypotheses. *Evolution (N. Y).* **64**: 1136–1142.

White, W. B. and R. G. Peterson. **1996**. An Antarctic circumpolar wave in surface pressure, wind, temperature and sea-ice extent. *Nature* **380**: 699–702.

Wickham, H. 2009. *ggplot2: Elegant Graphics for Data Analysis*. Springer-Verlag New York, New York.

Table 1. Nucleotide indices from all three mtDNA fragments. Note that neither Tajima's *D* or Fu and Li's F_s tests of neutrality were found to be significant for any mitochondrial fragments.

	16S-rDNA	COI	COII
Nucleotide diversity	Pi = 0.018	Pi = 0.038	Pi = 0.032
Number of segregating sites	30	76	74
Number of parsimony-informative sites	22	60	53
Tajima's *D* statistic	1.154 ($P > 0.10$)	0.925 ($P > 0.10$)	0.102 ($P > 0.10$)
Fu and Li's F_s	-0.366 ($P > 0.10$)	0.294 ($P > 0.10$)	-1.475 ($P > 0.10$)
Haplotype diversity (Hd)	0.772 (SD +/- 0.001)	0.946 (SD +/- 0.000)	0.937 (SD +/- 0.009)

Table 2. Pairwise F_{ST} genetic distances of the SNP data set between the three mtDNA clades (Roman numerals as in Figure 3) recovered from both Hunter & Halanych (2008) and mtDNA analyses presented here. All F_{ST} values recovered have a $P < 0.001$.

	SO (I)	SA (II)	SA (III)
SO (I)	-		
SA (II)	0.799	-	
SA (III)	0.711	0.363	-

Table 3. Summary statistics of the 955 SNP loci, inferred from the clusters identified by DAPC analyses as well as the complete data set for the following statistics: number of individuals (*n*), observed heterozygosity (*Ho*), mean gene diversity within population (*Hs*), overall gene diversity (*Ht*), gene diversity among samples (*Dst*), corrected gene diversity (*Htp*), global population differentiation (F_{ST}), corrected population differentiation (*Fstp*), and inbreeding coefficient (*Fis*). Numbers in parentheses represent cluster numbers presented in Figure 4.

Region (cluster)	*n*	*Ho*	*He*	*Hs*	*Ht*	*Dst*	*Htp*	*Fst*	*Fstp*	*Fis*
SA (1)	19	0.097	0.093	0.0867	0.094	0.007	0.09	0.07	0.11	-0.13
SA (2)	10	0.106	0.085	0.095	0.096	0.001	0.09	0.01	0.01	-0.12
Admixed (3)	5	0.067	0.056	0.067	0.065	-0.002	0.06	-0.03	-0.04	-0.01
SO (4)	27	0.155	0.158	0.161	0.157	-0.003	0.15	-0.02	-0.02	0.068
SO (5)	33	0.158	0.159	0.160	0.164	0.004	0.16	0.02	0.03	0.02
SA & SO	94	0.136	0.373	0.122	0.372	0.250	0.43	0.67	0.72	0.02

Table 4. Number of fixed SNP loci between the five clusters inferred from DAPC analyses. Loci had to be 100% fixed for opposite alleles within the two compared populations to be counted. Final row is the number of loci coded for both alleles within a population. Numbers in parentheses represent cluster numbers presented in Figure 4.

	SA (1)	SA (2)	SO (4)	SO (5)
SA (1)	-			
SA (2)	1	-		
SA (4)	287	292	-	
SO (5)	295	300	0	-
Heterozygous	233	217	452	425

Figure 1. (a) Aboral view of *Astrotoma agassizii*. (b) Oral view of *A. agassizii*. (c) Yo-Yo camera photo of the Southern Ocean benthic ecosystem where *A. agassizii* is the dominant species. Image was taken at a depth of 390 m in the Ross Sea at 74°10.9186S, 166°39.6616E. Photographs (a) and (b) kindly provided by Dr. Christoph Held.

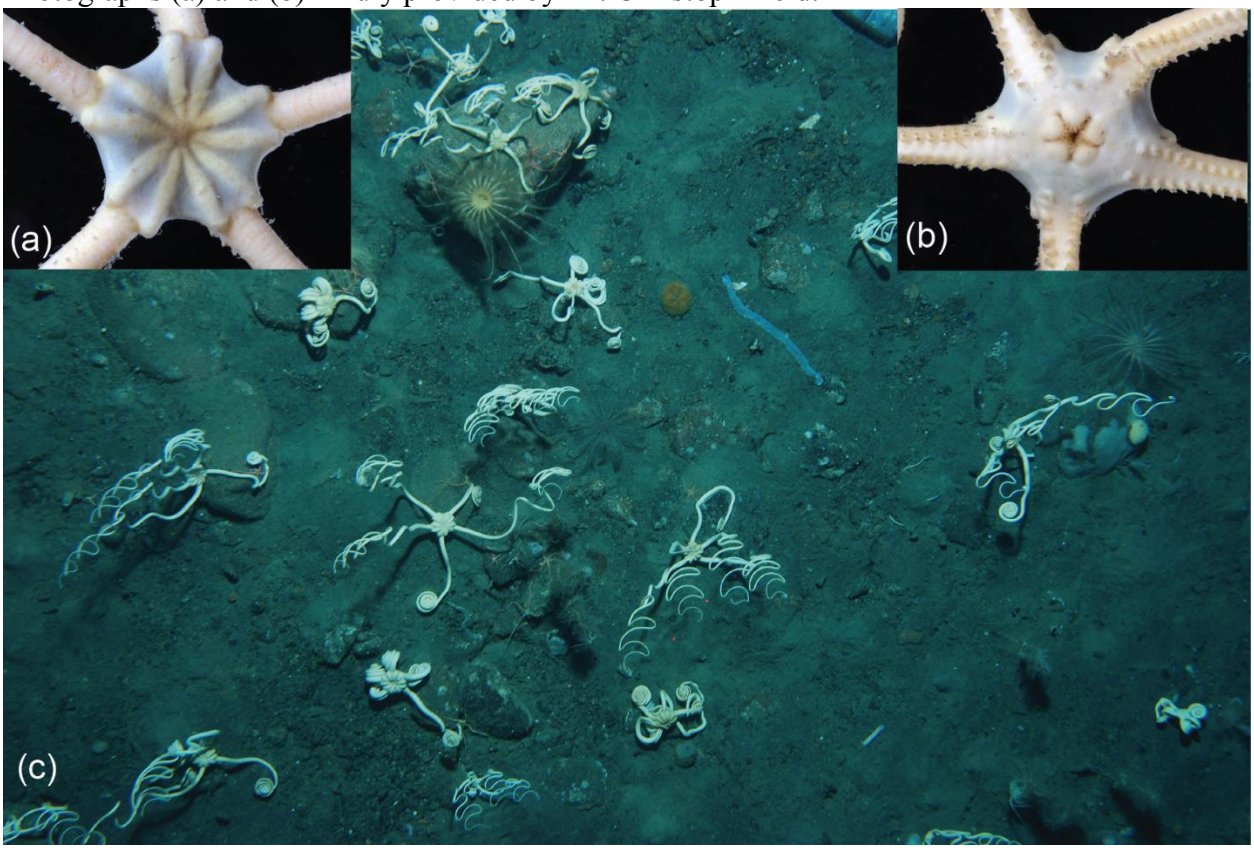

Figure 2. A) Sampling locations of *Astrotoma agassizii* and admixture results from single nucleotide polymorphism (SNP) analyses. Red dots represent sampling localities for individuals with both nuclear 2b-RAD and mitochondrial *COII* and *16S-rDNA* data. Light blue dots represent localities with *COII* and *16S-rDNA* data and light blue triangles represent localities with *COI* data. Due to the proximity of some localities, red dots had priority as they included the most data and may overlap with proximal light blue dots. Pie charts connected to each red dot represent the level of admixture that was found in the sampling locality recovered from LEA analyses. The burgundy color represents individuals that are admixed between genotypes common to South America and the Southern Ocean. Dotted line with arrowheads represents the approximate location and direction of the Antarctic Polar Front (APF) and Antarctic Circumpolar Current (ACC). B) LEA admixture coefficients per individual represented in a bar graph. Admixture coefficients are represented on the Y-axis and individuals are represented by a single vertical bar. Arrows along the top of the bar graph denote admixed individuals between the two regions.

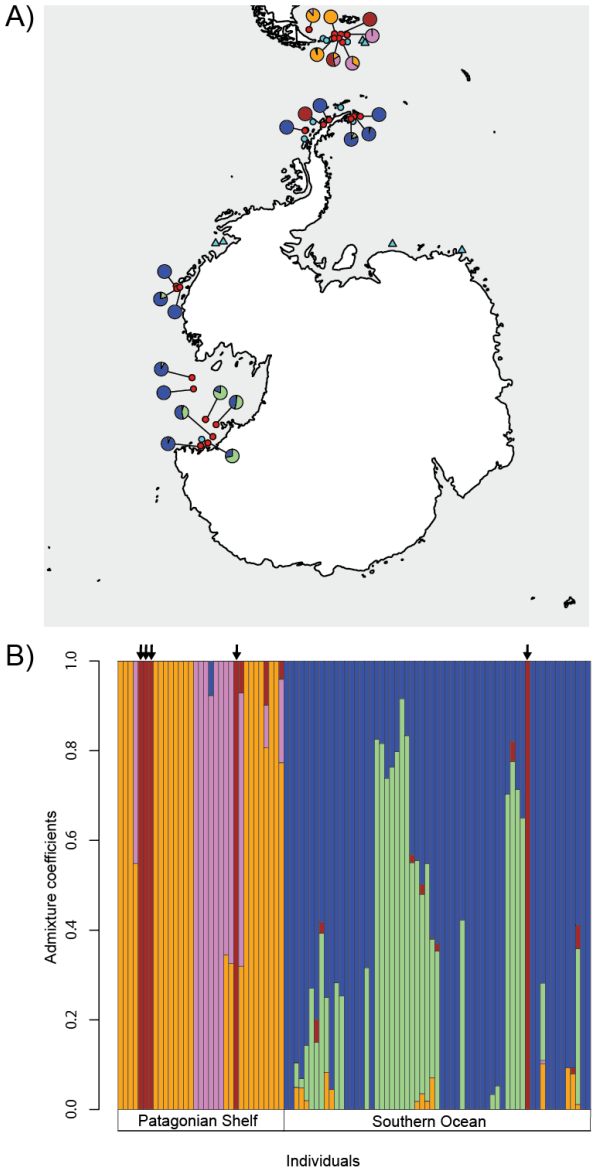

Figure 3. Haplotype network of *Astrotoma agassizii.* A) The network is based off *COII* and *16S-rDNA* data from 186 individuals along with uncorrected pairwise (*p*-) distances for *COII* on the left. Clades I., II., and III. in the *COII* and *16S-rDNA* haplotype network separate if a 95% connection limit is applied. B) Network based off 45 individuals amplified for *COI* and p-distances for *COI*. Filled black dots represent missing haplotypes.

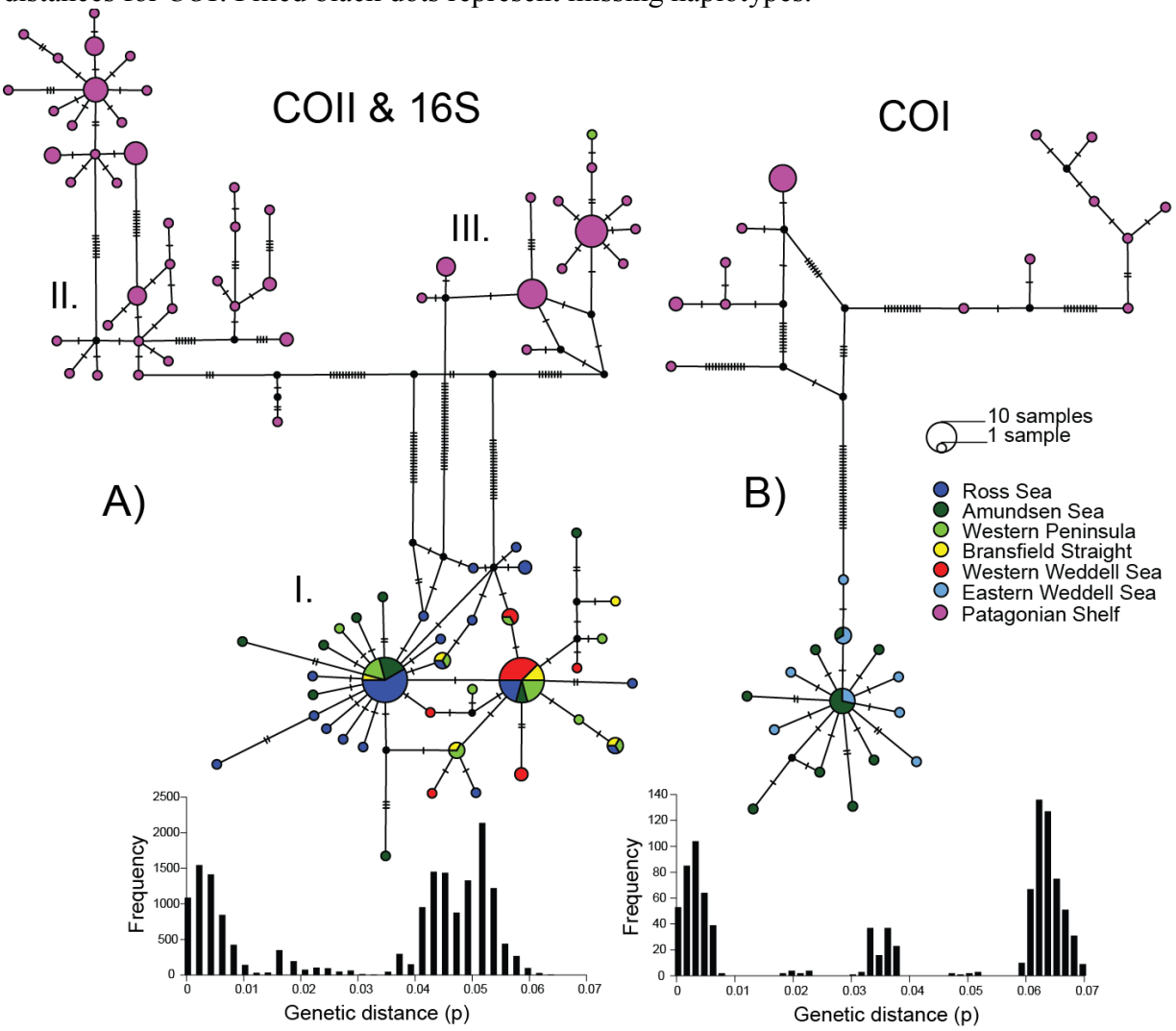

Figure 4. Discriminant Analyses of Principal Components (DAPC) for *Astrotoma agassizii* in both the Southern Ocean and South America based on SNP data. The numbers on each cluster are also presented on each peak in the histogram of density based on the discriminant function.

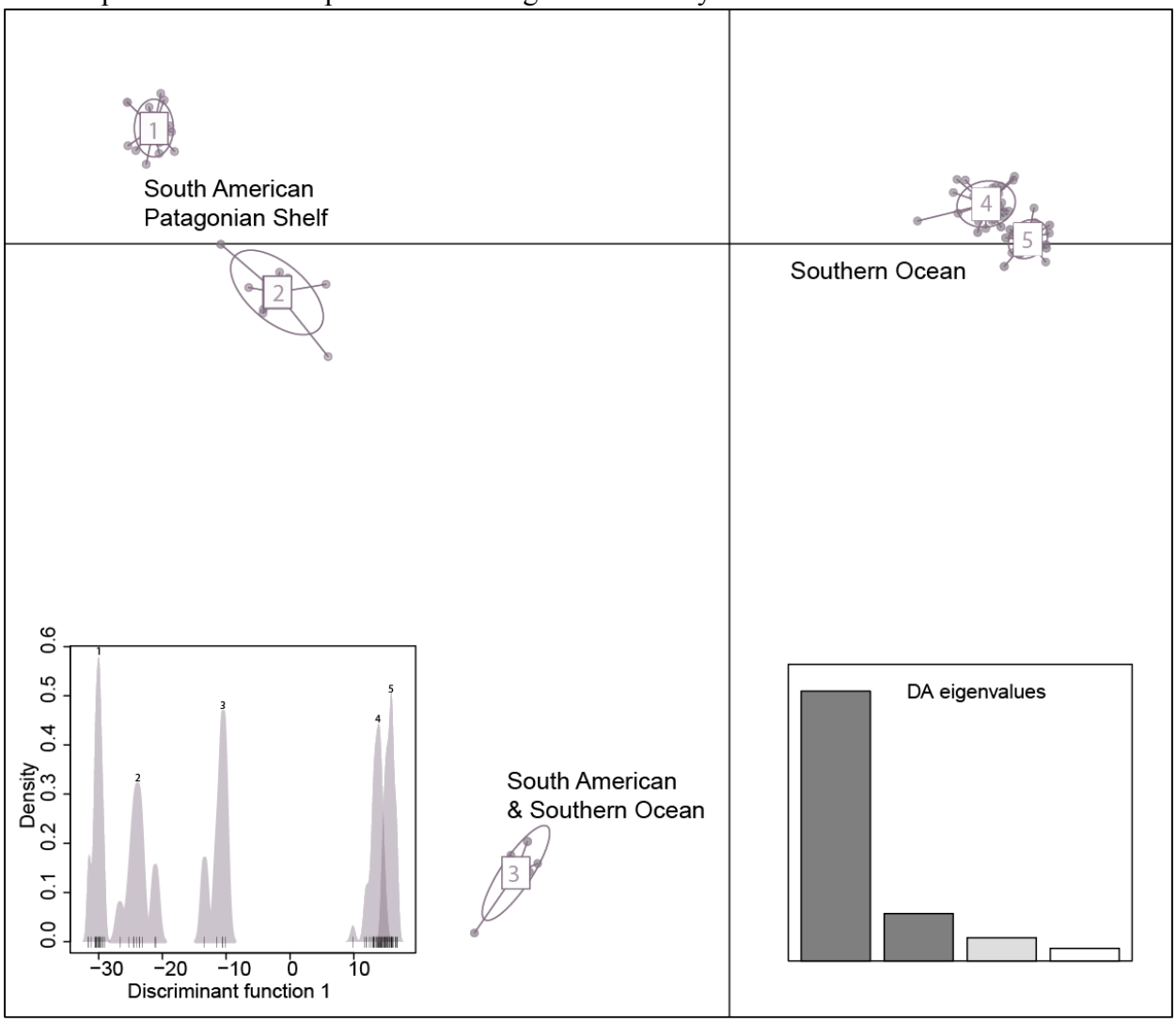

Chapter 4. Conservation of ophiuroid mitochondrial genome arrangements.

Abstract:

Ophiuroids are a conspicuous member of the benthic ecosystem as they are the most speciose of all classes of echinoderms and fill many ecological niches. With high levels of biodiversity, and ecosystem importance, understanding their evolutionary history is an important is an important goal. There have been great advances in understanding higher taxonomic relationships of ophiuroids using nuclear data but many species of ophiuroids for which molecular data have been collected, are limited only to *coI* barcoding information. Implying the importance of the utility of mitochondrial data to recover similar topologies as the nuclear data in ophiuroids needed to be addressed. For the purposes of this study, 17 mitochondrial genomes spanning the breadth of Ophiuroidea taxonomic diversity were utilized to explore evolutionary relationships through maximum likelihood analyses and comparative arrangements of the 37 mitochondrial genes. The three clades recovered from phylogenetic analyses support recent nuclear work of the two orders Ophintegrida and Euryophiurida. Further, only three mitochondrial genome arrangements were recovered from the 13 protein coding and 2 ribosomal RNA genes. As expected, tRNA genes were more likely to have undergone rearrangement but the order of all 37 genes were found to be conserved in all sampled Euryalida, a clade within Euryophiurida. Both clades within Euryophiurida, Euryalida and Ophiuridae, had conserved rearrangement of genes after the divergence of their last common ancestor. Euryalida has a rearrangement of the two ribosomal RNA genes, *rrnS* and *rrnL*, in contrast to Ophiuridae which had an inversion of the genes *nad1*, *nad2*, and *cob* onto the opposite strand.

Introduction:

Ophiuroids, or brittle stars, occur in all the world's oceans from the deep sea to intertidal zones and are more speciose than other extant lineages of echinoderms (Stöhr et al., 2012). Ophiuroidea fill a wide array of ecological niches from suspension feeding (Emson et al., 1991), scavenging, and even opportunistic generalists that will feed on anything from detritus material to cannibalizing smaller individuals of its species (Fratt and Dearborn, 1984). Additionally, ophiuroids possess both sexual and asexual reproduction, although asexual reproduction most often occurs in member with six arms (D Heimeier et al., 2010; Mladenov et al., 1983; Tominaga et al., 2004). Evolutionary relationships within Ophiuroidea are of great interest (Stöhr et al., 2012; O'Hara et al., 2014) and traditionally Ophiuroidea had been thought to comprise two lineages, Ophiurida and Euryalida (Smith et al., 1995). Fossil evidence suggests Euryalida separated more recently, within Ophiurida (Smith et al., 1995). Recent studies employing transcriptome data (O'Hara et al., 2014) and target-capture approaches (O'Hara et al., 2017) have improved understanding of ophiuroid evolutionary history and suggest Ophiuroidea comprises Euryophiurida and Ophintegrida. Euryophiurida is composed of the Euryalida, and some members of Ophiuridae (within traditionally recognized Ophiurida) and the *Ophiomusium* complex. Ophintegrida is composed of all remaining Ophiurida families.

Mitochondrial genomes can be useful molecular marker for phylogenetics and may be used in addition to nuclear data to confirm topology. Further, rare genomic changes such as gene rearrangements, inversions, transpositions, etc. can be studied in a comparative fashion among mitochondrial genomes, shedding further light on the evolutionary history of a group of organisms (Zhong et al., 2008). Additionally, some groups such as echinoderms, have a unique translation code. Currently there are only seven publicly available ophiuroid mitochondrial

genomes, with six published (Perseke et al., 2010, 2008; Scouras et al., 2004), out of approximately 2,100 currently recognized species (Stöhr et al., 2017). In comparison to other echinoderm classes, mitochondrial data of Ophiuroidea has been demonstrated to have accelerated molecular clocks and significant rearrangements of gene (Scouras et al., 2004). This contrasts the relatively conserved gene arrangement of echinoids, asteroids, and holothoroids (Scouras et al., 2004). The echinoid mtDNA genome order is the most conserved among all classes of echinoderms (Perseke et al., 2010). To date, all complete Ophiuroidea mitochondrial genomes have been recovered as circular and to contain all 37 genes of the typical bilaterian mtDNA complement (Perseke et al., 2010).

Here, we sought to assess whether phylogenetic analyses of mitochondrial genomes recover a topology consistent with nuclear data sets (O'Hara et al., 2017, 2014). Understanding the relative topologies recovered between nuclear and mitochondrial data sets has implications on the utility of mitochondrial genomes for animal phylogenetics (Moore, 1995). Additionally mitochondrial data, specifically *coI*, is widely utilized for barcoding of species along with population genetics and phylogenetics (Hajibabaei et al., 2007; Dorothea Heimeier et al., 2010). We sequenced 10 new ophiuroid mitochondrial genomes broadly spanning ophiuroid diversity, doubling the previously available data for brittle star mtDNA genomes. This study set out to test two hypotheses; 1) the mitochondrial rearrangements of coding genes and ribosomal RNA will remain conserved within the major phylogenetic clades identified by O'Hara et al (2014, 2017) and, 2) the inferred phylogenetic relationships recovered from the mitochondrial genomes will be consistent with that of the nuclear data set.

Methods:

Collection, Genome assembly, annotation and mapping

Collection and locality information for the 10 new ophiuroid specimens sampled herein are given in Table 1. Specimens were collected using Blake trawls, identified on the ship, and preserved in either >90% ethanol or frozen at -80°C. Identifications were subsequently confirmed once back in the laboratory. An additional 7 ophiuroid mitochondrial genomes were downloaded from NCBI (Table 1) for inclusion in this study.

Genomic DNA was extracted using Qiagen's DNeasy® Blood and Tissue kit following manufacturer's protocol. Library preparation and sequencing was performed by The Genomic Services Lab at Hudson Alpha Institute in Huntsville Alabama. Sequencing employed an Illumina HiSeq 2500 platform (San Diego, California) using 2 x 150 paired-end v4 chemistry. *De novo* assemblies of the paired-end reads were performed using Ray 2.2.0 (Boisvert et al., 2012) with a k-mer of 31. Mitochondrial genomes were identified using BLASTn (Altschul et al., 1990) with the mitochondrial genome of *Opiocomina nigra* (Perseke et al., 2010) serving as the query sequence. Contigs were initially annotated using the MITOS web server (Bernt et al., 2013) and annotations were edited manually using Artemis (Rutherford et al., 2000). Comparisons of the rearrangement of coding genes was visualized using Mauve (Darling et al., 2004).

Phylogenetic analyses

Phylogenetic analyses were performed on 17 ophiuroids (Table 1) along with two asteroids, *Acanthaster brevispinus* and *Acanthaster planci* (GenBank Accessions AB231476 and AB231475, respectively; Yasuda et al., 2006), used as an outgroup. Analyses were conducted on nucleotide and amino acid (AA) sequences from the 13 mitochondrial protein-coding genes

(*cox1, cox2, cox3, cob, atp6, atp8, nad1, nad2, nad3, nad4, nad5, nad6, nad4l*) and nucleotide sequences from the 2 ribosomal RNA genes (*rrnS* and *rrnL*). All 15 genes were individually aligned using MUSCLE (Edgar, 2004) in the MEGA 6 software package (Tamura et al., 2013). Resulting alignments were manually evaluated and minor corrections were made by hand. To remove any ambiguously aligned regions, alignments were trimmed using Gblocks (Talavera and Castresana, 2007) with default settings. Resulting trimmed alignments for each gene were then concatenated using FASconCAT (Kück and Meusemann, 2010) for use in phylogenetic analyses. To select an appropriate partition scheme and the best-fitting substitution model for each partition, PartitionFinderV1.1.1 (Lanfear et al., 2012) was used. Maximum likelihood (ML) analyses in RAxML (Stamatakis, 2014) were used to infer phylogenetic relationships, using 100 replicates of rapid bootstrapping to evaluate the consistency of the topology.

Results:

mtDNA genome composition:

Complete mitochondrial genomes, which included all 13 protein coding genes, 22 tRNA genes and 2 ribosomal RNA genes, were recovered for all 10 sequenced ophiuroids. Each sampled ophiuroid was found to have genes on both strands, which is typical of echinoderms (Perseke et al., 2010). These findings are consistent with previously available ophiuroid mtDNA genomes (Perseke et al., 2010, 2008; Scouras et al., 2004). Mitochondrial genome sizes (Table 2) within Euryalida were fairly conserved with *Astrospartus mediterraneus* having the smallest genome at 16,238 base pairs and *Astrotoma agassizii* having the largest mitochondrial genome at 16,524 base pairs. Ophintegrida had a larger range in mitochondrial genome size, from 15,845 base pairs in *Ophiacantha linea*, up to 17,383 base pairs in *Ophiocomina nigra.* Ophiuridae had

highest variation in mitochondrial genome sizes, ranging from *Ophionotus victoriae* at 15,932 base pairs to *Ophioplinthus gelida* with 18,387 base pairs.

Phylogenetic analyses:

Phylogenetic analyses of both amino acid alignments (Figure 2) and nucleotide alignments recovered a branching order consistent with that of O'Hara et al (2014; 2017), albeit with a much reduced taxon sampling. Our analyses recovered three main clades with Euryalida sister to Ophiuridae, supporting the Euryophiurida superorder, and all other families of ophiuroids comprised another clade supporting the Ophintegrida superorder.

Gene order conservation:

The respective arrangement of the 13 coding genes and 2 ribosomal RNA genes were conserved within Euryalida and Ophiuridae. Samples from Ophintegrida recovered 2 differing arrangements of the ribosomal genes. One arrangement of the 13 protein coding genes and 2 ribosomal RNA genes were unique within Ophintegrida. The mtDNA genome arrangement of Ophintegrida and Euryalida that differ, are in the order of *rrnS* and *rrnL* genes. Comparatively, mtDNA genomes of Ophintegrida and Ophiuridae differ on the strand *nad1*, *nad2*, and *cob* or located. Euryalida and Ophiuridae differ in both the order of *rrnS*, *rrnL*, and the strand that *nad1*, *nad2*, and *cob* are located. Ophiuridae's unique arrangement of *nad1, nad2,* and *cob*, is likely due to a transposal of these onto the opposite strand but in the same transcriptional order (Figure 2).

Across all three clades, the arrangement of coding and tRNA genes from *cox1* through *nad5* remained conserved. Figure 3 depicts the gene orders of all 37 mitochondrial genes for the ophiuroids examined herein. Interestingly, all Euryalids sampled have the same gene order,

including tRNAs. Although *Ophiacantha linea* and *Ophioceres incipiens* from Ophintegrida shared the same relative arrangement of coding and ribosomal genes as Euryalida, the arrangement of tRNA genes differed between these two species and from Euryalida. The relative order of tRNA genes for the unique arrangement of coding and ribosomal genes within Ophintegrida have been presented by Perseke et al., (2010). Within Ophiuridae, there are three unique arrangements of tRNA genes. *Ophionotus victoria*, *Ophiura albida*, and *Ophiura lutkeni* all possess identical arrangements of all 37 mitochondrial genes. Similarly, *Ophioplinths brevirima*, *Ophiosteira antarctica*, and *Ophiosteira sp*. also possessed identical mitochondrial gene arrangements. These two clades within Ophiuridae only differ by the relative position of *trnL1*. *Ophioplinthus gelida* had a unique arrangement of tRNA genes for *trnL1*, *trnY* and *trnV*.

Discussion:

mtDNA genome composition:

All ophiuroids possessed a conserved gene arrangement from *coI* through *nad5*, signifying that this region is under strict selection. Euryalida shares the same protein coding and ribosomal RNA genes with *Ophioceres incipiens* and *Ophiacantha linea* of Ophintegrida, but the divergent tRNA arrangement suggests that these were likely independently derived. The recovered phylogenetic tree from this study and O'Hara et al 2014 both suggest that *Ophioceres incipiens* and *Ophiacatha linea* are from two separate clades within Ophintegrida, suggesting that the rearrangement of *rrnS* and *rrnL* has occurred independently at least three times. With multiple rearrangements of the ribosomal RNA genes, the transcriptional order is likely not under strong selection as long as they are transcribed together. Within Euryalida, there is no difference in arrangement of any of the 37 mitochondrial genes, suggesting that this order is selected for or

sampling was not extensive enough to reveal additional changes. In Ophiuridae, only tRNAs showed signs of rearrangement, even within the two individuals of the genus *Ophioplinthus*.

Phylogenetic analyses:

Although the phylogenetic placement of Ophiuroidea among other classes of echindoerms has shown inconsistencies from mitochondrial data due to long branch attraction (Littlewood et al., 1997; Scouras and Smith, 2001), our recovered relationships within Ophiuroidea are consistent with recent analyses of nuclear protein-coding genes (O'Hara et al., 2017, 2014) (Figure 1). The three conserved clades provide further support to the two superorders within Ophiuroidea, specifically Euryophiurida and Ophintegrida, as suggested by O'Hara et al 2017. Previous work (Perseke et al., 2010) concluded that the ancestral gene arrangement in Ophiuroidea was that of *Ophiocomina nigra*, a member of clade Ophintegrida. If the arrangement in Ophintegrida represented by *Ophiocomina nigra* is the ancestral gene arrangement, the gene order of Euryalida can be explained by an inversion of *rrnS* and *rrnL* during the branching event of Euryalida from Ophiurida within Euryophiurida. Similarly, the arrangement of Ophiuridae can also be explained within Euryophiurida by the transposition of *nad1*, *nad2*, and *cob*.

Gene order conservation:

Euryalida and Ophiuridae diverged a minimum of 180 million years ago (Ma) as members of Euryophiurida (O'Hara et al., 2017), after the end-Permian mass extinction and subsequent radiation of Ophiuroidea species (Chen and McNamara, 2006). During the time when these lineage diverged to the last common ancestor in the crown group of Euryalida and Ophiuridae, mitochondrial rearrangements occurred that have since been conserved in Euryalida or

Ophiuridae sensu O'Hara et al. (2017, Figure 2). Using O'Hara's estimated times of divergence, we can estimate the relative times of rearrangements. Specifically, the two independent rearrangements of the ribosomal RNA genes recovered in Ophintegrida occurred within the last ~190 Ma for *Ophiacantha linea* and ~205 Ma for *Ophioceres incipiens*. Further sampling within the clades containing these respective families could further reduce this estimate. The sampling presented here is from across a wide evolutionary range of Ophintegrida and thus the two main arrangements of the 13 protein coding genes and 2 ribosomal RNA genes recovered, likely represent close estimates for others with the group. In general, rearrangement of tRNA genes remained between families with the exception of *Ophioplinthus gelida* which surprisingly varied from that of *Ophioplinthus brevirima* within Ophiuridae. Ultimately, only three arrangements of the 13 protein coding genes and 2 ribosomal RNA genes were recovered which is more conserved than other groups such as insects (Cameron, 2014) where rearrangements are typical between orders, but similar to annelids (Zhong et al., 2008). Although ophiuroid mitochondrial genome arrangements are considered to be more extensively rearranged compared to other classes of echinoderms, within ophiuroids the arrangements are fairly conserved and usually represent higher taxonomically separations.

Acknowledgements:

We would like to thank the support received from the National Science Foundation (NSF ANT-1043670 to ARM, NSF ANT- 1043745 & OPP- 0132032 to KMH) for the funding to collect the specimens and perform the research. This research was made possible with assistance from the Captains and crews of NBP12- 10, LMG13- 12, LMG04- 14, and LMG06- 05. This is Molette Biology Laboratory contribution XX and Auburn University Marine Biology Program contribution XXX.

Data accessibility:

Mitochondrial genomes are deposited in GenBank under accession codes XXX-XXX.

References:

Altschul, S.F., Gish, W., Miller, W., Myers, E.W., Lipman, D.J., 1990. Basic local alignment search tool. J. Mol. Biol. 215, 403–10. doi:10.1016/S0022-2836(05)80360-2

Bernt, M., Donath, A., Jühling, F., Externbrink, F., Florentz, C., Fritzsch, G., Pütz, J., Middendorf, M., Stadler, P.F., 2013. MITOS: Improved de novo metazoan mitochondrial genome annotation. Mol. Phylogenet. Evol. 69, 313–319. doi:10.1016/j.ympev.2012.08.023

Boisvert, S., Raymond, F., Godzaridis, E., Laviolette, F., Corbeil, J., 2012. Ray Meta: scalable de novo metagenome assembly and profiling. Genome Biol. 13, R122. doi:10.1186/gb-2012-13-12-r122

Cameron, S.L., 2014. Insect Mitochondrial Genomics: Implications for Evolution and Phylogeny. Annu. Rev. Entomol. 59, 95–117. doi:10.1146/annurev-ento-011613-162007

Chen, Z.Q., McNamara, K.J., 2006. End-Permian extinction and subsequent recovery of the Ophiuroidea (Echinodermata). Palaeogeogr. Palaeoclimatol. Palaeoecol. 236, 321–344. doi:10.1016/j.palaeo.2005.11.014

Darling, A.C.E., Mau, B., Blattner, F.R., Perna, N.T., 2004. Mauve : Multiple Alignment of Conserved Genomic Sequence With Rearrangements Mauve : Multiple Alignment of Conserved Genomic Sequence With Rearrangements. Genome Res. 14, 1394–1403. doi:10.1101/gr.2289704

Edgar, R.C., 2004. MUSCLE: Multiple sequence alignment with high accuracy and high throughput. Nucleic Acids Res. 32, 1792–1797. doi:10.1093/nar/gkh340

Emson, R., Mladenov, P., Barrow, K., 1991. The feeding mechanism of the basket star Gorgonocephalus arcticus. Can. J. Zool. 69, 449–455.

Fratt, D., Dearborn, J., 1984. Feeding biology of the Antarctic brittle star *Ophionotus victoriae* (Echinodermata: Ophiuroidea). Polar Biol. 3, 127–139.

Hajibabaei, M., Singer, G.A.C., Hebert, P.D.N., Hickey, D.A., 2007. DNA barcoding: how it complements taxonomy, molecular phylogenetics and population genetics. Trends Genet. 23, 167–172. doi:10.1016/j.tig.2007.02.001

Heimeier, D., Lavery, S., Sewell, M., 2010. Molecular species identification of *Astrotoma agassizii* from planktonic embryos: further evidence for a cryptic species complex. J. Hered. 101, 775–779. doi:10.1093/jhered/esq074

Heimeier, D., Lavery, S., Sewell, M. a., 2010. Using DNA barcoding and phylogenetics to identify Antarctic invertebrate larvae: Lessons from a large scale study. Mar. Genomics 3, 165–177. doi:10.1016/j.margen.2010.09.004

Kück, P., Meusemann, K., 2010. FASconCAT: Convenient handling of data matrices. Mol. Phylogenet. Evol. 56, 1115–1118. doi:10.1016/j.ympev.2010.04.024

Lanfear, R., Calcott, B., Ho, S.Y.W., Guindon, S., 2012. PartitionFinder: Combined selection of partitioning schemes and substitution models for phylogenetic analyses. Mol. Biol. Evol. 29, 1695–1701. doi:10.1093/molbev/mss020

Littlewood, D.T.J., Smith, A.B., Clough, K.A., Emson, R.H., 1997. The interrelationships of the echinoderm classes: morphological and molecular evidence. Biol. J. Linn. Soc. 61, 409–438. doi:10.1111/j.1095-8312.1997.tb01799.x

Mladenov, P. V., Emson, R.H., Colpit, L. V., Wilkie, I.C., 1983. Asexual reproduction in the west indian brittle star Ophiocomella ophiactoides (H.L. Clark) (Echinodermata: Ophiuroidea). J. Exp. Mar. Bio. Ecol. 72, 1–23. doi:10.1016/0022-0981(83)90016-3

Moore, W.S., 1995. Inferring Phylogenies from mtDNA Variation : Mitochondrial-Gene Trees Versus Nuclear-Gene Trees. Soc. Study Evol. 49, 718–726.

O'Hara, T.D., Hugall, A.F., Thuy, B., Moussalli, A., 2014. Phylogenomic Resolution of the Class Ophiuroidea Unlocks a Global Microfossil Record. Curr. Biol. 1–6. doi:10.1016/j.cub.2014.06.060

O'Hara, T.D., Hugall, A.F., Thuy, B., Stöhr, S., Martynov, A. V, 2017. Molecular Phylogenetics and Evolution Restructuring higher taxonomy using broad-scale phylogenomics : The living Ophiuroidea. Mol. Phylogenet. Evol. 107, 415–430. doi:10.1016/j.ympev.2016.12.006

Perseke, M., Bernhard, D., Fritzsch, G., Brümmer, F., Stadler, P.F., Schlegel, M., 2010. Mitochondrial genome evolution in Ophiuroidea, Echinoidea, and Holothuroidea: Insights in phylogenetic relationships of Echinodermata. Mol. Phylogenet. Evol. 56, 201–211. doi:10.1016/j.ympev.2010.01.035

Perseke, M., Fritzsch, G., Ramsch, K., Bernt, M., Merkle, D., Middendorf, M., Bernhard, D., Stadler, P.F., Schlegel, M., 2008. Evolution of mitochondrial gene orders in echinoderms. Mol. Phylogenet. Evol. 47, 855–864. doi:10.1016/j.ympev.2007.11.034

Rutherford, K., Parkhill, J., Crook, J., Horsnell, T., Rice, P., Rajandream, M.A., Barrell, B., 2000. Artemis: sequence visualization and annotation. Bioinformatics 16, 944–945. doi:10.1093/bioinformatics/16.10.944

Scouras, A., Beckenbach, K., Arndt, A., Smith, M.J., 2004. Complete mitochondrial genome DNA sequence for two ophiuroids and a holothuroid: The utility of protein gene sequence and gene maps in the analyses of deep deuterostome phylogeny. Mol. Phylogenet. Evol. 31, 50–65. doi:10.1016/j.ympev.2003.07.005

Scouras, A., Smith, M.J., 2001. A novel mitochondrial gene order in the crinoid echinoderm Florometra serratissima. Mol. Biol. Evol. 18, 61–73.

Smith, A.B., Paterson, G.L.J., Lafay, B., 1995. Ophiuroid phylogeny and higher taxonomy: morphological, molecular and palaeontological perspectives. Zool. J. Linn. Soc. 114, 213–243. doi:10.1111/j.1096-3642.1995.tb00117c.x

Stamatakis, A., 2014. RAxML version 8: a tool for phylogenetic analysis and post-analysis of large phylogenies. Bioinformatics 2010–2011. doi:10.1093/bioinformatics/btu033

Stöhr, S., O'Hara, T., Thuy, B., 2017. World Ophiuroidea database [WWW Document]. URL http://www.marinespecies.org/ophiuroidea (accessed 5.7.17).

Stöhr, S., O'Hara, T.D., Thuy, B., 2012. Global diversity of brittle stars (Echinodermata: Ophiuroidea). PLoS One 7, 1–14. doi:10.1371/journal.pone.0031940

Talavera, G., Castresana, J., 2007. Improvement of phylogenies after removing divergent and ambiguously aligned blocks from protein sequence alignments. Syst. Biol. 56, 564–77. doi:10.1080/10635150701472164

Tamura, K., Stecher, G., Peterson, D., Filipski, A., Kumar, S., 2013. MEGA6: Molecular evolutionary genetics analysis version 6.0. Mol. Biol. Evol. 30, 2725–2729. doi:10.1093/molbev/mst197

Tominaga, H., Nakamura, S., Komatsu, M., 2004. Reproduction and development of the conspicuously dimorphic brittle star *Ophiodaphne formata* (Ophiuroidea). Biol. Bull. 206,

25–34.
Yasuda, N., Hamaguchi, M., Sasaki, M., Nagai, S., Saba, M., Nadaoka, K., 2006. Complete mitochondrial genome sequences for Crown-of-thorns starfish Acanthaster planci and Acanthaster brevispinus. BMC Genomics 7, 17. doi:10.1186/1471-2164-7-17
Zhong, M., Struck, T.H., Halanych, K.M., 2008. Phylogenetic information from three mitochondrial genomes of Terebelliformia (Annelida) worms and duplication of the methionine tRNA. Gene 416, 11–21. doi:10.1016/j.gene.2008.02.020

Table 1. Collection information, including taxonomic designation, NCBI accession number, depth, and coordates of sampling location.

Taxon	Species	mtDNA genome	Depth (m)	Latitude	Longitude
Ophintegrida					
Ophiurida					
Amphiuridae	*Amphiopholis squamata*	NC_013876			
Ophiacanthidae	*Ophiacantha linea*	NC_023254			
Ophiactidae	*Ophiopholis aculeata*	AF314589			
Ophiocomidae	*Ophiocomina nigra*	NC_013874			
Ophiolepididae	*Ophioceres incipiens*	This study	277	63 23.05 S	60 03.40 W
Euryophiurida					
Euryalida					
Gorgonocephalidae	*Astrohamma tuberculatum*	This study	612	72 12.25 S	103 35.78 W
	Astrospartus mediterraneus	NC_103878			
	Astrotoma agassizii (SA)	This study	854	53 47 S	49 33 W
	Astrotoma agassizii (SO)	This study	457	76 28.76 S	165 44.26 W
	Gorgonocephalus chilensis	This study	664	64 24.67 S	61 57.79 W
Ophiurida					
Ophiuridae	*Ophionotus victoriae*	This study	122	67 44.42 S	69 17.37 W
	Ophioplinthus brevirima	This study	228	63 23.31 S	60 07.20 W
	Ophioplinthus gelida	This study	228	63 23.31 S	60 07.20 W
	Ophiosteira antarctica	This study	570	75 19.77 S	176 59.10 W
	Ophiosteira sp	This study	570	75 19.77 S	176 59.10 W
	Ophiura albida	NC_010691			
	Ophiura lutkenii	AY184223			

Table 2. Genome size, and base composition of assembled Ophiuroidea mitochondrial genomes.

Taxon	Species	Length	GC%
Ophintegrida			
Ophiurida			
Amphiuridae	*Amphiopholis squamata*	16,907	33.25
Ophiacanthidae	*Ophiacantha linea*	15,845	31.43
Ophiactidae	*Ophiopholis aculeata*	16,472	36.35
Ophiocomidae	*Ophiocomina nigra*	17,383	39.42
Ophiolepididae	*Ophioceres incipiens*	18,107	39.49
Euryophiurida			
Euryalida			
Gorgonocephalidae	*Astrohamma tuberculatum*	16,464	28.10
	Astrospartus mediterraneus	16,524	29.13
	Astrotoma agassizii (SA)	16,361	27.93
	Astrotoma agassizii (SO)	16,238	28.76
	Gorgonocephalus chilensis	15,932	33.70
Ophiurida			
Ophiuridae	*Ophionotus victoriae*	16,438	26.34
	Ophioplinthus brevirima	15,967	31.57
	Ophioplinthus gelida	18,387	34.01
	Ophiosteira antarctica	16,979	30.63
	Ophiosteira sp	16,66	31.12
	Ophiura albida	16,580	31.51
	Ophiura lutkenii	17,329	34.13

Figure 1. Phylogenetic relationships recovered from Maximum Likelihood analyses utilizing both nucleotide and amino acid alignments. Both analyses recovered identical topologies. Support values not shown have 100% bootstrap support for both analyses. Nucleotide support values are on the left, amino acid support values are on the right. Arrows show the corresponding gene arrangement of the 13 protein coding and 2 ribosomal RNA genes.

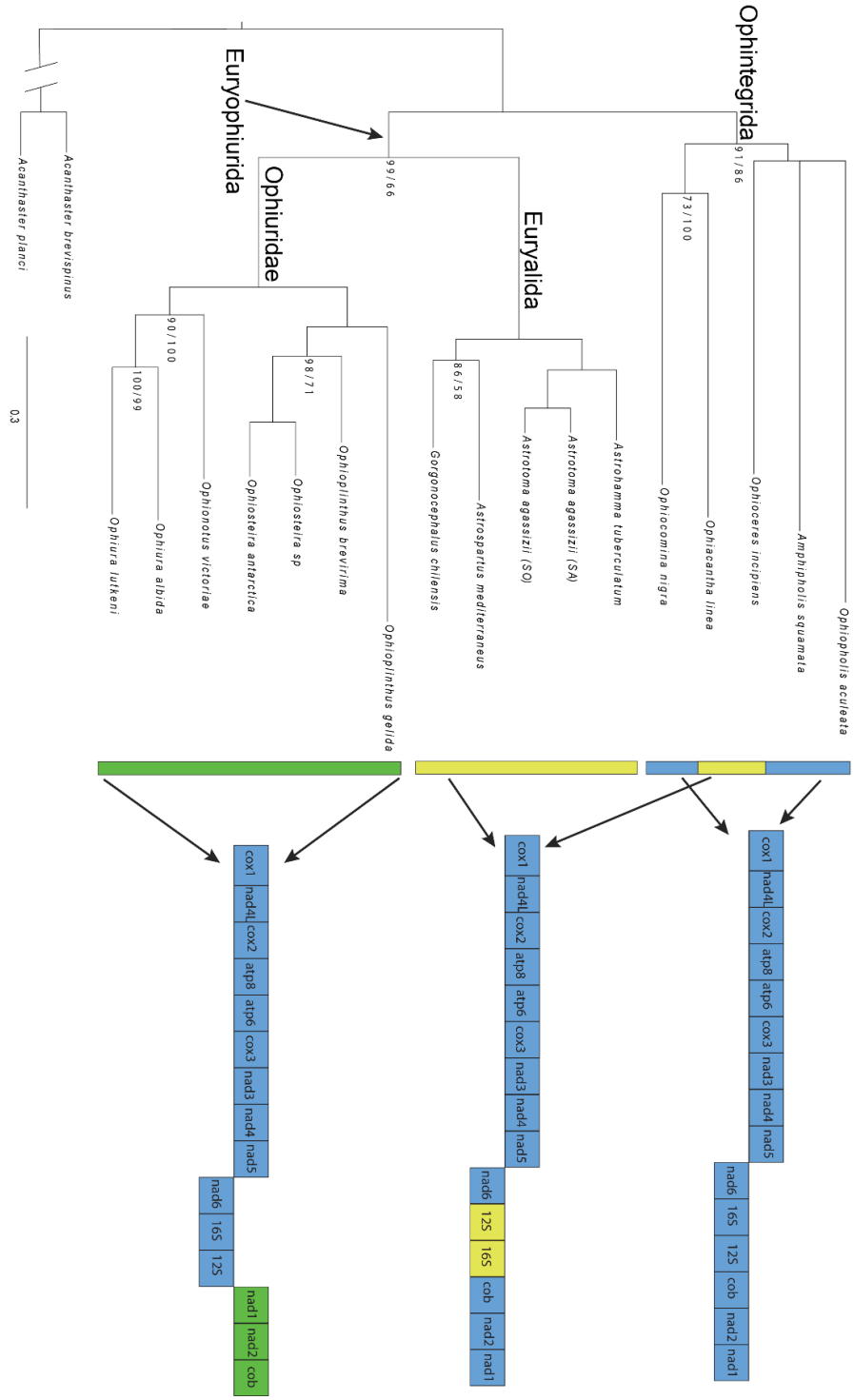

Figure 2. Gene order of all 37 mitochondrial genes for all 17 specimens. Gene orders with more than one specimen are noted above the order.

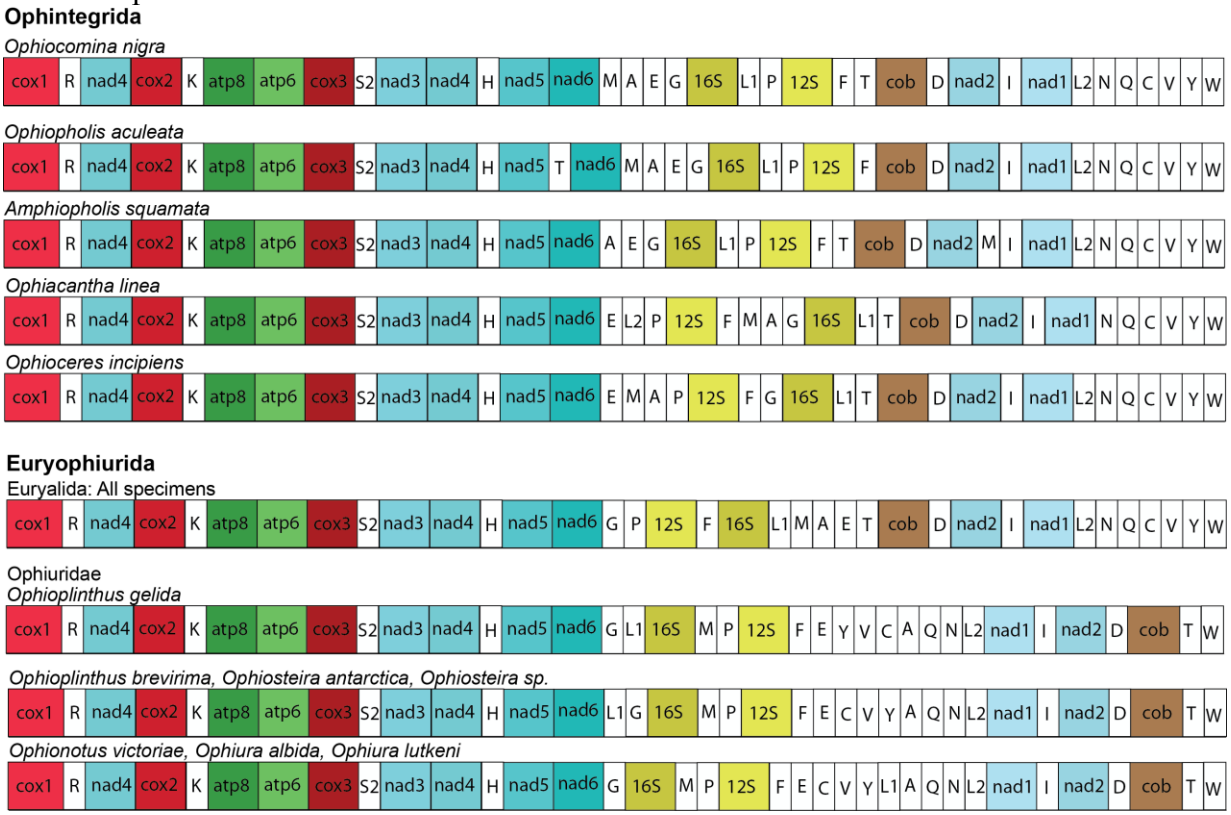

Chapter 5. Conclusions

The Southern Ocean is a uniquely isolated ecosystem, influenced by glacial cycles (Clarke and Crame, 1992; Thatje et al., 2005), complex oceanographic currents (García et al., 2002; Kaiser et al., 2011; Thatje, 2012), and open ocean barriers which may not be as limiting as previously thought. Results of this work suggest that 1) the circumpolar ophiuroids *Ophionotus victoriae* and *Astrotoma agassizii* are not homogenous through their range as geographic structure was identified, 2) the Antarctic Polar Front does not serve as an absolute barrier to dispersal for *Astrotoma agassizii* and, 3) the mitochondrial genome of all sampled Ophiuroidea were conserved to three different arrangements of the 13 coding genes and 2 ribosomal RNA genes

To date, most benthic invertebrate phylogeographic work in the Southern Ocean has focused mostly on a handful of mitochondrial markers (e.g., Hunter and Halanych, 2010, 2008; Leese et al., 2010; Leese and Held, 2008; Wilson et al., 2007), but some nuclear markers including microsatellites have been employed (e.g., Baird et al., 2012; Leese et al., 2008) . For the A focal point phylogeographic work herein, high-resolution whole genome single nucleotide polymorphism (SNP) data was generated by the 2b-RAD protocol (Wang et al., 2012) to sample numerous nuclear loci. Inclusion of SNP data allowed the opportunity to look for admixture that would have gone unrecognized, and also provided the ability to identify fine scale genetic structure (Herrera and Shank, 2016; Lamer et al., 2014; Reitzel et al., 2013). To date, this work on *Ophionotus victoriae* (Galaska et al., 2017) and *Astrotoma agassizii* are the largest phylogeographic studies in the Southern Ocean of benthic invertebrates to utilize SNP data. Use of SNP data provided increased resolution and identified four distinct geographic populations in *Ophionotus victoriae* in comparison to mitochondrial data which recovered only three

populations that had less distinct geographic boundaries. In *Astrotoma agassizii*, mitochondrial data only provided evidence for one homogenous population in the Southern Ocean while the SNP data was able to reveal geographic structure between the Ross Sea and the rest of the tested range. Additionally, genetic connectivity of *Astrotoma agassizii* across the Antarctic Polar Front was more apparent with SNP data than mitochondrial data suggesting current or recent admixture.

Although our sampling covered a large portion of the Southern Ocean, including the entire Western Antarctic, there is a need for further sampling or collaboration to fill in the gaps of the Eastern Antarctic. Results presented in this work have shown the ability of these circumpolar organisms to maintain genetic connectivity over thousands of kilometers, from the Ross Sea to the western side of the Weddell Sea, but the inclusion of Eastern Antarctic samples would allow further testing of competing hypotheses. For example, additional samples would allow the hypothesis of a recent (within the last 1.5 MY) trans-Antarctic seaway connecting the Ross and Weddell Sea (Barnes and Hillenbrand, 2010) to be tested. Although lacking SNP data from the eastern Weddell Sea, the mitochondrial data of *Ophionotus victoriae* (Galaska et al., 2017) and other current phylogeographic studies (personal correspondence and collaborations) provide evidence potentially supporting this hypothesis. Additional data from the eastern Weddell and Amery Ice Shelf would allow the direct ability to test this hypothesis.

The work put forth in this dissertation also focused on the biodiversity and the evolutionary relationships within Ophiuroidea. Although, recent work has mostly resolved major phylogenetic relationships of Ophiuroidea using transcriptomic (O'Hara et al., 2014) and an exon capture approach (O'Hara et al., 2017), our interest was in the phylogenetic signal of mitochondrial genomes of Ophiuroidea as they were reported to possess an unusually high

nucleotide substitution rate and inconsistent gene arrangement compared to other classes of echinoderms (Perseke et al., 2008). Phylogenetic analyses of the 13 coding genes and 2 ribosomal genes revealed that mtDNA data provided the same branching order as recent multi-locus nuclear data sets (O'Hara et al. 2014, 2017). This branching order supports the reorganization of Ophiuroidea into two major lineages, Euryophiurida and Ophintegrida. Additionally, three distinct gene arrangements of the 13 protein coding genes and 2 ribosomal RNA genes were identified. The conserved order of protein-coding and ribosomal genes was observed across all sampled Euryalida, and was found within Ophintegrida.

Overall this work has provided substantial contributions to the knowledge of ophiuroid phylogeography, biodiversity, and to Southern Ocean ecology. My work has shown that reproductive strategy is not always the best indicator for species dispersal. This work also serves as an example of why future phylogeographic work should embrace the data types that provide higher genetic resolution than traditionally employed markers. Further, mitochondrial genomes still serve as a viable option for phylogenetic inference during the current push for large nuclear data sets, at least for brittle stars. Possibly the most impactful contribution of this work is that the Antarctic Polar Front which was often seen an absolute barrier to dispersal for many benthic invertebrates, does in fact have bi-directional migration and investigation of additional non-endemic species will likely yield similar results.

References:

Baird, H.P., Miller, K.J., Stark, J.S., 2012. Genetic population structure in the antarctic benthos: Insights from the widespread amphipod, orchomenella franklini. PLoS One 7. doi:10.1371/journal.pone.0034363

Barnes, D.K. a., Hillenbrand, C.-D., 2010. Faunal evidence for a late quaternary trans-Antarctic seaway. Glob. Chang. Biol. 16, 3297–3303. doi:10.1111/j.1365-2486.2010.02198.x

Clarke, A., Crame, J.A., 1992. The Southern Ocean benthic fauna and climate change: A historical perspective. Philos. Trans. R. Soc. B Biol. Sci. 339, 299–309.

Galaska, M.P., Sands, C.J., Santos, S.R., Mahon, A.R., Halanych, K.M., 2017. Geographic structure in the Southern Ocean circumpolar brittle star Ophionotus victoriae (Ophiuridae) revealed from mtDNA and single-nucleotide polymorphism data. Ecol. Evol. 7, 1–11. doi:10.1002/ece3.2617

García, M.A., Castro, C.G., Ríos, A.F., Doval, M.D., Rosón, G., Gomis, D., López, O., 2002. Water masses and distribution of physico-chemical properties in the Western Bransfield Strait and Gerlache Strait during Austral summer 1995/96. Deep. Res. Part II Top. Stud. Oceanogr. 49, 585–602. doi:10.1016/S0967-0645(01)00113-8

Herrera, S., Shank, T.M., 2016. RAD sequencing enables unprecedented phylogenetic resolution and objective species delimitation in recalcitrant divergent taxa. Mol. Phylogenet. Evol. 100, 70–79. doi:10.1101/019745

Hunter, R.L., Halanych, K.M., 2010. Phylogeography of the Antarctic planktotrophic brittle star *Ophionotus victoriae* reveals genetic structure inconsistent with early life history. Mar. Biol. 157, 1693–1704. doi:10.1007/s00227-010-1443-3

Hunter, R.L., Halanych, K.M., 2008. Evaluating connectivity in the brooding brittle star

Astrotoma agassizii across the drake passage in the Southern Ocean. J. Hered. 99, 137–48. doi:10.1093/jhered/esm119

Kaiser, S., Griffiths, H.J., Barnes, D.K. a., Brandão, S.N., Brandt, A., O'Brien, P.E., 2011. Is there a distinct continental slope fauna in the Antarctic? Deep Sea Res. Part II Top. Stud. Oceanogr. 58, 91–104. doi:10.1016/j.dsr2.2010.05.017

Lamer, J.T., Sass, G.G., Boone, J.Q., Arbieva, Z.H., Green, S.J., Epifanio, J.M., 2014. Restriction site-associated DNA sequencing generates high-quality single nucleotide polymorphisms for assessing hybridization between bighead and silver carp in the United States and China. Mol. Ecol. Resour. 14, 79–86. doi:10.1111/1755-0998.12152

Leese, F., Agrawal, S., Held, C., 2010. Long-distance island hopping without dispersal stages: transportation across major zoogeographic barriers in a Southern Ocean isopod. Naturwissenschaften 97, 583–94. doi:10.1007/s00114-010-0674-y

Leese, F., Held, C., 2008. Identification and characterization of microsatellites from the Antarctic isopod Ceratoserolis trilobitoides: nuclear evidence for cryptic species. Conserv. Genet. 9, 1369–1372. doi:10.1007/s10592-007-9491-z

Leese, F., Kop, A., Wägele, J.-W., Held, C., 2008. Cryptic speciation in a benthic isopod from Patagonian and Falkland Island waters and the impact of glaciations on its population structure. Front. Zool. 5, 19. doi:10.1186/1742-9994-5-19

O'Hara, T.D., Hugall, A.F., Thuy, B., Moussalli, A., 2014. Phylogenomic Resolution of the Class Ophiuroidea Unlocks a Global Microfossil Record. Curr. Biol. 1–6. doi:10.1016/j.cub.2014.06.060

O'Hara, T.D., Hugall, A.F., Thuy, B., Stöhr, S., Martynov, A. V, 2017. Molecular Phylogenetics and Evolution Restructuring higher taxonomy using broad-scale phylogenomics : The living

Ophiuroidea. Mol. Phylogenet. Evol. 107, 415–430. doi:10.1016/j.ympev.2016.12.006

Perseke, M., Fritzsch, G., Ramsch, K., Bernt, M., Merkle, D., Middendorf, M., Bernhard, D., Stadler, P.F., Schlegel, M., 2008. Evolution of mitochondrial gene orders in echinoderms. Mol. Phylogenet. Evol. 47, 855–864. doi:10.1016/j.ympev.2007.11.034

Reitzel, A.M., Herrera, S., Layden, M.J., Martindale, M.Q., Shank, T.M., 2013. Going where traditional markers have not gone before: utility of and promise for RAD sequencing in marine invertebrate phylogeography and population genomics. Mol. Ecol. 22, 2953–2970. doi:10.1111/mec.12228

Thatje, S., 2012. Effects of Capability for Dispersal on the Evolution of Diversity in Antarctic Benthos. Integr. Comp. Biol. 52, 470–482. doi:10.1093/icb/ics105

Thatje, S., Hillenbrand, C.-D., Larter, R., 2005. On the origin of Antarctic marine benthic community structure. Trends Ecol. Evol. 20, 534–40. doi:10.1016/j.tree.2005.07.010

Wang, S., Meyer, E., McKay, J.K., Matz, M. V, 2012. 2b-RAD: a simple and flexible method for genome-wide genotyping. Nat. Methods 9, 808–10. doi:10.1038/nmeth.2023

Wilson, N.G., Hunter, R.L., Lockhart, S.J., Halanych, K.M., 2007. Multiple lineages and absence of panmixia in the “circumpolar” crinoid Promachocrinus kerguelensis from the Atlantic sector of Antarctica. Mar. Biol. 152, 895–904. doi:10.1007/s00227-007-0742-9

Appendix 1.

Supplementary Table 1. Sampling information sorted by locality. Blank spaces represent data that was not available.

Sampling Group	Latitude	Longitude	# of 16S	# of COI	# of 2b-RAD	Year	Depth (m)	Cruise	Station	AMOVA Region
787	-76.998275	-175.0932	9	9	0	2013	541	NBP-12-10	22	Ross
803	-76.245261	174.50412	9	9	3	2013	604	NBP-12-10	23	Ross
806	-76.9038	169.96525	10	10	10	2013	764	NBP-12-10	24	Ross
826	-74.70781	168.40783	3	3	1	2013	489	NBP-12-10	26	Ross
818	-75.833465	166.50549	11	11	0	2013	552	NBP-12-10	25	Ross
762	-78.06324	-169.99115	6	6	6	2013	549	NBP-12-10	21	Ross
531	-71.699	-93.693667	9	9	6	2013	670	NBP-12-10	3	Bell/Amund
843	-74.995422	165.74422	6	6	2	2013	1101	NBP-12-10	28	Ross
867	-63.805542	-60.479083	9	9	8	2013	428	LMG-13-12	3	W. Peninsula
877	-62.995875	-58.598617	10	10	10	2013	320	LMG-13-12	4	W. Peninsula
895	-64.302283	-56.136417	7	7	7	2013	290	LMG-13-12	6	Weddell
900	-64.303633	-56.141533	0	0	5	2013	276	LMG-13-12	6b	Weddell
913	-64.134392	-56.860217	10	10	8	2013	310	LMG-13-12	8	Weddell
914	-63.742367	-57.431867	8	8	5	2013	692	LMG-13-12	9	Weddell
917	-63.685783	-56.859	10	10	7	2013	400	LMG-13-12	10	Weddell
1051	-64.64	-64.245383	0	0	1	2013	695	LMG-13-12	27	W. Peninsula

1042	-64.846183	-62.959483	10	10	10	2013	301	LMG-13-12	26	W. Peninsula
57	-63.666667	-57.329167	8	8	0	2004	335	LMG-04-14	40	Weddell
59	-63.666667	-57.329167	3	3	0	2004	335	LMG-04-14	40	Weddell
312	-64.350361	-61.759953	8	8	0	2006	334	LMG-06-05	17	W. Peninsula
398	-67.717028	-68.243286	7	7	0	2006	170	LMG-06-05	47	W. Peninsula
422	-65.183694	-64.243283	10	10	0	2006	285	LMG-06-05	58	W. Peninsula
82	-62.850361	-59.45995	5	5	0	2004	900	LMG-04-14	47	W. Peninsula
92	-63.383694	-60.05995	15	15	0	2004	277	LMG-04-14	51	W. Peninsula
321	-64.350361	-57.076617	5	5	0	2006	146	LMG-06-05	21	Weddell
73	-62.100361	-58.393283	10	10	0	2004	276	LMG-04-14	44	W. Peninsula
362	-67.733694	-69.293283	10	10	0	2006	122	LMG-06-05	33	W. Peninsula
114	-62.933694	-60.65995	10	10	0	2004	161	LMG-04-14	64	W. Peninsula
194	-58.783694	-26.343283	9	9	0	200R	270	LMG-04-14	34	Oceanic islands
195	-57.088533	-30.398971	6	6	0	2006	130	LMG-04-14	32	Oceanic islands
196	-56.00683	2.6013889	8	8	0	2006	648	LMG-04-14	50	Oceanic islands
177	-54.816665	-3.5	10	10	0	2004	169	LMG-04-14	58	Oceanic islands
AGT-21A	-67.546004	-70.189001	0	1	0	2009	507	JR230	N/A	W. Peninsula
EI-AGT-4	-61.334004	-55.195	0	9	0	2006	201	JR144	N/A	W. Peninsula

EI-AGT-3	-61.385998	-55.192999	0	5	0	2006	482	JR144	N/A	W. Peninsula
PB-AGT-1B	-61.035998	-46.955	0	1	0	2006	1630	JR144	N/A	Oceanic islands
ST-AGT-3	-59.481	-27.278999	0	2	0	2006	549	JR144	N/A	Oceanic islands
ST-EBS-4	-59.47	-27.276001	0	1	0	2006	307	JR144	N/A	Oceanic islands
ST-AGT-1	-59.518003	-27.436	0	9	0	2006	1545	JR144	N/A	Oceanic islands
LI-AGT-4	-62.525	-61.826997	0	2	0	2006	192	JR144	N/A	W. Peninsula
RGBT-02	-61.965998	-57.244002	0	1	0	2006	129	JR144	N/A	W. Peninsula
LI-AGT-1	-62.276	-61.595999	0	4	0	2006	1511	JR144	N/A	W. Peninsula
BIO6-AGT-2B	-71.179002	-109.894	0	19	0	2008	998	JR179	N/A	Bell/Amund
BIO6-AGT-2A	-71.175003	-109.863	0	22	0	2008	1079	JR179	N/A	Bell/Amund
BIO6-AGT-2C	-71.182	-109.926	0	15	0	2008	986	JR179	N/A	Bell/Amund
BIO6-AGT-1B	-71.152001	-110.013	0	1	0	2008	1491	JR179	N/A	Bell/Amund
BIO6-AGT-1A	-71.146001	-109.971	0	1	0	2008	1530	JR179	N/A	Bell/Amund
PS77-252-3	-64.694001	-60.517999	0	1	0	2011	316	PS77	N/A	Weddell
PS77-248-3	-65.924	-60.332	0	1	0	2011	433	PS77	N/A	Weddell
PS77-250-6	-65.383999	-61.548001	0	5	0	2011	566	PS77	N/A	Weddell
PS77-235-8	-65.528002	-61.551999	0	1	0	2011	448	PS77	N/A	Weddell
PS77-237-2	-66.209002	-60.162001	0	1	0	2011	382	PS77	N/A	Weddell
PS77-265-2	-70.794	-10.67	0	4	0	2011	633	PS77	N/A	Weddell

PS77-260-6	-70.84	-10.597	0	2	0	2011	259	PS77	N/A	Weddell
PS77-312-2	-54.47	3.1849998	0	5	0	2011	297	PS77	N/A	Oceanic islands
PS77-291-1	-70.841998	-10.587	0	3	0	2011	267	PS77	N/A	Weddell
PS77-312-4	-54.481	3.1889998	0	4	0	2011	300	PS77	N/A	Oceanic islands
PS77-312-3	-54.502001	3.2249999	0	4	0	2011	264	PS77	N/A	Oceanic islands
PS77-308-1	-70.854999	-10.589001	0	1	0	2011	223	PS77	N/A	Weddell
PS77-301-1	-70.850999	-10.588001	0	1	0	2011	225	PS77	N/A	Weddell
PS77-284-1	-70.972	-10.504002	0	1	0	2011	289	PS77	N/A	Weddell
PS77-275-3	-70.934	-10.496	0	1	0	2011	238	PS77	N/A	Weddell
PS77-222-5	-62.297002	-58.678	0	1	0	2011	873	PS77	N/A	W. Peninsula
PS77-239-3	-66.195001	-60.148998	0	5	0	2011	362	PS77	N/A	Weddell
PS77-226-7	-64.914001	-60.620998	0	5	0	2011	226	PS77	N/A	Weddell
PS77-228-3	-64.918001	-60.537	0	5	0	2011	279	PS77	N/A	Weddell
PS77-233-3	-65.557999	-61.621998	0	5	0	2011	324	PS77	N/A	Weddell
PS77-228-4	-64.929	-60.564999	0	1	0	2011	315	PS77	N/A	Weddell
AGT-2B	-67.983001	-68.438	0	1	0	2009	585	JR230	N/A	W. Peninsula
BIO5-AGT-3C	-73.986	-107.39	0	1	0	2008	541	JR179	N/A	Bell/Amund
BIO4-AGT-2C	-74.477	-104.257	0	5	0	2008	1150	JR179	N/A	Bell/Amund

Supplementary Table 2. F_{ST} values for 2b-RAD data based on sampling locality. Significant values ($P < 0.05$).

Fst P values	1042	1051	531	762	803	806	826	843	867	877	895	900	913	914
1042	-													
1051	0.0715	-												
531	0.0880	0.1606	-											
762	0.0516	0.1385	0.1173	-										
803	0.0597	0.1926	0.1341	0.0883	-									
806	0.0426	0.0784	0.0905	0.0484	0.0630	-								
826	0.0784	0.4402	0.1694	0.1204	0.2034	0.0773	-							
843	0.0708	0.2972	0.1433	0.1041	0.1584	0.0652	0.3118	-						
867	0.0430	0.0962	0.0956	0.0605	0.0735	0.0480	0.0966	0.0865	-					
877	0.0427	0.0708	0.0807	0.0609	0.0620	0.0515	0.0725	0.0651	0.0445	-				
895	0.0817	0.1382	0.1102	0.1019	0.1113	0.0890	0.1254	0.1269	0.0861	0.0555	-			
900	0.0871	0.1705	0.1235	0.1157	0.1249	0.0931	0.1461	0.1511	0.0950	0.0584	0.0639	-		
913	0.0987	0.1478	0.1223	0.1290	0.1339	0.1114	0.1422	0.1332	0.1085	0.0680	0.0746	0.0890	-	
914	0.1095	0.1974	0.1492	0.1400	0.1613	0.1180	0.2008	0.1854	0.1183	0.0718	0.0876	0.1121	0.0664	-
917	0.1019	0.1584	0.1317	0.1295	0.1326	0.1170	0.1534	0.1426	0.1109	0.0673	0.0751	0.0957	0.0506	0.0735

Supplementary Table 3. PCA χ^2 results for genetic populations identified by STRUCTURE *K*=4. Significant values (P<0.01)* and (P<0.001)** are in bold.

χ^2	Ross/W. Peninsula	Bellingshausen	Weddell A/Bransfield	Weddell B
Ross/W. Peninsula	-	**-**	**-**	**-**
Bellingshausen	**66.451****	-	**-**	**-**
Weddell A/Bransfield	**54.004****	**35.626****	-	-
Weddell B	**60.923****	**42.120****	**25.034***	-

Supplementary Table 4. PCA χ^2 results for samples labeled by geographic region. Significant values (P<0.01)* and (P<0.001)** are in bold.

χ^2	Ross Sea	Bellingshausen Sea	Western Peninsula	Bransfield Strait	Weddell Sea
Ross Sea	-	**-**	-	-	**-**
Bellingshausen Sea	**80.403****	-	**-**	**-**	**-**
Western Peninsula	17.080	**84.254****	-	-	**-**
Bransfield Strait	**27.269***	**32.062****	12.454	-	-
Weddell Sea	**96.670****	**42.525****	**56.393****	20.925	-

Supplementary Table 5. Analysis of molecular variance statistics for *O. victoriae* based on 16S data.

Source of variation	d.f.	Sum of squares	σ^2	Percentage of variation
Among groups	4	270.700	0.780	22.95361
Among populations within groups	3	81.044	0.946	27.81462
Within populations	243	406.744	1.674	49.23177
Total	250	758.518	3.400	

Supplementary Table 6. Analysis of molecular variance statistics for *O. victoriae* based on COI & 16S data.

Source of variation	d.f.	Sum of squares	σ^2	Percentage of variation
Among groups	4	8997.445	19.178	19.76305
Among populations within groups	3	3444.274	41.491	42.75669
Within populations	243	8838.085	36.371	37.48025
Total	250	21279.805	97.040	

Supplementary Table 7. Summary statistics for DIYABC v2.1.0 historical scenario analyses. Values indicate for each summary statistics the proportion of simulated data sets which have a value below the observed one. A total of 7,000,000 simulated datasets were performed.

Summary statistics	observed	scenario 1	scenario 2	scenario 3	scenario 4	scenario 5	scenario 6	scenario 7
FM1_1_1&2	-0.1697	0.0373 (*)	0.0001(***)	0.0430 (*)	0.0021 (**)	0.0002(***)	0.0843	0.0027(**)
FM1_1_1&3	-0.0956	0.1208	0.2014	0.1263	0.1204	0.004(**)	0.0212(*)	0.2312
FM1_1_1&4	-0.1632	0.1739	0.3219	0.329	0.1741	0.0517	0.1159	0.5176
FM1_1_2&3	-0.1725	0.0788	0.0011(**)	0.0792	0.0795	0.1183	0.0079(**)	0.0073(**)
FM1_1_2&4	-0.2344	0.0927	0.0249(*)	0.2831	0.2835	0.2077	0.0827	0.0828
FM1_1_3&4	-0.1145	0.1748	0.2845	0.2065	0.1756	0.284	0.333	0.3363
FV1_1_1&2	-0.0344	0.0865	0.0013(**)	0.0839	0.0095 (**)	0.0014(**)	0.1586	0.0101(*)
FV1_1_1&3	-0.0128	0.1144	0.1876	0.1173	0.1141	0.0036(**)	0.0192(*)	0.2153
FV1_1_1&4	-0.033	0.1232	0.2619	0.2964	0.1229	0.0412(*)	0.097	0.4748
FV1_1_2&3	-0.0366	0.1632	0.0095(**)	0.1783	0.164	0.2468	0.0352(*)	0.0354(*)
FV1_1_2&4	-0.0535	0.1479	0.0586	0.3617	0.3616	0.2946	0.1256	0.147
FV1_1_3&4	-0.0188	0.1642	0.2653	0.1944	0.1648	0.265	0.314	0.3249
FMO_1_1&2	-0.0953	0.3585	0.1321	0.3068	0.1262	0.0284(*)	0.5871	0.063
FMO_1_1&3	-0.0541	0.1823	0.3146	0.1287	0.1958	0.0029(**)	0.0172(*)	0.2962
FMO_1_1&4	-0.1055	0.3069	0.5676	0.5555	0.3054	0.1526	0.2445	0.7857
FMO_1_2&3	-0.0948	0.4465	0.1976	0.4493	0.4418	0.6734	0.2164	0.1408
FMO_1_2&4	-0.1346	0.6428	0.5181	0.7985	0.7754	0.832	0.5877	0.5562
FMO_1_3&4	-0.0587	0.24	0.3915	0.2036	0.2267	0.3888	0.4364	0.3878
NM1_1_1&2	-0.083	0.4113	0.1002	0.343	0.224	0.0675	0.5258	0.1583
NM1_1_1&3	-0.035	0.1654	0.2874	0.1583	0.1651	0.0085(**)	0.0342(*)	0.2812
NM1_1_1&4	-0.0715	0.2666	0.4215	0.4097	0.2673	0.1026	0.1802	0.5975
NM1_1_2&3	-0.084	0.292	0.0808	0.3621	0.2923	0.4583	0.1778	0.1536
NM1_1_2&4	-0.1198	0.3517	0.219	0.5184	0.5183	0.4989	0.311	0.3373
NM1_1_3&4	-0.0477	0.1994	0.3389	0.2575	0.2001	0.3385	0.3856	0.3901
NV1_1_1&2	-0.0223	0.3108	0.0323	0.2584	0.1082	0.0309(*)	0.4229	0.0922

NV1_1_1&3	-0.0058	0.1235	0.2105	0.1218	0.1233	0.0044(**)	0.0213(*)	0.2227
NV1_1_1&4	-0.017	0.1142	0.2507	0.2725	0.1141	0.0339(*)	0.084	0.4429
NV1_1_2&3	-0.0226	0.2362	0.0331	0.2857	0.2365	0.3749	0.0911	0.0848
NV1_1_2&4	-0.038	0.2141	0.0975	0.4271	0.4272	0.376	0.1829	0.2073
NV1_1_3&4	-0.0103	0.1671	0.2785	0.2065	0.1678	0.2784	0.3266	0.3366
NMO_1_1&2	-0.0811	0.7052	0.458	0.7795	0.5542	0.4575	0.9014	0.5234
NMO_1_1&3	-0.0348	0.2912	0.485	0.2663	0.2984	0.028(*)	0.0752	0.4799
NMO_1_1&4	-0.0709	0.486	0.6799	0.7097	0.4882	0.3776	0.456	0.8504
NMO_1_2&3	-0.0828	0.7679	0.512	0.7284	0.7654	0.8823	0.5502	0.5036
NMO_1_2&4	-0.1145	0.8138	0.7435	0.9053	0.8857	0.93	0.7749	0.7788
NMO_1_3&4	-0.0467	0.4107	0.6151	0.4236	0.413	0.6226	0.6698	0.6017

Supplementary Table 8. Genbank accession numbers for each haplotype and corresponding sequences.

Genbank accession COI	Sequence
KY048218	DSOPH1899
	DSOPH1900
	Op913_3E_3
FJ917329	194.1E.02
	195.1E.05
	DSOPH1903
	DSOPH2142
	DSOPH2143
	DSOPH2144
	DSOPH2148
	DSOPH2152
KY048223	DSOPH2157
	DSOPH2159
KY048231	DSOPH2198
	DSOPH2212
	DSOPH2251
	DSOPH2678
	DSOPH2685
	DSOPH2734
	Op913_3E_10
KY048226	DSOPH2186
	DSOPH2215
	DSOPH2217
	DSOPH2254
	DSOPH2256
	DSOPH2258
	DSOPH2684
	DSOPH2699
	DSOPH2743
	Op531_3E_6
KY048234	DSOPH2203
	DSOPH2207
	DSOPH2218
	Op803_4C_1
	Op806_3C_2
KY048229	DSOPH2193
	DSOPH2206
	DSOPH2208
	DSOPH2211

	DSOPH2216
	DSOPH2230
	DSOPH2252
	DSOPH2259
	DSOPH2272
	DSOPH2676
	DSOPH2738
KY048233	DSOPH2201
	DSOPH2202
	DSOPH2209
	DSOPH2731
	DSOPH2752
KY048228	DSOPH2191
	DSOPH2199
	DSOPH2229
	DSOPH2255
	DSOPH2273
	DSOPH2733
	DSOPH2736
	DSOPH2903
	Op531_3E_13
	Op531_3E_9
KY048232	DSOPH2200
	DSOPH2276
FJ917310	321.2C.04
	57.3C.05
	57.3C.10
	57.3C.12
	59.2C.03
	59.2C.06
	59.2C.07
	DSOPH1912
	DSOPH2161
	DSOPH2204
	DSOPH2888
	DSOPH3835
	Op913_3E_1
	Op913_3E_2
	Op913_3E_4
	Op913_3E_5
	Op913_3E_6
	Op913_3E_9
	Op914_3E_8
	Op914_3E_9

	Op917_3E_10
	Op917_3E_4
	Op917_3E_6
	Op917_3E_7
KY048265	Op914_3E_3
	Op914_3E_5
KY048261	Op762_3C_2
	Op787_6C_4
	Op806_3C_1
	Op806_7C
	Op806_8C_1
	Op818_2E
	Op818_3C_3
	Op818_4C_3
	Op818_4C_4
	Op826_3C_2
	Op843_3C_1
	Op843_7C_1
	Op843_7C_4
FJ917348	422.1C.10
	DSOPH2568
	DSOPH2964
FJ917339	312.3C.07
	312.3C.09
	422.1C.01
	422.1C.04
	422.1C.05
	422.1C.08
	422.1C.14
	E82.2C.01
	E82.2C.02
	DSOPH2327
	DSOPH724
	Op1042_3E_2
	Op1042_3E_3
	Op1042_3E_4
	Op1042_3E_9
	Op867_4E_10
	Op867_4E_2
	Op867_4E_3
	Op867_4E_6
	Op867_4E_8
	Op867_4E_9
	Op877_2E_1

	Op877_2E_8
FJ917337	312.3C.01
	312.3C.03
	312.3C.16
	398.1E.12
	422.1C.03
	422.1C.06
	E82.2C.04
	E82.2C.05
	DSOPH1908
	DSOPH2154
	DSOPH2346
	DSOPH2571
	DSOPH2904
	DSOPH2962
	DSOPH2963
	DSOPH3033
	DSOPH3035
	DSOPH3185
	DSOPH3216
	DSOPH3239
	DSOPH3807
	DSOPH3810
	DSOPH3859
	DSOPH3871
	DSOPH446
	DSOPH721
	DSOPH722
	DSOPH725
	Op1042_3E_1
	Op1042_3E_6
	Op531_3E_11
	Op762_2E
	Op762_5C_1
	Op762_6C_1
	Op762_6C_2
	Op787_5C_1
	Op787_5C_2
	Op787_5C_3
	Op787_5C_4
	Op787_6C_1
	Op787_6C_2
	Op787_6C_3
	Op787_6C_5

	Op803_3C_1
	Op803_3C_2
	Op803_3C_3
	Op803_3C_4
	Op803_3C_5
	Op803_3C_6
	Op803_4C_2
	Op803_4C_3
	Op806_2E
	Op806_3C_3
	Op806_3C_4
	Op806_8C_2
	Op806_8C_3
	Op806_8C_4
	Op818_3C_1
	Op818_3C_2
	Op818_3C_4
	Op818_3C_5
	Op818_4C_1
	Op818_4C_2
	Op818_4C_5
	Op826_2E
	Op826_3C_1
	Op843_2E
	Op843_7C_2
	Op843_7C_3
	Op867_4E_5
	Op867_4E_7
	Op877_2E_3
	Op877_2E_7
	Op877_2E_9
FJ917340	312.3C.15
	DSOPH1756
	DSOPH2155
	DSOPH2971
	DSOPH3098
	Op1042_3E_5
	Op867_4E_1
	Op877_2E_5
FJ917333	194.1E.07
	195.1E.04
FJ917328	194.1E.01
	194.1E.06
	195.1E.03

	195.1E.06
	195.1E.08
	DSOPH1904
	DSOPH2149
FJ917332	194.1E.05
	195.1E.07
	DSOPH2145
FJ917324	177.1E.01
	177.1E.05
	196.1E.07
	DSOPH3146
FJ917326	177.1E.04
	177.1E.07
	177.1E.10
	177.1E.12
	196.1E.01
	196.1E.04
	196.1E.05
	196.1E.06
	196.1E.08
	DSOPH3043
	DSOPH3045
	DSOPH3046
	DSOPH3145
	DSOPH3147
	DSOPH3157
	DSOPH3160
FJ917313	196.1E.10
	57.3C.13
	92.10C
	Op913_3E_7
	Op917_3E_5
	Op917_3E_8
	Op917_3E_9
FJ917312	114.5C
	57.3C.11
	DSOPH1909
	Op914_3E_10
KY048252	DSOPH3528
	DSOPH3873
	Op1042_3E_7
KY048243	DSOPH2914
	DSOPH3872
KY048242	DSOPH2902

	DSOPH2905	
	DSOPH2906	
KY048239	DSOPH2729	
	Op531_3E_4	
	Op531_3E_8	
KY048230	DSOPH2195	
	DSOPH2213	
	DSOPH2253	
	DSOPH2260	
	DSOPH2264	
	DSOPH2359	
	DSOPH2680	
	DSOPH2730	
	DSOPH2732	
	DSOPH2747	
	DSOPH2753	
	DSOPH678	
KY048246	DSOPH3096	
	DSOPH3311	
FJ917327	177.1E.02	
	177.1E.06	
	177.1E.09	
	177.1E.11	
	DSOPH3144	
FJ917316	114.10C	
	114.4C	
	114.7C	
	114.8C	
	362.1C.09	
	362.1C.12	
	398.1E.02	
	398.1E.14	
	92.11C	
	92.13C	
	92.15C	
	92.17C	
	92.5C	
	92.6C	
	E73.2C.09	
	DSOPH3848	
	DSOPH3892	
	Op877_2E_2	
FJ917322	114.13C	
	114.6C	

	312.3C.02
	398.1E.07
	E73.2C.06
	DSOPH1910
	DSOPH2918
	DSOPH3809
	DSOPH3876
FJ917319	321.2C.03
	321.2C.06
	92.12C
	E73.2C.08
	DSOPH1898
	DSOPH2257
	Op895_3E_2
	Op895_3E_4
	Op895_3E_8
	Op913_3E_8
	Op914_3E_2
FJ917311	57.3C.08
	Op917_3E_2
FJ917343	362.1C.07
	398.1E.01
	398.1E.15
FJ917320	114.3C
	92.16C
	E73.2C.10
	DSOPH2924
	DSOPH3837
	DSOPH3839
	Op877_2E_10
	Op877_2E_4
	Op877_2E_6
FJ917342	362.1C.01
	362.1C.10
FJ917318	321.2C.01
	92.8C
	E73.2C.02
	E73.2C.11
	DSOPH3808
	DSOPH3847
	DSOPH3850
	DSOPH3851
	Op914_3E_6
	Op914_3E_7

FJ917309	362.1C.02
	362.1C.03
	362.1C.04
	362.1C.05
	57.3C.03
	57.3C.14
	92.14C
	92.9C
	E73.2C.01
	E73.2C.05
	DSOPH1263
	DSOPH2156
	Op895_3E_5
	Op895_3E_7
KY048241	DSOPH2867
FJ917347	422.1C.07
KY048262	Op762_4C_1
FJ917346	422.1C.02
KY048256	Op1042_3E_10
FJ917338	312.3C.05
FJ917345	398.1E.13
KY048257	Op1042_3E_8
KY048248	DSOPH3120
KY048247	DSOPH3097
KY048245	DSOPH3044
KY048235	DSOPH2205
KY048260	Op531_3E_5
KY048237	DSOPH2566
KY048236	DSOPH2275
KY048240	DSOPH2742
KY048221	DSOPH2150
KY048259	OP531_3E_12
KY048238	DSOPH2567
KY048227	DSOPH2187
KY048258	Op531_3E_10
KY048225	DSOPH2160
KY048249	DSOPH3158
FJ917317	92.7C
FJ917344	362.1C.11
KY048254	DSOPH3838
KY048255	DOPH3849
KY048268	DSOPH3811
KY048253	DSOPH3836
FJ917353	E73.2C.12

KY048222	DSOPH2151
FJ917331	194.1E.04
KY048264	Op895_3E_3
FJ917314	92.3C
KY048220	DSOPH2146
KY048219	DSOPH1911
FJ917330	194.1E.03
FJ917354	E82.2C.03
KY048267	Op917_3E_3
KY048263	Op895_3E_10
FJ917321	114.2C
FJ917351	E73.2C.03
FJ917315	92.4C
FJ917323	114.11C
KY048251	DSOPH3226
FJ917341	321.2C.02
KY048266	Op917_3E_1
FJ917335	194.1E.09
FJ917334	194.1E.08
KY048244	DSOPH2923
KY048224	DSOPH2158
FJ917336	196.1E.03
KY048250	DSOPH3159
Genbank accession 16S	Sequence
KY048203	Op1042_3E_1
	Op877_2E_9
KY048209	Op531_3E_12
	Op531_3E_13
	Op531_3E_4
	Op531_3E_6
	Op531_3E_8
	Op913_3E_10
KY048214	Op803_4C_1
	Op806_3C_2
FJ917301	177.1E.01
	177.1E.05
	195.1E.07
KY048204	Op1042_3E_5
	Op877_2E_5
FJ917305	Op1042_3E_10
	Op1042_3E_6
	Op762_3C_2
	Op762_5C_1

	Op762_6C_1
	Op787_5C_3
	Op787_6C_3
	Op787_6C_4
	Op803_3C_2
	Op803_3C_3
	Op803_3C_4
	Op803_4C_2
	Op803_4C_3
	Op806_3C_1
	Op806_3C_3
	Op806_3C_4
	Op806_7C
	Op806_8C_1
	Op806_8C_3
	Op806_8C_4
	Op818_2E
	Op818_3C_1
	Op818_3C_3
	Op818_3C_5
	Op818_4C_1
	Op818_4C_2
	Op818_4C_3
	Op818_4C_4
	Op818_4C_5
	Op826_2E
	Op826_3C_2
	Op843_2E
	Op843_3C_1
	Op843_7C_1
	Op843_7C_2
	Op843_7C_4
	Op867_4E_1
	Op867_4E_3
	Op867_4E_5
	Op867_4E_7
	Op877_2E_7
	Op877_2E_8
	312.3C.01
	312.3C.03
	312.3C.16
	398.1E.12
	422.1C.03
	422.1C.06

	E82.2C.04
	E82.2C.05
	312.3C.05
	312.3C.15
	398.1E.13
	422.1C.02
	422.1C.10
FJ917306	Op1042_3E_2
	Op1042_3E_3
	Op1042_3E_4
	Op1042_3E_9
	Op867_4E_10
	Op867_4E_2
	Op867_4E_6
	Op867_4E_8
	Op867_4E_9
	Op877_2E_1
	312.3C.07
	312.3C.09
	422.1C.01
	422.1C.04
	422.1C.05
	422.1C.08
	422.1C.14
	E82.2C.01
	E82.2C.02
	422.1C.07
KY048206	Op1042_3E_8
	Op877_2E_3
FJ917291	57.3C.05
	321.2C.04
FJ917293	Op913_3E_1
	Op913_3E_2
	Op913_3E_3
	Op913_3E_4
	Op913_3E_5
	Op913_3E_6
	Op913_3E_9
	Op914_3E_3
	Op914_3E_5
	Op914_3E_8
	Op914_3E_9
	Op917_3E_10
	Op917_3E_4

	Op917_3E_6
	Op917_3E_7
	57.3C.10
	57.3C.12
	59.2C.03
	59.2C.06
	59.2C.07
KY048208	Op531_3E_11
	Op762_2E
	Op787_5C_1
	Op787_5C_2
	Op787_5C_4
	Op787_6C_1
	Op787_6C_2
	Op787_6C_5
	Op803_3C_1
	Op803_3C_5
	Op803_3C_6
	Op806_2E
	Op806_8C_2
	Op818_3C_2
	Op818_3C_4
	Op826_3C_1
FJ917296	Op877_2E_2
	Op895_3E_10
	92.3C
	92.6C
	92.15C
	92.17C
	114.8C
	362.1C.09
	398.1E.02
	398.1E.14
	E43.2C.03
	114.2C
	114.6C
	114.13C
	312.3C.02
	398.1E.07
	E73.2C.06
	114.11C
FJ917304	194.1E.03
	E73.2C.02
FJ917294	Op877_2E_10

	Op877_2E_6	
	Op895_3E_3	
	Op895_3E_4	
	Op895_3E_8	
	Op913_3E_7	
	Op913_3E_8	
	Op914_3E_2	
	Op914_3E_6	
	Op917_3E_1	
	Op917_3E_3	
	Op917_3E_5	
	Op917_3E_8	
	Op917_3E_9	
	57.3C.11	
	57.3C.13	
	92.10C	
	196.1E.10	
	92.4C	
	321.2C.01	
	E73.2C.11	
	92.12C	
	321.2C.03	
	321.2C.06	
	92.16C	
	114.3C	
	196.1E.07	
	177.1E.04	
	177.1E.10	
	177.1E.12	
	196.1E.01	
	196.1E.04	
	196.1E.06	
	196.1E.08	
	194.1E.01	
	194.1E.06	
	195.1E.06	
	195.1E.08	
	194.1E.02	
	195.1E.05	
	194.1E.04	
	194.1E.07	
	194.1E.08	
	194.1E.09	
	196.1E.03	

	321.2C.02	
	362.1C.07	
	398.1E.01	
	398.1E.15	
	E73.2C.03	
	E73.2C.12	
	E82.2C.03	
	195.1E.03	
	195.1E.04	
FJ917302	177.1E.06	
	177.1E.09	
	177.1E.11	
	177.1E.02	
FJ917300	Op877_2E_4	
	Op914_3E_10	
	114.5C	
	E73.2C.10	
KY048213	Op762_6C_2	
	Op843_7C_3	
FJ917295	Op895_3E_7	
	57.3C.14	
	92.9C	
	92.14C	
	362.1C.02	
	362.1C.03	
	362.1C.04	
	362.1C.05	
	E73.2C.01	
	92.7C	
	177.1E.07	
	196.1E.05	
	362.1C.01	
	362.1C.10	
	362.1C.11	
	E73.2C.05	
FJ917299	92.11C	
	92.13C	
	114.4C	
	114.7C	
	114.10C	
	362.1C.12	
	E73.2C.09	
FJ917292	Op917_3E_2	
	57.3C.08	

KY048210	Op531_3E_5
KY048211	Op531_3E_9
KY048207	Op531_3E_10
KY048212	Op762_4C_1
KY048205	Op1042_3E_7
FJ917298	92.8C
FJ917297	92.5C
FJ917303	194.1E.05
KY048217	Op914_3E_7
KY048215	Op895_3E_2
FJ917308	E73.2C.08
FJ917290	57.3C.03
KY048216	Op895_3E_5

Supplementary Figure 1. Historical scenarios evaluated using Bayesian computation (ABC). In these scenarios t# represents time in generations and is based off the four genetic populations identified by STRUCTURE. **Scenario 1**. The three geographic regions split at approximately the same time with a more recent diversification in the Weddell Sea. **Scenario 2**. Initial separation of the Bellingshausen Sea with a subsequent split between the Ross with the most recent diversification in the Weddell Sea, consistent with a trans-Antarctic seaway hypothesis. **Scenario 3**. Diversification of all populations at approximately the same time, possibly due to isolation in refugium. **Scenario 4**. Initial separation of the Ross Sea with a much more recent diversification in the Bellingshausen and two in the Weddell Sea. **Scenario 5**. Initial separation of the Ross, then Bellingshausen and finally diversification in the Weddell, consistent with West to East distribution and diversification through the ACC. **Scenario 6**. An initial separation of Western and Easter Antarctica with later diversification in both regions. **Scenario 7**. Initial isolation of the Bellingshausen Sea and a much more recent diversification between the three remaining populations.

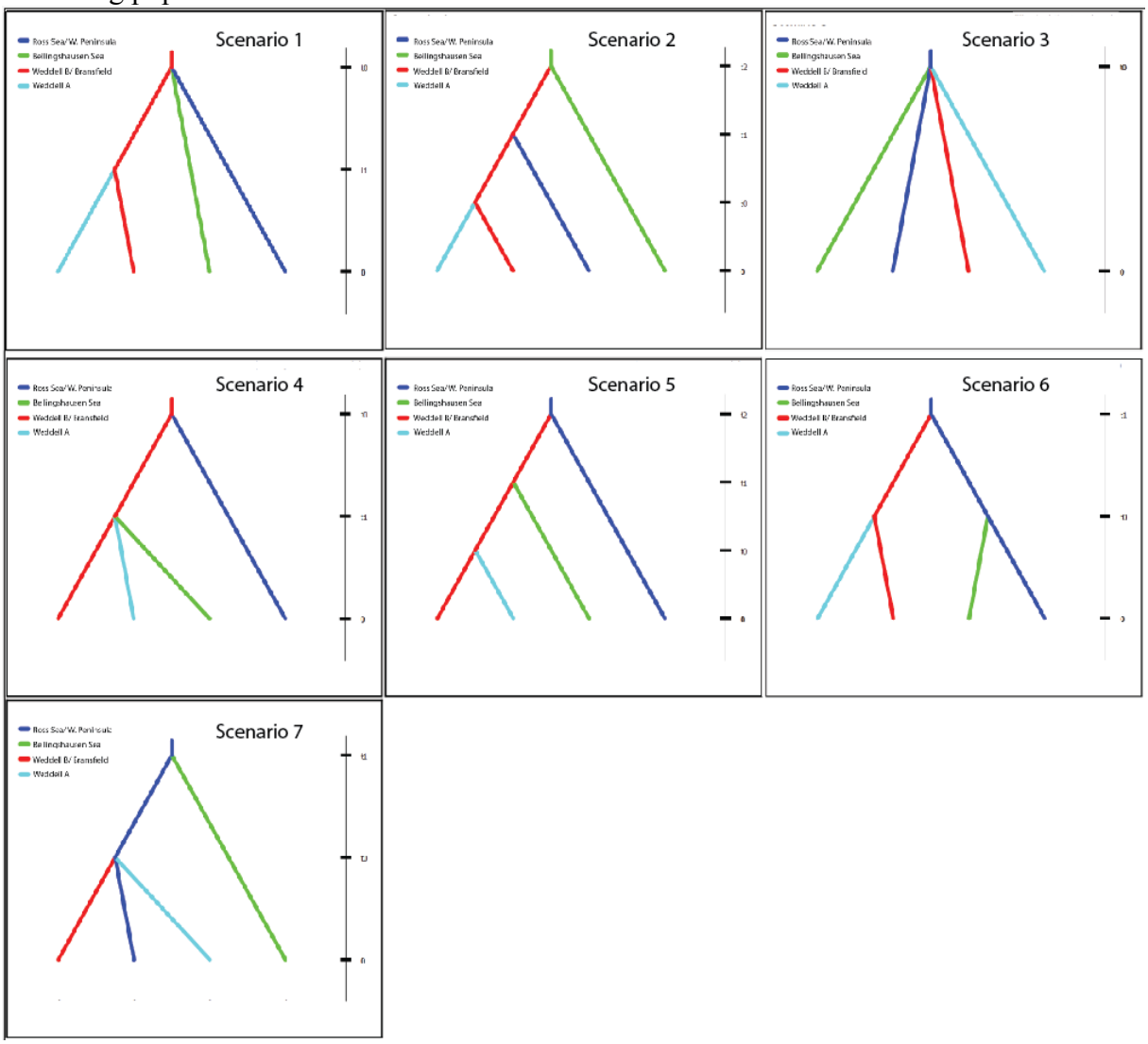

Supplementary Figure 2. STRUCTURE HARVESTER (Earl & vonHoldt 2012) average calculations of DeltaK based on the 1999 SNP loci.

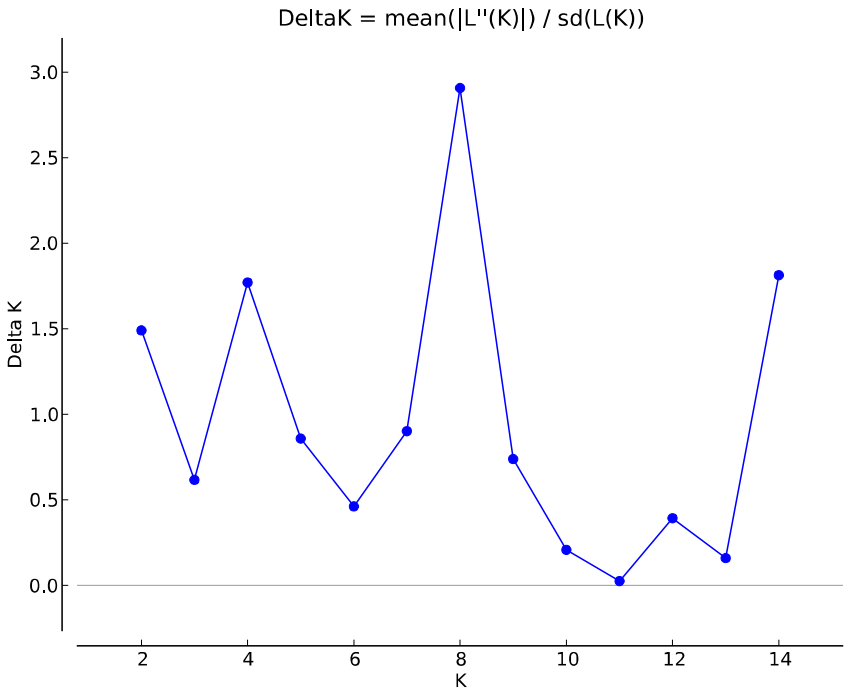

Supplementary Figure 3. Patterns of population structure for *Ophionotus victoriae* based on SNP data analyzed in STRUCTURE 2.3.4. (Pritchard et al. 2000) and visualized in DISTRUCT (Rosenberg 2004) testing for the true number of populations (*K*). *K*=2 is presented in the graph above.

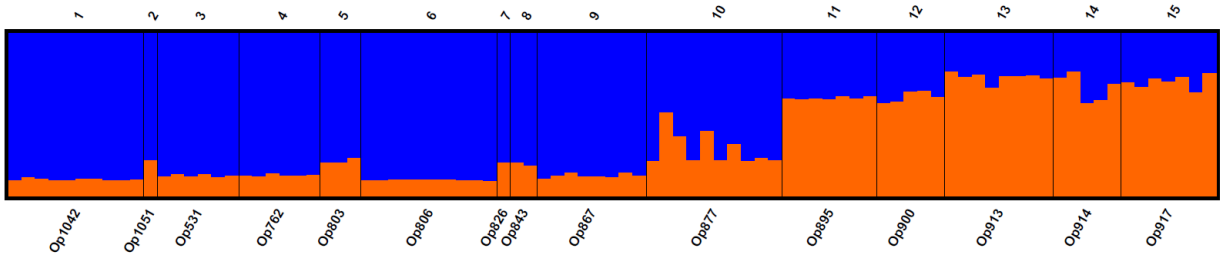

Supplementary Figure 4. Patterns of population structure for *Ophionotus victoriae* based on SNP data analyzed in STRUCTURE 2.3.4. (Pritchard et al. 2000) and visualized in DISTRUCT (Rosenberg 2004) testing for the true number of populations (*K*). *K*=8 is presented in the graph above.

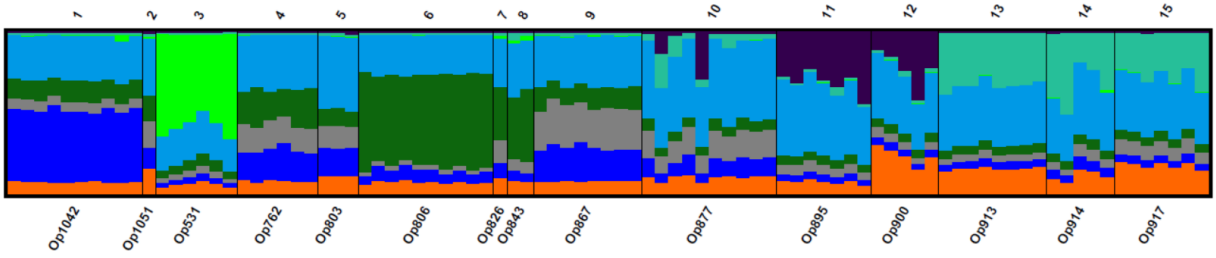

Supplementary Figure 5. PCA results based on SNP data for samples labeled by the geographic regions of the Ross Sea, Bellingshausen Sea, western Antarctic Peninsula, Bransfield Straits and Weddell Sea. Sampling locality Op867 was at the boundary of the western Antarctic Peninsula and Bransfield Strait and is likely bathed in Weddell Sea water coming through Antarctic Sound and southwest along continental edge of the Peninsula. Thus for Op 867 samples, we have circled the gray X used to denote western Antarctic Peninsula samples as they appear to cluster themselves with either other samples further southwest on the Antarctic Peninsula or with samples from the Weddell Sea.

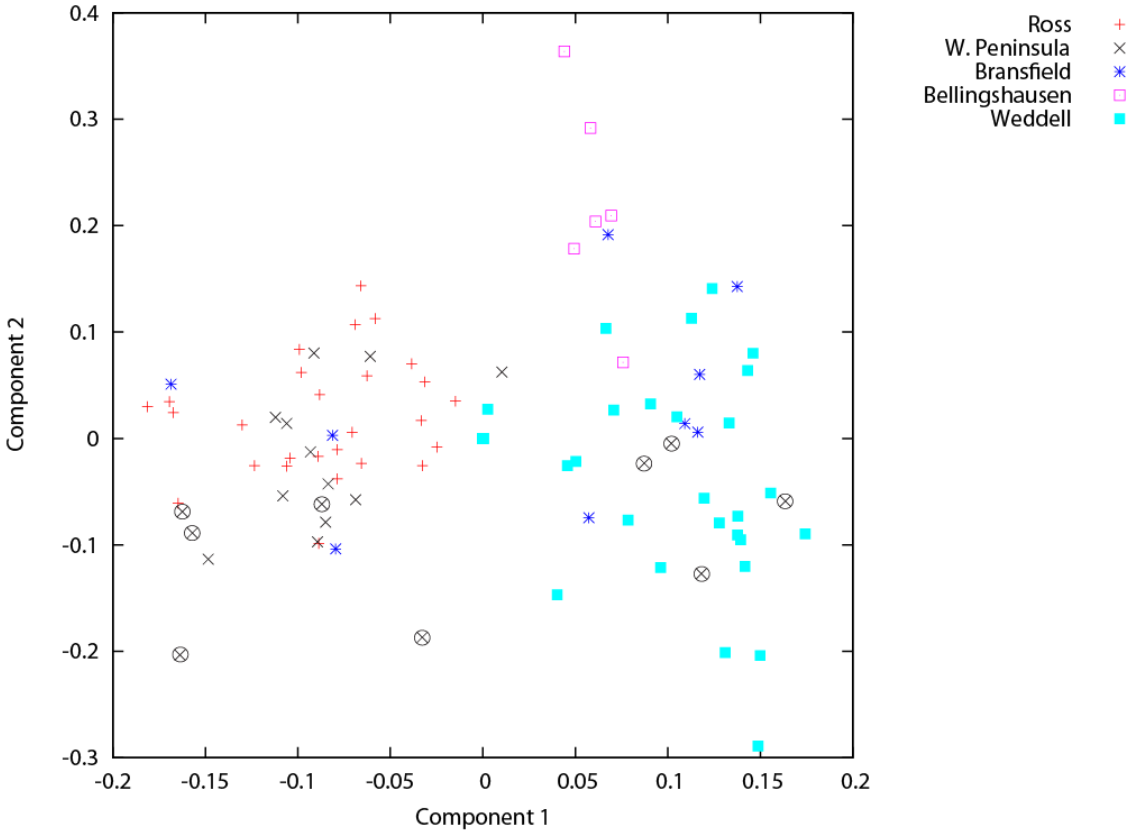

Appendix 2.

Appendix Table 1. Sampling information including locality, depth and molecular analyses used for every individual *Astrotoma agassizii* specimen.

Sample ID	Location	Latitude	Longitude	Depth (m)	COI	COII	16S	2b-RAD
143.1C	Antarctic Pen.	-65.623733	-67.784617	217	NO	YES	YES	NO
15.1C	Patagonian Shelf	-54.455333	-63.8776	108	NO	YES	YES	NO
152.3C	Antarctic Pen.	-65.663333	-68.03	278	NO	YES	YES	YES
152.4C	Antarctic Pen.	-65.663333	-68.03	278	NO	YES	YES	NO
152.5C	Antarctic Pen.	-65.663333	-68.03	278	NO	YES	YES	NO
152.6C	Antarctic Pen.	-65.663333	-68.03	278	NO	YES	YES	NO
160.2C	Antarctic Pen.	-64.688333	-65.926667	368	NO	YES	YES	NO
160.4C	Antarctic Pen.	-64.688333	-65.926667	368	NO	YES	YES	NO
160.5C	Antarctic Pen.	-64.688333	-65.926667	368	NO	YES	YES	NO
160.6C	Antarctic Pen.	-64.688333	-65.926667	368	NO	YES	YES	NO
17.3C.1	Patagonian Shelf	-54.470683	-62.202583	321	NO	YES	YES	NO
17.3C.3	Patagonian Shelf	-54.470683	-62.202583	321	NO	YES	YES	NO
17.3C.5	Patagonian Shelf	-54.470683	-62.202583	321	NO	YES	YES	NO
17.3C.6	Patagonian Shelf	-54.470683	-62.202583	321	NO	YES	YES	NO
17.3C.7	Patagonian Shelf	-54.470683	-62.202583	321	NO	YES	YES	NO
17.3C.8	Patagonian Shelf	-54.470683	-62.202583	321	NO	YES	YES	NO
17.3C.9	Patagonian Shelf	-54.470683	-62.202583	321	NO	YES	YES	NO
17.4E.1	Patagonian Shelf	-54.470683	-62.202583	321	NO	YES	YES	NO
17.4E.2	Patagonian Shelf	-54.470683	-62.202583	321	NO	YES	YES	NO
17.4E.4	Patagonian Shelf	-54.470683	-62.202583	321	NO	YES	YES	NO
17.4E.5	Patagonian Shelf	-54.470683	-62.202583	321	NO	YES	YES	NO
17.4E.6	Patagonian Shelf	-54.470683	-62.202583	321	NO	YES	YES	NO
17.4E.7	Patagonian Shelf	-54.470683	-62.202583	321	NO	YES	YES	NO

17.4E.8	Patagonian Shelf	-54.470683	-62.202583	321	NO	YES	YES	NO
17.4E.9	Patagonian Shelf	-54.470683	-62.202583	321	NO	YES	YES	NO
235.1C.1	Patagonian Shelf	-53.270233	-66.385833	96	NO	YES	YES	NO
235.1C.11	Patagonian Shelf	-53.270233	-66.385833	96	NO	YES	YES	NO
235.1C.12	Patagonian Shelf	-53.270233	-66.385833	96	NO	YES	YES	YES
235.1C.13	Patagonian Shelf	-53.270233	-66.385833	96	NO	YES	YES	YES
235.1C.14	Patagonian Shelf	-53.270233	-66.385833	96	NO	YES	YES	NO
235.1C.15	Patagonian Shelf	-53.270233	-66.385833	96	NO	NO	NO	YES
235.1C.16	Patagonian Shelf	-53.270233	-66.385833	96	NO	YES	YES	NO
235.1C.17	Patagonian Shelf	-53.270233	-66.385833	96	NO	YES	YES	NO
235.1C.18	Patagonian Shelf	-53.270233	-66.385833	96	NO	YES	YES	NO
235.1C.20	Patagonian Shelf	-53.270233	-66.385833	96	NO	YES	YES	YES
235.1C.5	Patagonian Shelf	-53.270233	-66.385833	96	NO	YES	YES	NO
235.1C.6	Patagonian Shelf	-53.270233	-66.385833	96	NO	YES	YES	NO
235.1C.9	Patagonian Shelf	-53.270233	-66.385833	96	NO	YES	YES	NO
25.1C	Patagonian Shelf	-54.470683	-62.202583	321	NO	YES	YES	NO
251.10C	Patagonian Shelf	-54.470683	-62.202583	170	NO	YES	YES	NO
251.12C	Patagonian Shelf	-53.783333	-60.7	170	NO	YES	YES	YES
251.13C	Patagonian Shelf	-53.783333	-60.7	170	NO	YES	YES	NO
251.14C	Patagonian Shelf	-53.783333	-60.7	170	NO	YES	YES	NO
251.15C	Patagonian Shelf	-53.783333	-60.7	170	NO	YES	YES	YES
251.17C	Patagonian Shelf	-53.783333	-60.7	170	NO	YES	YES	YES

251.18C	Patagonian Shelf	-53.783333	-60.7	170	NO	YES	YES	NO
251.1C	Patagonian Shelf	-53.783333	-60.7	170	NO	YES	YES	NO
251.20C	Patagonian Shelf	-53.783333	-60.7	170	NO	YES	YES	NO
251.3C	Patagonian Shelf	-53.783333	-60.7	170	NO	YES	YES	NO
251.4C	Patagonian Shelf	-53.783333	-60.7	170	NO	YES	YES	NO
251.5C	Patagonian Shelf	-53.783333	-60.7	170	NO	YES	YES	NO
251.6C	Patagonian Shelf	-53.783333	-60.7	170	NO	YES	YES	NO
251.7C	Patagonian Shelf	-53.783333	-60.7	170	NO	YES	YES	NO
251.9C	Patagonian Shelf	-53.783333	-60.7	170	NO	YES	YES	NO
259.1C.1	Patagonian Shelf	-53.783333	-61.8	403	NO	YES	YES	YES
259.1C.10	Patagonian Shelf	-53.783333	-61.8	403	NO	YES	YES	YES
259.1C.2	Patagonian Shelf	-53.783333	-61.8	403	NO	NO	NO	YES
259.1C.4	Patagonian Shelf	-53.783333	-61.8	403	NO	NO	NO	YES
259.1C.5	Patagonian Shelf	-53.783333	-61.8	403	NO	YES	YES	NO
259.1C.6	Patagonian Shelf	-53.783333	-61.8	403	NO	YES	YES	YES
259.1C.8	Patagonian Shelf	-53.783333	-61.8	403	NO	YES	YES	YES
259.1C.9	Patagonian Shelf	-53.783333	-61.8	403	NO	YES	YES	YES
262.2C.1	Patagonian Shelf	-53.783333	-59.55	854	NO	YES	YES	NO
262.2C.10	Patagonian Shelf	-53.783333	-59.55	854	NO	YES	YES	NO
262.2C.13	Patagonian Shelf	-53.783333	-59.55	854	NO	YES	YES	NO
262.2C.14	Patagonian Shelf	-53.783333	-59.55	854	NO	YES	YES	YES
262.2C.16	Patagonian Shelf	-53.783333	-59.55	854	NO	YES	YES	YES

262.2C.17	Patagonian Shelf	-53.783333	-59.55	854	NO	NO	NO	YES
262.2C.18	Patagonian Shelf	-53.783333	-59.55	854	NO	YES	YES	NO
262.2C.19	Patagonian Shelf	-53.783333	-59.55	854	NO	YES	YES	NO
262.2C.20	Patagonian Shelf	-53.783333	-59.55	854	NO	NO	NO	YES
262.2C.2	Patagonian Shelf	-53.783333	-59.55	854	NO	YES	YES	YES
262.2C.3	Patagonian Shelf	-53.783333	-59.55	854	NO	YES	YES	NO
262.2C.4	Patagonian Shelf	-53.783333	-59.55	854	NO	YES	YES	NO
262.2C.5	Patagonian Shelf	-53.783333	-59.55	854	NO	YES	YES	NO
262.2C.6	Patagonian Shelf	-53.783333	-59.55	854	NO	YES	YES	NO
262.2C.7	Patagonian Shelf	-53.783333	-59.55	854	NO	YES	YES	YES
262.2C.8	Patagonian Shelf	-53.783333	-59.55	854	NO	YES	YES	NO
262.2C.9	Patagonian Shelf	-53.783333	-59.55	854	NO	YES	YES	NO
268.1C.1	Patagonian Shelf	-54.816667	-60.266667	110	NO	YES	YES	YES
268.1C.2	Patagonian Shelf	-54.816667	-60.266667	110	NO	YES	YES	YES
271.1C.1	Patagonian Shelf	-54.341333	-60.993833	125	NO	YES	YES	YES
271.1C.2	Patagonian Shelf	-54.341333	-60.993833	125	NO	YES	YES	YES
276.1C.1	Patagonian Shelf	-54.382267	-61.8828	274	NO	YES	YES	YES
276.1C.10	Patagonian Shelf	-54.382267	-61.8828	274	NO	NO	NO	YES
276.1C.2	Patagonian Shelf	-54.382267	-61.8828	274	NO	NO	NO	YES
276.1C.3	Patagonian Shelf	-54.382267	-61.8828	274	NO	NO	NO	YES
276.1C.4	Patagonian Shelf	-54.382267	-61.8828	274	NO	NO	NO	YES
276.1C.5	Patagonian Shelf	-54.382267	-61.8828	274	NO	NO	NO	YES

276.1C.6	Patagonian Shelf	-54.382267	-61.8828	274	NO	YES	YES	YES
276.1C.7	Patagonian Shelf	-54.382267	-61.8828	274	NO	YES	YES	YES
276.1C.8	Patagonian Shelf	-54.382267	-61.8828	274	NO	YES	YES	NO
29.10C	Patagonian Shelf	-54.6904	-59.3918	207	NO	YES	YES	NO
29.12C.1	Patagonian Shelf	-54.6904	-59.3918	207	NO	YES	YES	NO
29.12C.2	Patagonian Shelf	-54.6904	-59.3918	207	NO	YES	YES	NO
29.12C.3	Patagonian Shelf	-54.6904	-59.3918	207	NO	YES	YES	NO
29.13C	Patagonian Shelf	-54.6904	-59.3918	207	NO	YES	YES	NO
29.14C	Patagonian Shelf	-54.6904	-59.3918	207	NO	YES	YES	NO
29.15C	Patagonian Shelf	-54.6904	-59.3918	207	NO	YES	YES	NO
29.16C	Patagonian Shelf	-54.6904	-59.3918	207	NO	YES	YES	NO
29.17C	Patagonian Shelf	-54.6904	-59.3918	207	NO	YES	YES	NO
29.18C	Patagonian Shelf	-54.6904	-59.3918	207	NO	YES	YES	NO
29.6C	Patagonian Shelf	-54.6904	-59.3918	207	NO	YES	YES	NO
29.8C	Patagonian Shelf	-54.6904	-59.3918	207	NO	YES	YES	NO
29.9C	Patagonian Shelf	-54.6904	-59.3918	207	NO	YES	YES	NO
33.2C.2	Patagonian Shelf	-54.6904	-59.3918	207	NO	YES	YES	NO
33.2C.4	Patagonian Shelf	-54.6904	-59.3918	207	NO	YES	YES	NO
33.2C.6	Patagonian Shelf	-54.6904	-59.3918	207	NO	YES	YES	NO
34.1C.1	Patagonian Shelf	-54.6904	-59.3918	207	NO	YES	YES	NO
34.1C.2	Patagonian Shelf	-54.6904	-59.3918	207	NO	YES	YES	NO
355.2C	Antarctic Pen.	-66.61105	-68.309433	261	NO	YES	YES	NO
407.1C.1	Antarctic Pen.	-65.66405	-68.037067	282	NO	YES	YES	NO

407.1C.2	Antarctic Pen.	-65.66405	-68.037067	282	NO	YES	YES	NO
407.1C.3	Antarctic Pen.	-65.66405	-68.037067	282	NO	YES	YES	NO
407.1C.4	Antarctic Pen.	-65.66405	-68.037067	282	NO	YES	YES	NO
407.1C.5	Antarctic Pen.	-65.66405	-68.037067	282	NO	YES	YES	NO
407.1C.6	Antarctic Pen.	-65.66405	-68.037067	282	NO	YES	YES	NO
407.1C.7	Antarctic Pen.	-65.66405	-68.037067	282	NO	YES	YES	NO
46.2C	Patagonian Shelf	-54.674833	-63.233333	254	NO	YES	YES	NO
46.3C	Patagonian Shelf	-54.674833	-63.233333	254	NO	YES	YES	NO
81.10C	Bransfield	-62.85	-59.45	900	NO	YES	YES	NO
81.11C	Bransfield	-62.85	-59.45	900	NO	YES	YES	NO
81.3C	Bransfield	-62.85	-59.45	900	NO	YES	YES	NO
81.5C	Bransfield	-62.85	-59.45	900	NO	YES	YES	NO
81.6C	Bransfield	-62.85	-59.45	900	NO	YES	YES	NO
81.7C	Bransfield	-62.85	-59.45	900	NO	YES	YES	NO
81.8C	Bransfield	-62.85	-59.45	900	NO	YES	YES	NO
81.9C	Bransfield	-62.85	-59.45	900	NO	YES	YES	NO
Op660_2C	Amundsen Sea	-73.296662	-129.918777	506	NO	YES	YES	NO
Op660_3C	Amundsen Sea	-73.296662	-129.918777	506	NO	YES	YES	YES
Op660_4C	Amundsen Sea	-73.296662	-129.918777	506	NO	YES	YES	YES
Op666_10C	Amundsen Sea	-73.498535	-129.918777	516	NO	YES	YES	YES
Op666_11C	Amundsen Sea	-73.498535	-129.918777	516	NO	YES	YES	YES
Op666_2C	Amundsen Sea	-73.498535	-129.918777	516	NO	YES	YES	YES
Op666_3C	Amundsen Sea	-73.498535	-129.918777	516	NO	YES	YES	YES
Op666_4C	Amundsen Sea	-73.498535	-129.918777	516	NO	YES	YES	YES
Op666_5C	Amundsen Sea	-73.498535	-129.918777	516	NO	YES	YES	YES
Op666_6C	Amundsen Sea	-73.498535	-129.918777	516	NO	YES	YES	YES
Op666_7C	Amundsen Sea	-73.498535	-129.918777	516	NO	YES	YES	YES
Op666_8C	Amundsen Sea	-73.498535	-129.918777	516	NO	YES	YES	YES
Op666_9C	Amundsen Sea	-73.498535	-129.918777	516	NO	YES	YES	YES

Op682_2C	Amundsen Sea	-73.710433	-129.056117	655	NO	YES	YES	YES
Op734_2E	Ross Sea	-76.341217	-170.850495	531	NO	YES	YES	YES
Op750_2C	Ross Sea	-76.479417	-165.737762	457	NO	YES	YES	YES
Op750_3C	Ross Sea	-76.479417	-165.737762	457	NO	YES	YES	YES
Op750_4C	Ross Sea	-76.479417	-165.737762	457	NO	YES	YES	YES
Op750_5C	Ross Sea	-76.479417	-165.737762	457	NO	YES	YES	YES
Op750_6C	Ross Sea	-76.479417	-165.737762	457	NO	YES	YES	NO
Op796_2E	Ross Sea	-76.245262	174.50412	604	NO	YES	YES	NO
Op796_3C_1	Ross Sea	-76.245262	174.50412	604	NO	YES	YES	YES
Op796_3C_2	Ross Sea	-76.245262	174.50412	604	NO	YES	YES	YES
Op796_3C_3	Ross Sea	-76.245262	174.50412	604	NO	YES	YES	YES
Op796_3C_4	Ross Sea	-76.245262	174.50412	604	NO	YES	YES	YES
Op796_4C_1	Ross Sea	-76.245262	174.50412	604	NO	YES	YES	YES
Op796_4C_2	Ross Sea	-76.245262	174.50412	604	NO	YES	YES	YES
Op796_4C_3	Ross Sea	-76.245262	174.50412	604	NO	YES	YES	YES
Op796_4C_4	Ross Sea	-76.245262	174.50412	604	NO	YES	YES	NO
Op805_2E	Ross Sea	-76.9038	169.96525	764	NO	YES	YES	YES
Op805_3E_1	Ross Sea	-76.9038	169.96525	764	NO	YES	YES	YES
Op805_3E_2	Ross Sea	-76.9038	169.96525	764	NO	YES	YES	YES
Op822_2E	Ross Sea	-75.833465	166.505493	552	NO	YES	YES	YES
Op822_3C	Ross Sea	-75.833465	166.505493	552	NO	YES	YES	YES
Op829_2E	Ross Sea	-74.70781	168.407827	489	NO	YES	YES	NO
Op833_10C	Ross Sea	-74.181977	166.661027	390	NO	YES	YES	YES
Op833_11C	Ross Sea	-74.181977	166.661027	390	NO	YES	YES	YES
Op833_12C	Ross Sea	-74.181977	166.661027	390	NO	YES	YES	YES
Op833_13C	Ross Sea	-74.181977	166.661027	390	NO	YES	YES	YES
Op833_14C	Ross Sea	-74.181977	166.661027	390	NO	NO	NO	YES
Op833_15C	Ross Sea	-74.181977	166.661027	390	NO	YES	YES	YES
Op833_2C	Ross Sea	-74.181977	166.661027	390	NO	YES	YES	YES
Op833_3C	Ross Sea	-74.181977	166.661027	390	NO	NO	NO	YES
Op833_4C	Ross Sea	-74.181977	166.661027	390	NO	YES	YES	YES
Op833_5C	Ross Sea	-74.181977	166.661027	390	NO	YES	YES	YES
Op833_6C	Ross Sea	-74.181977	166.661027	390	NO	YES	YES	YES
Op833_7C	Ross Sea	-74.181977	166.661027	390	NO	NO	NO	YES
Op833_8C	Ross Sea	-74.181977	166.661027	390	NO	YES	YES	YES
Op833_9C	Ross Sea	-74.181977	166.661027	390	NO	YES	YES	YES
Op844_2E	Ross Sea	-74.995422	165.744217	1101	NO	YES	YES	NO

Op844_3C_1	Ross Sea	-74.995422	165.744217	1101	NO	YES	YES	YES
Op844_3C_2	Ross Sea	-74.995422	165.744217	1101	NO	YES	YES	YES
Op844_3C_3	Ross Sea	-74.995422	165.744217	1101	NO	YES	YES	YES
Op844_3C_4	Ross Sea	-74.995422	165.744217	1101	NO	NO	NO	YES
Op856_2E	Antarctic Pen.	-64.997867	-63.3009	525	NO	YES	YES	YES
Op860_2E	Antarctic Pen.	-64.4112	-61.963167	664	NO	YES	YES	YES
Op887_2E	W. Weddell Sea	-63.700525	-56.07855	293	NO	NO	NO	YES
Op887_2C	W. Weddell Sea	-63.700525	-56.07855	293	NO	YES	YES	YES
Op887_3E	W. Weddell Sea	-63.700525	-56.07855	293	NO	YES	YES	YES
Op887_5C	W. Weddell Sea	-63.700525	-56.07855	293	NO	YES	YES	YES
Op887_6C	W. Weddell Sea	-63.700525	-56.07855	293	NO	YES	YES	YES
Op887_7C	W. Weddell Sea	-63.700525	-56.07855	293	NO	YES	YES	YES
Op887_8C	W. Weddell Sea	-63.700525	-56.07855	293	NO	YES	YES	YES
Op894_1E	W. Weddell Sea	-64.302283	-56.136417	290	NO	YES	YES	NO
Op894_2C	W. Weddell Sea	-64.302283	-56.136417	290	NO	YES	YES	NO
Op894_3E	W. Weddell Sea	-64.302283	-56.136417	290	NO	YES	YES	NO
Op894_4C	W. Weddell Sea	-64.302283	-56.136417	290	NO	YES	YES	NO
Op909_2E	W. Weddell Sea	-64.035167	-56.72825	220	NO	YES	YES	YES
Op909_3E	W. Weddell Sea	-64.035167	-56.72825	220	NO	YES	YES	YES
Op909_4C	W. Weddell Sea	-64.035167	-56.72825	220	NO	YES	YES	YES
Op909_5C	W. Weddell Sea	-64.035167	-56.72825	220	NO	YES	YES	NO
Op938_2E	W. Weddell Sea	-63.5763	-54.629367	227	NO	YES	YES	NO
Op938_3C	W. Weddell Sea	-63.5763	-54.629367	227	NO	YES	YES	YES
DSOPH2092	Patagonian Shelf	-54.31452	-56.67918	197.62	YES	NO	NO	NO
DSOPH2093	Patagonian Shelf	-54.31452	-56.67918	197.62	YES	NO	NO	NO

DSOPH2096	Patagonian Shelf	-54.31452	-56.67918	197.62	YES	NO	NO	NO
DSOPH2097	Patagonian Shelf	-54.31452	-56.67918	197.62	YES	NO	NO	NO
DSOPH2098	Patagonian Shelf	-54.31452	-56.67918	197.62	YES	NO	NO	NO
DSOPH2099	Patagonian Shelf	-54.31452	-56.67918	197.62	YES	NO	NO	NO
DSOPH2100	Patagonian Shelf	-54.31452	-56.67918	197.62	YES	NO	NO	NO
DSOPH2336	Amundsen Sea	-74.40986	-104.65477	502.47	YES	NO	NO	NO
DSOPH2337	Amundsen Sea	-74.40986	-104.65477	502.47	YES	NO	NO	NO
DSOPH2338	Amundsen Sea	-74.40986	-104.65477	502.47	YES	NO	NO	NO
DSOPH2339	Amundsen Sea	-74.40986	-104.65477	502.47	YES	NO	NO	NO
DSOPH2340	Amundsen Sea	-74.40986	-104.65477	502.47	YES	NO	NO	NO
DSOPH2341	Amundsen Sea	-74.40986	-104.65477	502.47	YES	NO	NO	NO
DSOPH2425	Amundsen Sea	-74.40986	-104.65477	502.47	YES	NO	NO	NO
DSOPH2426	Amundsen Sea	-74.40986	-104.65477	502.47	YES	NO	NO	NO
DSOPH2427	Amundsen Sea	-74.39886	-104.62954	488.37	YES	NO	NO	NO
DSOPH2428	Amundsen Sea	-74.39886	-104.62954	488.37	YES	NO	NO	NO
DSOPH2692	Amundsen Sea	-74.39	-104.76392	517.91	YES	NO	NO	NO
DSOPH2694	Amundsen Sea	-74.39088	-104.76726	505.81	YES	NO	NO	NO
DSOPH2700	Amundsen Sea	-73.97488	-107.42227	552.75	YES	NO	NO	NO
DSOPH2952	E. Weddell Sea	-70.781333	-10.6815	633.5	YES	NO	NO	NO
DSOPH2953	E. Weddell Sea	-70.781333	-10.6815	633.5	YES	NO	NO	NO
DSOPH2954	E. Weddell Sea	-70.781333	-10.6815	633.5	YES	NO	NO	NO
DSOPH2955	E. Weddell Sea	-70.781333	-10.6815	633.5	YES	NO	NO	NO
DSOPH2956	E. Weddell Sea	-70.781333	-10.6815	633.5	YES	NO	NO	NO
DSOPH3091	E. Weddell Sea	-70.8345	-10.628833	276.7	YES	NO	NO	NO
DSOPH3095	E. Weddell Sea	-70.831167	-10.5765	281.7	YES	NO	NO	NO
DSOPH3176	E. Weddell Sea	-70.842667	-10.584	250.5	YES	NO	NO	NO
DSOPH3251	E. Weddell Sea	-70.8155	-10.544833	282.7	YES	NO	NO	NO
DSOPH3343	Patagonian Shelf	-54.501	-56.137167	290.5	YES	NO	NO	NO
DSOPH3344	Patagonian Shelf	-54.501	-56.137167	290.5	YES	NO	NO	NO
DSOPH3345	Patagonian Shelf	-54.501	-56.137167	290.5	YES	NO	NO	NO
DSOPH3346	Patagonian Shelf	-54.501	-56.137167	290.5	YES	NO	NO	NO
DSOPH3551	Patagonian Shelf	-54.546833	-56.166667	293.7	YES	NO	NO	NO
DSOPH3552	Patagonian Shelf	-54.546833	-56.166667	293.7	YES	NO	NO	NO

DSOPH3553	Patagonian Shelf	-54.546833	-56.166667	293.7	YES	NO	NO	NO
DSOPH3554	Patagonian Shelf	-54.546833	-56.166667	293.7	YES	NO	NO	NO
DSOPH3555	Patagonian Shelf	-54.546833	-56.166667	293.7	YES	NO	NO	NO
DSOPH3714	Patagonian Shelf	-54.567333	-56.177333	299.5	YES	NO	NO	NO
DSOPH3715	Patagonian Shelf	-54.567333	-56.177333	299.5	YES	NO	NO	NO
DSOPH3716	Patagonian Shelf	-54.567333	-56.177333	299.5	YES	NO	NO	NO
DSOPH3717	Patagonian Shelf	-54.567333	-56.177333	299.5	YES	NO	NO	NO
DSOPH3718	Patagonian Shelf	-54.567333	-56.177333	299.5	YES	NO	NO	NO
DSOPH3719	Patagonian Shelf	-54.567333	-56.177333	299.5	YES	NO	NO	NO
DSOPH4450	E. Weddell Sea	-75.76453	-30.45297	430	YES	NO	NO	NO

Appendix Table 2. NCBI accession number and sample ID for mtDNA fragments COI, COII, & 16S.

COI Accession	Sample ID	COII Accession	Sample ID	16S Accession	Sample ID
KY986616	DSOPH3714	EF565778	81.3C	EF565817	143.1C
KY986607	DSOPH2097	KY986638	Op887_6C		81.9C
KY986609	DSOPH2099	KY986618	OP660_3C		Op666_5C
KY986608	DSOPH2098	EF565787	407.1C.6		Op750_6C
KY986610	DSOPH2100	KY986633	Op833_6C	EF565816	152.3C
KY986606	DSOPH2096	EF565784	152.3C		152.4C
KY986604	DSOPH2092	KY986635	Op844_2E		152.5C
KY986605	DSOPH2093	KY986627	Op796_3C_1		152.6C
KY986614	DSOPH3552	KY986620	Op666_3C		160.2C
KY986611	DSOPH3343	KY986634	Op833_8C		160.4C
	DSOPH3344	KY986621	Op666_4C		160.5C
	DSOPH3345	KY986629	Op796_4C_2		160.6C
	DSOPH3554	KY986628	OP796_3C_2		355.2C
	DSOPH3555	KY986639	Op887_7C		407.1C.1
	DSOPH3716	KY986623	Op666_8C		407.1C.2
	DSOPH3717	EF565786	152.6C		407.1C.3
	DSOPH3718	KY986619	Op660_4C		407.1C.4
KY986617	DSOPH3715	KY986626	Op750_4C		407.1C.5
	DSOPH3719	KY986636	Op844_3C_3		407.1C.7
KY986613	DSOPH3551	KY986624	Op750_2C		81.10C
KY986615	DSOPH3553	KY986625	Op750_3C		81.11C
KY986612	DSOPH3346	KY986622	Op666_5C		81.5C
KY986600	DSOPH3091	KY986631	Op829_2E		81.6C
KY986592	DSOPH2339	KY986632	Op833_15C		81.7C
	DSOPH4450	EF565764	251.5C		81.8C
	DSOPH2953	KY986637	Op856_2E		Op660_2C
KY986594	DSOPH2341	EF565757	29.10C		Op666_10C
	DSOPH2426	EF565755	29.8C		Op666_11C
	DSOPH2427	EF565758	29.12C.2		Op666_2C
	DSOPH2692	EF565759	29.12C.3		Op666_4C
	DSOPH2700	EF565763	251.4C		Op666_6C
	DSOPH2955	EF565765	251.7C		Op666_7C
	DSOPH2956	EF565767	251.15C		Op666_8C
KY986589	DSOPH2336	EF565766	251.13C		Op666_9C
KY986602	DSOPH3176	EF565769	259.1C.10		Op734_2E
KY986599	DSOPH2954	EF565749	17.4E.1		Op750_2C
KY986601	DSOPH3095	EF565752	17.4E.6		Op750_3C
KY986603	DSOPH3251	EF565768	259.1C.9		Op750_4C
KY986590	DSOPH2337	EF565747	17.3C.5		Op750_5C
KY986596	DSOPH2428	EF565751	17.4E.5		Op796_2E

KY986598	DSOPH2952	EF565749	25.1C	Op796_3C_1
KY986597	DSOPH2694	EF565753	17.3C.8	Op796_3C_2
KY986595	DSOPH2425	EF565772	262.2C.7	Op796_3C_3
KY986593	DSOPH2340	EF565773	262.2C.8	Op796_3C_4
KY986591	DSOPH2338	EF565776	262.2C.16	Op796_4C_1
		EF565771	262.2C.5	Op796_4C_2
		EF565774	262.2C.9	Op796_4C_3
		EF565775	262.2C.10	Op796_4C_4
		EF565745	15.1C	Op805_2E
		EF565777	276.1C.8	Op805_3E_1
		EF565782	160.4C	Op805_3E_2
			407.1C.2	Op822_2E
			81.8C	Op822_3C
			Op887_8C	Op829_2E
		EF565785	152.4C	Op833_10C
			Op909_2E	Op833_11C
			Op909_3E	Op833_12C
		KY986640	Op894_1E	Op833_13C
			Op894_2C	Op833_15C
		EF565779	160.5C	Op833_2C
			407.1C.1	Op833_5C
			407.1C.4	Op833_6C
			407.1C.7	Op833_8C
			81.5C	Op833_9C
			Op660_2C	Op844_2E
			Op666_11C	Op844_3C_1
			Op666_2C	Op844_3C_2
			Op666_6C	Op844_3C_3
			Op666_9C	Op860_2E
			Op682_2C	Op887_2C
			Op734_2E	Op887_3E
			Op750_5C	Op887_5C
			Op796_3C_3	Op887_6C
			Op796_3C_4	Op887_7C
			Op796_4C_1	Op894_1E
			Op805_2E	Op894_2C
			Op805_3E_2	Op894_3E
			Op822_2E	Op894_4C
			Op822_3C	Op909_2E
			Op833_10C	Op909_3E
			Op833_11C	Op909_4C
			Op833_13C	Op909_5C
			Op833_4C	Op938_2E
			Op833_5C	Op938_3C

		Op833_9C	EF565815	81.3C
	EF565781	407.1C.5		Op660_3C
		81.7C	EF565797	251.10C
		Op833_12C		251.12C
	EF565780	152.5C		251.13C
		160.2C		251.14C
		160.6C		251.17C
		355.2C		251.18C
		81.10C		251.1C
		81.11C		251.20C
		81.6C		251.3C
		Op666_10C		251.4C
		Op666_7C		251.5C
		Op796_2E		251.6C
		Op805_3E_1		251.7C
		Op833_2C		251.9C
		Op844_3C_1		262.2C.6
		Op844_3C_2		271.1C.1
		Op860_2E		29.10C
		Op887_2C		29.12C.1
		Op887_3E		29.12C.2
		Op887_5C		29.12C.3
		Op894_3E		29.13C
		Op894_4C		29.14C
		Op909_4C		29.15C
		Op909_5C		29.16C
		Op938_2E		29.17C
		Op938_3C		29.18C
	KY986630	Op796_4C_3		29.6C
		Op796_4C_4		29.8C
	EF565783	143.1C		29.9C
		407.1C.3		33.2C.2
		81.9C		33.2C.4
		Op750_6C		33.2C.6
	EF565754	251.6C		34.1C.1
		271.1C.1		34.1C.2
		29.12C.1		Op856_2E
		29.13C	EF565809	262.2C.1
		29.15C		262.2C.14
		29.17C		262.2C.4
		29.18C		262.2C.9
		29.6C		271.1C.2
		33.2C.2	EF565811	262.2C.13
		34.1C.1		268.1C.2

	EF565756	251.10C	EF565790	15.1C
		251.12C		235.1C.1
		251.17C		262.2C.10
		251.18C		262.2C.2
		251.20C		262.2C.5
		251.3C		262.2C.7
		251.9C		262.2C.8
		262.2C.6		268.1C.1
		29.14C		276.1C.8
		29.16C		46.3C
		29.9C	EF565795	17.3C.9
		33.2C.4		17.4E.2
	EF565746	17.3C.1		17.4E.6
		17.3C.3		17.4E.7
		17.3C.6		46.2C
		17.3C.7	EF565798	235.1C.11
		17.3C.9		235.1C.12
		17.4E.2		235.1C.14
		17.4E.7		235.1C.16
		17.4E.8		235.1C.17
		17.4E.9		235.1C.5
		235.1C.12		235.1C.6
		235.1C.13		235.1C.9
		235.1C.16	EF565807	259.1C.6
		235.1C.17		259.1C.9
		235.1C.20	EF565791	17.3C.1
		235.1C.5		17.3C.6
		235.1C.6		276.1C.1
		235.1C.9	EF565793	17.3C.5
		259.1C.1		17.3C.7
		259.1C.5		17.4E.1
		259.1C.6		17.4E.5
		259.1C.8		17.4E.8
		262.2C.18		17.4E.9
		276.1C.1		25.1C
		276.1C.6		259.1C.5
		46.2C		259.1C.8
	EF565761	235.1C.11		262.2C.18
		235.1C.14		276.1C.6
	EF565750	17.4E.4	KY986584	Op660_4C
		235.1C.1	KY986586	Op682_2C
		46.3C	KY986585	Op666_3C
	EF565762	235.1C.18	KY986587	Op833_4C
		276.1C.7	EF565819	407.1C.6

	EF565770	262.2C.1	KY986588	Op887_8C
		262.2C.13	EF565804	251.15C
		262.2C.14	EF565814	276.1C.7
		262.2C.19	EF565799	235.1C.18
		262.2C.2	EF565812	262.2C.16
		262.2C.3	EF565808	259.1C.10
		262.2C.4	EF565806	259.1C.1
		268.1C.1	EF565794	17.3C.8
		268.1C.2	EF565796	17.4E.4
		271.1C.2	EF565801	235.1C.13
	EF565760	251.14C	EF565802	235.1C.20
		251.1C	EF565792	17.3C.3
		33.2C.6	EF565810	262.2C.3
		34.1C.2	EF565813	262.2C.19

Appendix Figure 1. Optimal K graph based on BIC values for DAPC analyses.

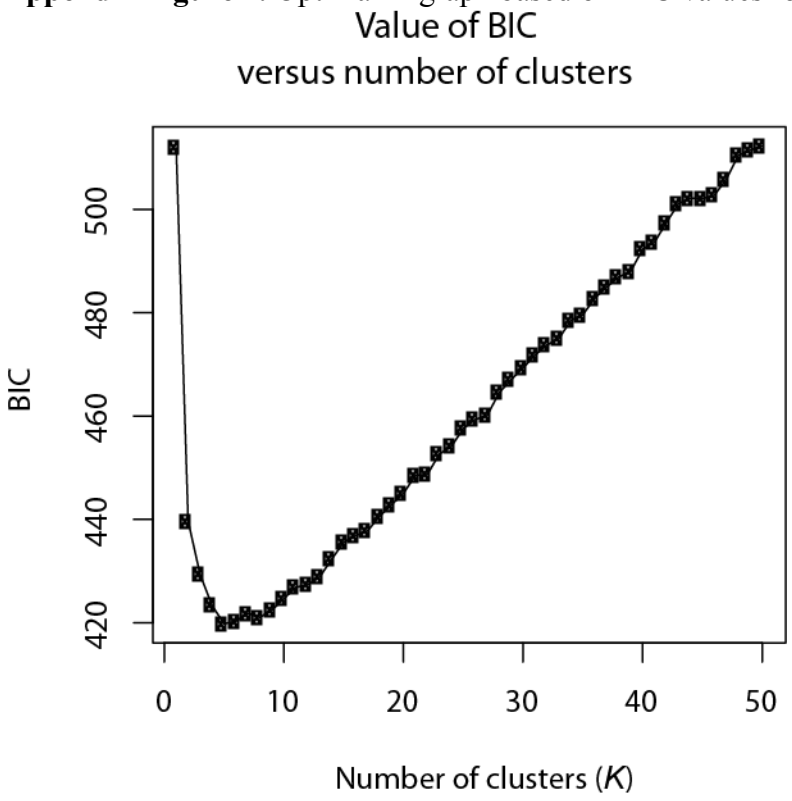

Appendix Figure 2. Optimal K graph based on minimal cross entropy for admixture analyses in LEA.

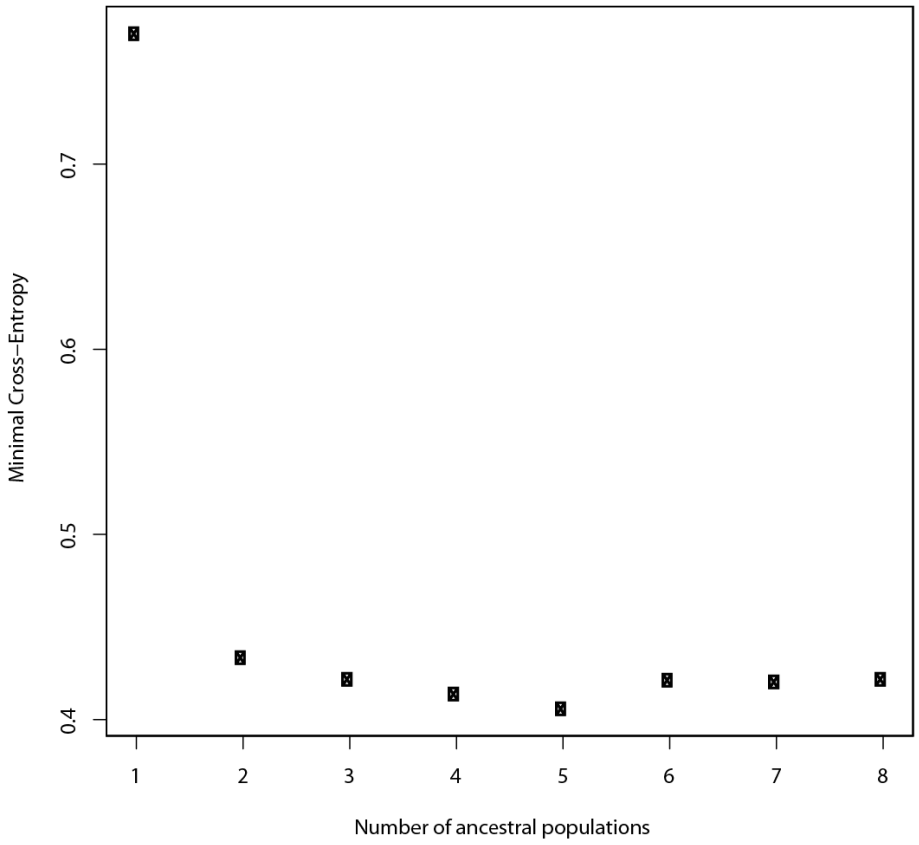

Appendix Figure 3. Patterns of population structure for *Astrotoma agassizii* in both the Southern Ocean and South America based on SNP data analyzed in STRUCTURE 2.3.4. (Falush *et al.*, 2003) and visualized in DISTRUCT (Rosenberg, 2004) testing for the true number of populations (*K*). *K*=2 is presented in the graph above as our most likely value of *K*.

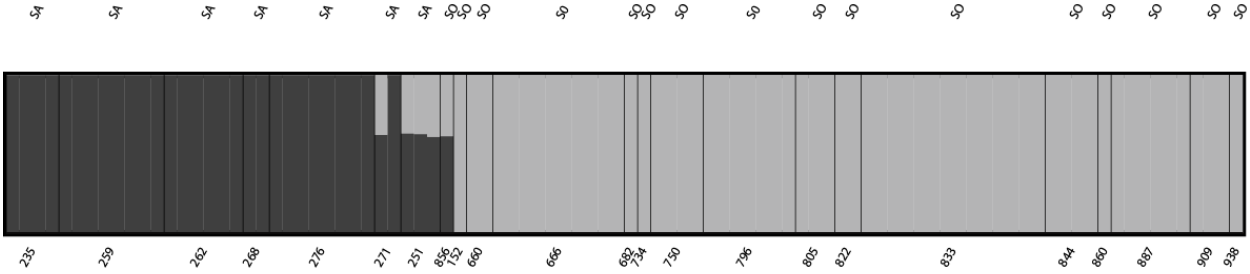

Appendix Figure 4. Patterns of population structure for *Astrotoma agassizii* in the Southern Ocean based on SNP data analyzed in STRUCTURE 2.3.4. (Falush *et al.*, 2003) and visualized in DISTRUCT (Rosenberg, 2004) testing for the true number of populations (*K*). *K*=4 is presented in the graph above as our most likely value of *K*.

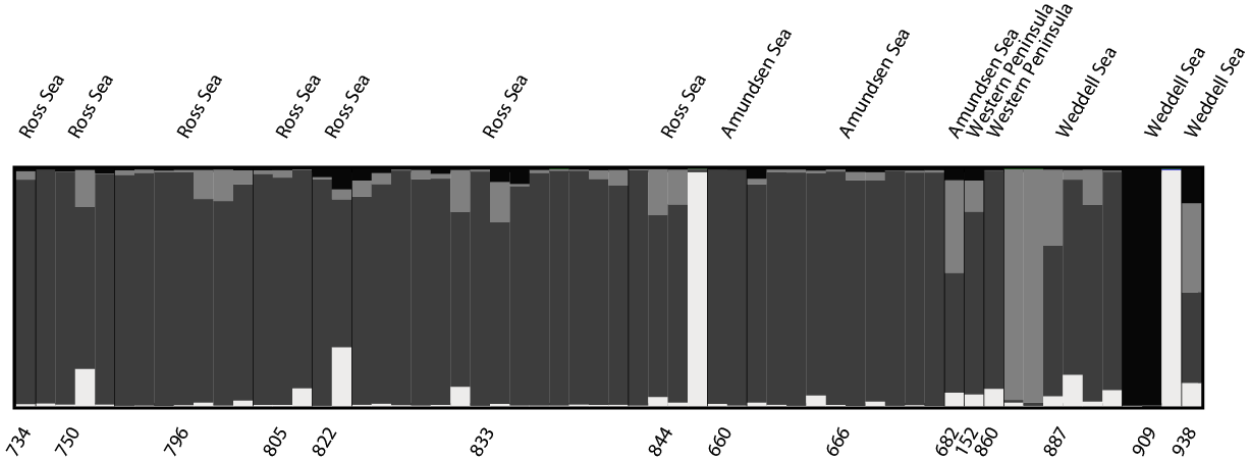

Appendix Figure 5. Patterns of population structure for *Astrotoma agassizii* in South American waters and Op856_2e from the Southern Ocean based on SNP data analyzed in STRUCTURE 2.3.4. (Falush *et al.*, 2003) and visualized in DISTRUCT (Rosenberg, 2004) testing for the true number of populations (*K*). *K*=3 is presented in the graph above as our most likely value of *K*.

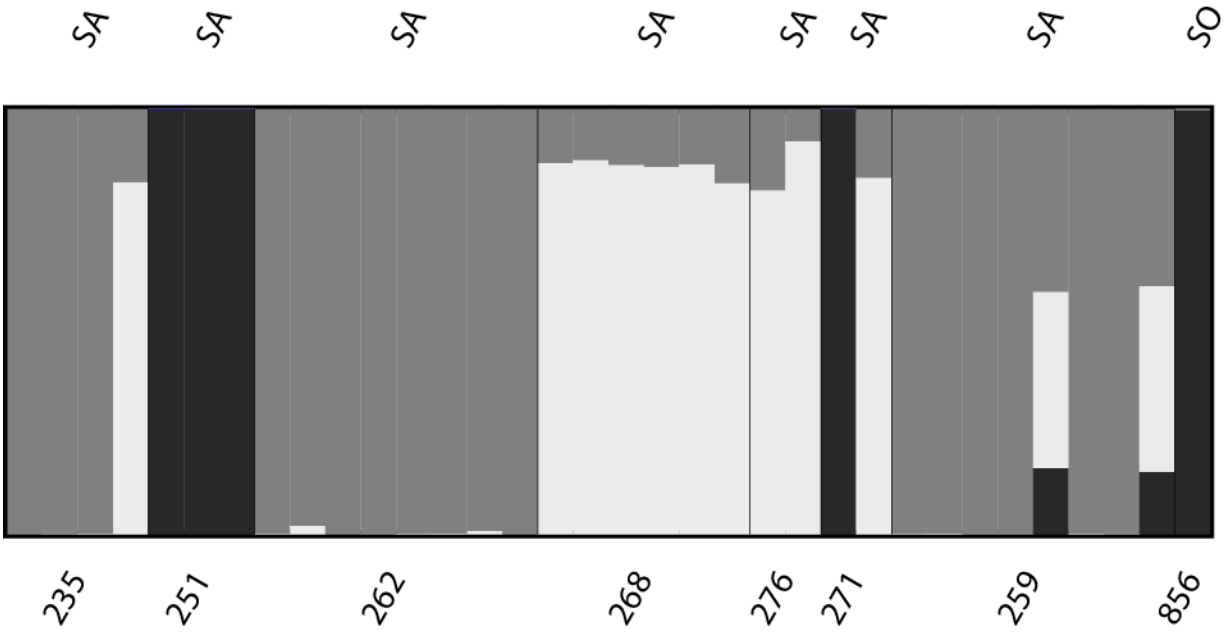

Appendix Figure 6. Admixture of *Astrotoma agassizii* from the South American Patagonian Shelf and from the Southern Ocean analyzed in LEA v1.0 (Frichot and François, 2015) assuming *K*=2.